SUBSURFACE ELECTRICAL RESISTIVITY INVESTIGATION AT THE N.Y.S.C. PROPOSED PERMANENT ORIENTATION CAMP, PAIKO, NIGER STATE, NIGERIA

BY

BALOGUN HAFIZ

DEPARTMENT OF PHYSICS,
FACULTY OF SCIENCE,
AHMADU BELLO UNIVERSITY, ZARIA

OCTOBER, 2015.

SUBSURFACE ELECTRICAL RESISTIVITY INVESTIGATION AT THE N.Y.S.C. PROPOSED PERMANENT ORIENTATION CAMP, PAIKO, NIGER STATE, NIGERIA

BY

BALOGUN HAFIZ
B.Sc. PHYSICS (A.B.U. 2008)
M.Sc./SCIEN/00640/2010-2011

BEING A RESEARCH THESIS SUBMITTED TO THE POSTGRADUATE SCHOOL, AHMADU BELLO UNIVERSITY, ZARIA, NIGERIA IN PARTIAL FULFILLMENT OF THE REQUIREMENTS FOR THE AWARD OF MASTER OF SCIENCE (M.Sc.) DEGREE IN APPLIED GEOPHYSICS

DEPARTMENT OF PHYSICS,
FACULTY OF SCIENCE,
AHMADU BELLO UNIVERSITY, ZARIA,
NIGERIA.

OCTOBER, 2015.

DECLARATION

I declare that the work titled **'*SUBSURFACE ELECTRICAL RESISTIVITY INVESTIGATION AT THE N.Y.S.C. PROPOSED PERMANENT ORIENTATION CAMP, PAIKO, NIGER STATE NIGERIA'*** has been performed by me in the Department of Physics under the supervision of Dr. P.O. Sule and Dr. A.L. Ahmed. The information derived from the literature has been duly acknowledged in the text and a list of references provided. No part of this thesis was previously presented for another degree or diploma at any university.

BALOGUN, Hafiz

| --- | --- | --- |
| Name of student | Signature | Date |

CERTIFICATION

This thesis titled **'*SUBSURFACE ELECTRICAL RESISTIVITY INVESTIGATION AT THE N.Y.S.C. PROPOSED PERMANENT ORIENTATION CAMP, PAIKO, NIGER STATE, NIGERIA'*** meets the regulations governing the award of Masters of Science Degree of Ahmadu Bello University, Zaria and is approved for its contribution to knowledge and literary presentation.

Dr. P. O. Sule

Chairman, Supervisory Committee	Signature	Date

Dr. A.L. Ahmed

Member, Supervisory Committee	Signature	Date

Dr. U. Sadiq

Head of Department	Signature	Date

Professor Kabir Bala

Dean, Postgraduate School	Signature	Date

DEDICATION

I dedicate this work to my late daddy, Mallam Abdullateef Ayodeji Balogun; this programme started when he was alive but was not privileged to witness this golden period. Well, Allah knows the best. Daddy, may your soul continue to rest in the bosom of the Most High and may Aljanatu Fridaus be your final abode. I really missed you. Adieu beloved daddy.

ACKNOWLEDGEMENT

First and foremost, my sincere thanks and appreciations are to God Almighty for His countless blessings upon me and for enabling me to achieve this important milestone in my life.Ya-Allah, Ya-Hafiz; glory be to Your holy name for making this work successful.

My sincere appreciation goes to my supervisors, Dr. P.O. Sule and Dr. A.L. Ahmed for creating time out of their busy schedule to give me audience, correct my mistakes and offer necessary contributions to the success of this work. May Allah bless you both on earth and in hereafter.

To my beloved mummy, Alhaja M. A. Balogun, words cannot express my gratitude and prayers for you. May you live long to reap the fruit of your labour. I owe you a lot sweet mum forever.

My immeasurable thanks also go to my siblings: mama D., Brother Lanre (big bross), Suliyat and Saheed (Engr. to be insha Allah). May the good Lord continue to strengthen our brotherly and sisterly relationship.

My sweetheart, my love and my jewel (SAHADAT IYABODE MUSTAPHA), thanks for standing firm by me. Thanks for your encouragement, your moral support and your prayers. I am indebted to you. You are a darling indeed! May Allah bless our union and lift us to a greater and unimagined height.

My uncle Alhaji Bukoye, you are acknowledged with high esteem. May Ya-Allah, Ya-Azeez and Ya-Hafiz continue to enrich your pocket in fold and bless you and your family in your endeavours.To my friend Mr. Mike (the Aviation man), my unquantifiable appreciation goes to you for your encouragement, contribution and motivation towards bringing this work to success. May the Almighty make you successful in your endeavours. You are more than a friend.

ABSTRACT

Electrical resistivity method was used in carrying out geophysical investigation at the Niger State National Youth Service Corp (N.Y.S.C.) proposed permanent orientation camp, Paiko of Paikoro Local Government Area (L.G.A.), with a view to determine the depth to the bedrock and thickness of the weathered basement. The Vertical Electrical Sounding (VES) using Schlumberger electrode array was carried out along five (5) profiles having a total of fifty (50) VES stations. On each profile, were ten (10) VES stations. The data were acquired using ABEM terrameter, Signal Averaging System (SAS) 1000. The field data obtained were analysed and interpreted using computer software (IPI2win and surfer 10) which gives an automatic interpretation of the apparent resistivity data. Results from the interpretation suggest three (3) layers in most parts of the study area. However, there is a case of two (2) layers at a station (VES A6). The resistivity value for the topsoil varies from 10 to 751Ωm with thickness ranging from 0.98 to 4.23m (except for VES A6 where the topsoil has been probably washed off by erosion). The weathered basement has resistivity values ranging from 9 to 968Ωm and thickness of between 0.67 and 24.50m. The fresh basement (bedrock) has resistivity values as high as 2718Ωm. The topsoil is characterized by a top lateritic soil underlain by a silty/sandy clay soil. These soils have great amount of dissolved salts resulting in their low resistivity values. The weathered basements are medium to fine grain, porous or fractured rocks containing water. They are referred to as the aquiferrous zones. The geologic sections derived, suggest that the weathered basement entirely represents a promising aquifer which can serve as the source of water to the area throughout the year. The parameters of investigation have helped in determining the depth to the aquiferous zone, identifying strategic areas such as VES A4, E4, A9, B1, B6, C4, D3 and E3 for siting high-rise buildings, potential positions for the location of boreholes such as VES A1, A3, A7, A8, A10, B2, B4, B5, B7, B8, B9, C3, C6, C9, D2, D7, E1, E2, E8 and E9 and possible depth of sewage system in order to avoid groundwater contamination. This survey revealed that the average depth to the bedrock (Fresh Basement) is about 15.00m with the lowest depth to it as 2.01m and with the highest depth to it as 26.81m. The aquifer in the area has an average depth of about 10.00m and therefore the depth of sewage system should be less than 10.00m in order to avoid groundwater contamination.

TABLE OF CONTENTS

	Page
COVER PAGE	i
TITLE PAGE	ii
DECLARATION	iii
CERTIFICATION	iv
DEDICATION	v
ACKNOWLEDGEMENT	vi
ABSTRACT	vii
TABLE OF CONTENTS	viii
LIST OF TABLES	xi
LIST OF FIGURES	xii
LIST OF APPENDICES	xiv
ABBREVIATION, SYMBOLS AND DEFINITIONS	xvii
CHAPTER ONE: INTRODUCTION	1
1.1 General Overview	1
1.2 Location of the Study Area	3
1.3 Climate, Relief and Vegetation	6
1.4 Aim and Objectives of the Survey	6
1.5 Justification	7
CHAPTER TWO: LITERATURE REVIEW	8
2.1 Some Previous Works in the Study Area	8
2.2 General Geology of the Study Area	10

CHAPTER THREE : MATERIALS AND METHODOLOGY 14

3.1 Fieldwork Planning 14

3.1.1 Choice of Electrode Configuration 14

3.1.2 Resistivity Values of Rocks and Minerals 14

3.1.3 Electrical Properties of Earth Materials and Parameters 20

3.1.3.1 Electrical Conductivity 20

3.1.3.2 Electrical Potentials 22

3.1.3.3 Magnetic Permeability 24

3.2 Basis and Theory of D.C. Resistivity Method 25

3.3 Vertical Electrical Sounding (VES) 29

3.4 Electrode Configuration 30

3.4.1 Schlumberger Array 30

3.4.2 Wenner Array 31

3.5 Preliminary Operations 32

3.5.1 Field procedure 34

3.5.2 Difficulties encountered in the field 36

3.5.3 Precautionary Measures used to overcome the difficulties 37

3.5.4 Data Collection 37

3.6 Instrumentation 38

3.7 IPI2win Model overview 38

3.8 Data Managing 40

CHAPTER FOUR: INTERPRETATION AND GENERAL DISCUSSION OF RESULTS 43

4.1 General Statement 43

4.2 Interpretation 44

4.3 General Discussion of Results 44

4.3.1 Geoelectric Sections along Profiles 48

4.3.2 PROFILE A 52

4.3.3 PROFILE B 52

4.3.4 PROFILE C 55

4.3.5 PROFILE D 55

4.3.6 PROFILE E 55

4.4 Isoresistivity Contour Maps 59

4.5 Depth-to-Bedrock Map 59

4.6 Depth-to-and Thickness of Weathered Basement Maps 66

CHAPTER FIVE: SUMMARY, CONCLUSION AND RECOMMENDATIONS 69

5.1 Summary 69

5.2 Conclusion 69

5.3 Recommendations 71

REFERENCES 72

APPENDIX I VES Curves for the acquired field data 77

APPENDIX II The Results of the interpreted VES Curves 102

LIST OF TABLES

Table 3.1 Resistivities of some Igneous, Metamorphic and Sedimentary Rocks 19

Table 4.1 A borehole Lithology of Paiko obtained from IBB University, Lapai 49

Table 4.2 Typical Resistivity values compiled from previous works 49

Table 4.3 Typical Resistivity values of common rock materials and selected ore minerals 50

Table 4.4 Resistivity values adopted for this work 51

LIST OF FIGURES

Figure 1.1 Map of Niger State showing Paikoro L.G.A. 4

Figure 1.2 Map of Paiko showing the study site 5

Figure 2.1 Geological Map of Nigeria showing the study Area 11

Figure 2.2 Geological Map of Niger State showing the Study Area 13

Figure 3.1 Schlumberger Symmetrical Electrode Array 27

Figure 3.2 Wenner Electrode Array 33

Figure 3.3 Study site showing Profiles and VES points 35

Figure 3.4 ABEM Terrameter (SAS 1000) with other equipment used to carry out the survey 39

Figure 4.1 Curve at VES A4 45

Figure 4.2 Curve at VES A9 45

Figure 4.3 Curve at VES B9 46

Figure 4.4 Curve at VES C5 46

Figure 4.5 Curve at VES D7 47

Figure 4.6 Curve at VES E3 47

Figure 4.7 Geoelectric section along Profile A 53

Figure 4.8 Geoelectric section along Profile B 54

Figure 4.9 Geoelectric section along Profile C 56

Figure 4.10 Geoelectric section along Profile D 57

Figure 4.11 Geoelectric section along Profile E 58

Figure 4.12 Isoresistivity Map at 5.00m depth 60

Figure 4.13 Isoresistivity Map at 15.00m depth 61

Figure 4.14 Isoresistivity Map at 27.00m depth 62

Figure 4.15 Depth to Bedrock Contour Map 64

Figure 4.16 3D Surface plot of the Bedrock 65

Figure 4.17: Depth-to-Weathered Basement Contour map 67

Figure 4.18: Thickness of Weathered Basement Contour map 68

LIST OF APPENDICES

CURVE AT VES A1	77
CURVE AT VES A2	77
CURVE AT VES A3	78
CURVE AT VES A4	78
CURVE AT VES A5	79
CURVE AT VES A6	79
CURVE AT VES A7	80
CURVE AT VES A8	80
CURVE AT VES A9	81
CURVE AT VES A10	81
CURVE AT VES B1	82
CURVE AT VES B2	82
CURVE AT VES B3	83
CURVE AT VES B4	83
CURVE AT VES B5	84
CURVE AT VES B6	84
CURVE AT VES B7	85
CURVE AT VES B8	85
CURVE AT VES B9	86
CURVE AT VES B10	86
CURVE AT VES C1	87

CURVE AT VES C2 87
CURVE AT VES C3 88
CURVE AT VES C4 88
CURVE AT VES C5 89
CURVE AT VES C6 89
CURVE AT VES C7 90
CURVE AT VES C8 90
CURVE AT VES C9 91
CURVE AT VES C10 91
CURVE AT VES D1 92
CURVE AT VES D2 92
CURVE AT VES D3 93
CURVE AT VES D4 93
CURVE AT VES D5 94
CURVE AT VES D6 94
CURVE AT VES D7 95
CURVE AT VES D8 95
CURVE AT VES D9 96
CURVE AT VES D10 96
CURVE AT VES E1 97
CURVE AT VES E2 97
CURVE AT VES E3 98
CURVE AT VES E4 98
CURVE AT VES E5 99

CURVE AT VES E6 99

CURVE AT VES E7 100

CURVE AT VES E8 100

CURVE AT VES E9 101

CURVE AT VES E10 101

ABBREVIATIONS, SYMBOLS AND DEFINITIONS

VES	Vertical Electrical Sounding
m	Metre
Ω	ohms
Ωm	ohm-metre
°	Degree
′	Minute
″	Second
ρ	True resistivity
ρ_a	Apparent resistivity
mV	Millivolt
I	Current
A	Cross sectional area
U	Electric Potential
L	Length
K_f	Geometric factor
MN	Potential electrode separation
AB	Current electrode separation
π	Pi (= 3.1416)
i.e.	That is
et al.	And others
σ	Conductivity

j	Current density
E	Electric field
$\emptyset$	Fractional pore volume (porosity)
ϕ	Adsorption (zeta) potential
S_w	Fraction of the pores containing water
ρ_w	Resistivity of water
kHz	Kilohertz
K_E	Dielectric constant
K_M	Magnetic susceptibility
η	Viscosity
ΔP	Pressure difference
R^1	Gas constant (8.31 joules/°C)
V_t	Voltage
F	Faraday constant (9.65 x 10^4 C/mol)
I_a and I_c	Mobilities of anions and cations reapectively
D_1 and D_2	Solution concentrations
cgs	Centimetre-gramme-second
mks	Metre-Kilogramme-Second
θ	Absolute temperature
n	Valence
μ	Magnetic permeability
F_r	Formation resistivity factor

ρ_s	Resistivity of solution
ρ_r	Resistivity of rock
α	Temperature coefficient of resistivity
V_f	Fractional volume
ρ_h	Resistivity in horizontal direction
ρ_v	Resistivity in vertical direction
E_s	Nernst potential

CHAPTER ONE: INTRODUCTION

1.1 General overview

The use of geophysics for engineering studies and groundwater exploration has increased over the last few years due to rapid advances in computer software and associated numerical modelling solutions. The Vertical Electrical Sounding (VES) has proved very popular with groundwater prospecting and engineering investigations due to simplicity of the technique (Harold and Mooney, 1980). The electrical geophysical survey method is the detection of the surface effects produced by the flow of electric current inside the earth. The electrical techniques have been used in a wide range of geophysical investigations such as mineral exploration, engineering studies, geothermal exploration, archeological investigations and geological mapping. Electrical methods are generally classified according to the energy source involved, i.e., natural or artificial. Thus, self potential (SP) and telluric current come under natural source methods, while resistivity, electromagnetic (EM) and induced polarization (IP) methods are artificial source methods (Kunetz, 1966). The electrical D.C. Resistivity method that has been used in carrying out the present survey is of artificial source using the ABEM terrameter Signal Averaging System (SAS) 1000.

The statistics of failure of town planning and boreholes and even the contamination of groundwater throughout the nation have increased tremendously as a result of no or inadequate geophysical investigations. These have great effects on the environment and particularly on the inhabitants. In some areas, buildings will be choked up without provision for drainage system, proper refuse and sewage disposal, e.t.c. and these can adversely affect the people in such areas. A case study is the borehole at Paiko Central Market that failed after few months, also the

contamination of Minna Central Mosque borehole by a nearby pit latrine (Muhammed *et al*., 2008). Properties worth billions of dollars have been lost in many countries due to structural disasters. Some common structural failures in Nigeria today include the failures of bridges, towers and failures of low and high rise buildings such as National Youth Service Corp (N.Y.S.C.) gymnasium where Man-O-War facilities are kept and even corp members' hostels in orientation camps. Most of these failures were caused by swelling clays (Blyth and Freitas, 1988). Therefore, the developments of new towns as well as N.Y.S.C. orientation camp sites generally require a detailed evaluation of the subsurface of the sites. Subsurface study of a new site is necessary so as to provide subsurface and aerial information that normally assists civil engineers, builders and town planners in the design, planning and siting of foundations of civil engineering structures (Omoyoloye *et al*., 2008). Water is an essential and inevitable commodity in human life. It is needed for agricultural and industrial purposes, domestic uses and for human consumption. Hence, access to clean uncontaminated water in the N.Y.S.C. orientation camps must be taken into consideration. Most of the world surface water is found to be polluted either from anthropogenic activities by man or nature, such as salinity, oil spillage, industrial waste and so on (Olarewaju *et al*., 1996). These factors have necessitated the purification of surface water before consumption or other uses incurring high costs. Hence, this has given rise to exploration of groundwater as alternative source of water supply. Groundwater is found within the pore spaces of soil or rock called the aquifer (Offodile, 1992). The nature of the aquifer is a function of subsurface geological composition that plays an important role in determining the circulation of water from the surface (infiltration) to subsurface water through recharge processes. The composition of aquifer varies between locations, as each location has a unique geological

lithology giving rise to variation in groundwater depth among different places. Detailed knowledge of the aquifer as well as understanding of the aquifer composition is important for optimum groundwater exploration.

Successful groundwater exploration largely depends on the pre-drilling information (survey) because most groundwater explorations fail due to inadequate pre-drilling information (Gomes, 2006). As a result, credence is lent to the development of groundwater in the present study site owing to the lack of any known surface water nearby and around the site. Hence, methods used for locating viable groundwater aquifers and their hydrological conditions should be effective so as to accurately ascertain the groundwater potential at the survey site and geophysical methods particularly the Electrical Resistivity methods are playing a satisfactory role in groundwater investigations. Though the use of geophysics for planning new N.Y.S.C. site, new towns and estates is yet to be fully embraced, this study has shown that the adoption of geophysical studies can aid in appropriate allocation of spaces for residence, high-rise buildings, recreational facilities and buried utilities like underground sewage channels within N.Y.S.C. camps.

1.2 Location of the Study Area

The area under study in Paiko lies between latitude 9°26'59.51"N and 9°27'17.49"N and Longitude 6°38'40.58"E and 6°38'50.01"E. Paiko hosts the Secretariat of Paikoro Local Government Area, of Niger State. It has an estimated population of about 158,086 people and covering a total area of 2,066 km^2 with other small villages, settlements and hamlets (Figure 1.1). It is part of Sheet 185 North-Central Nigeria and is located at about 25 km along Minna-Suleja express way (Figure 1.2). The terrain is relatively flat and accessible by road.

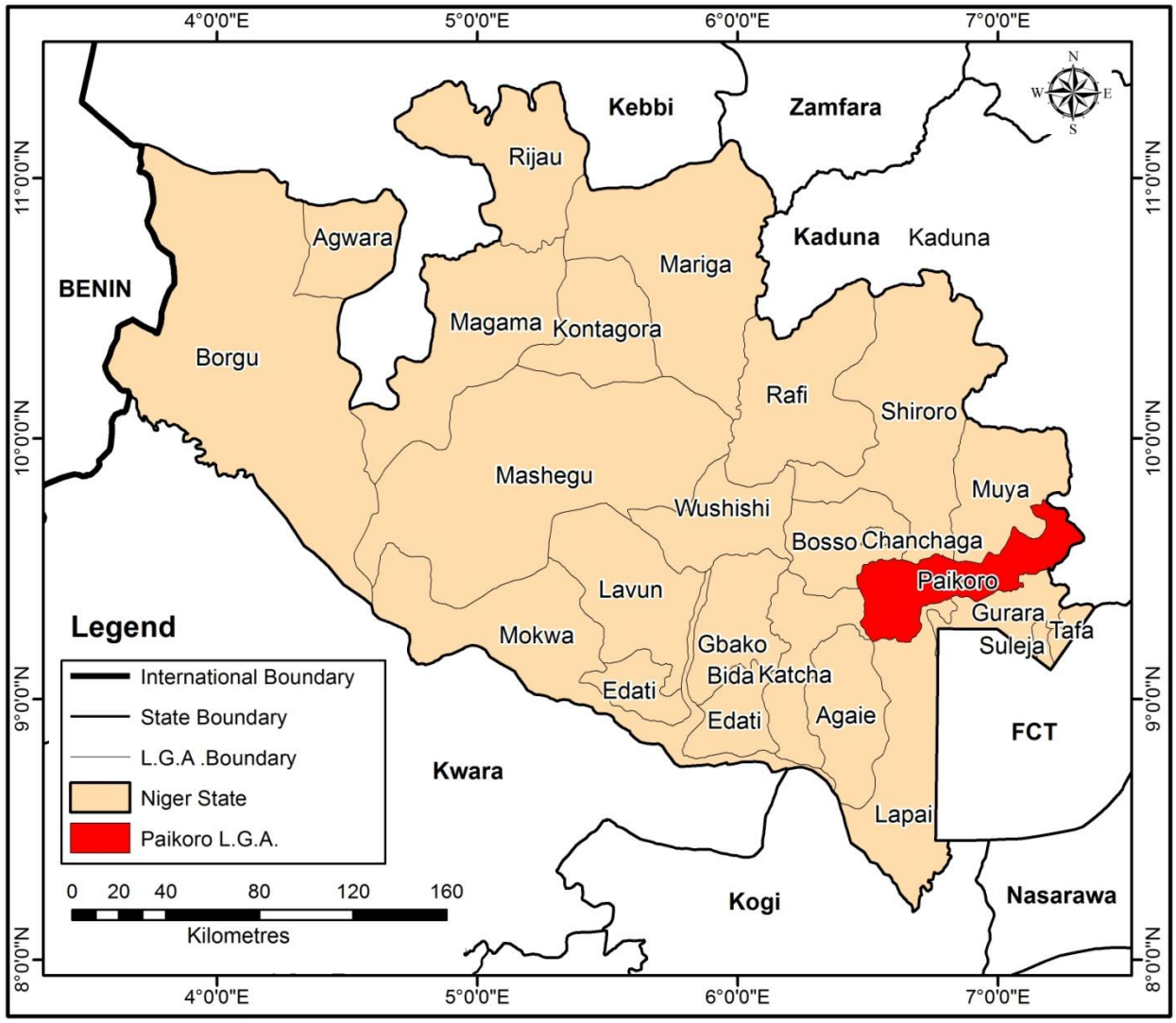

Figure 1.1: Map of Niger State showing Paikoro L.G.A. (Adapted and modified from the administrative Map of Nigeria).

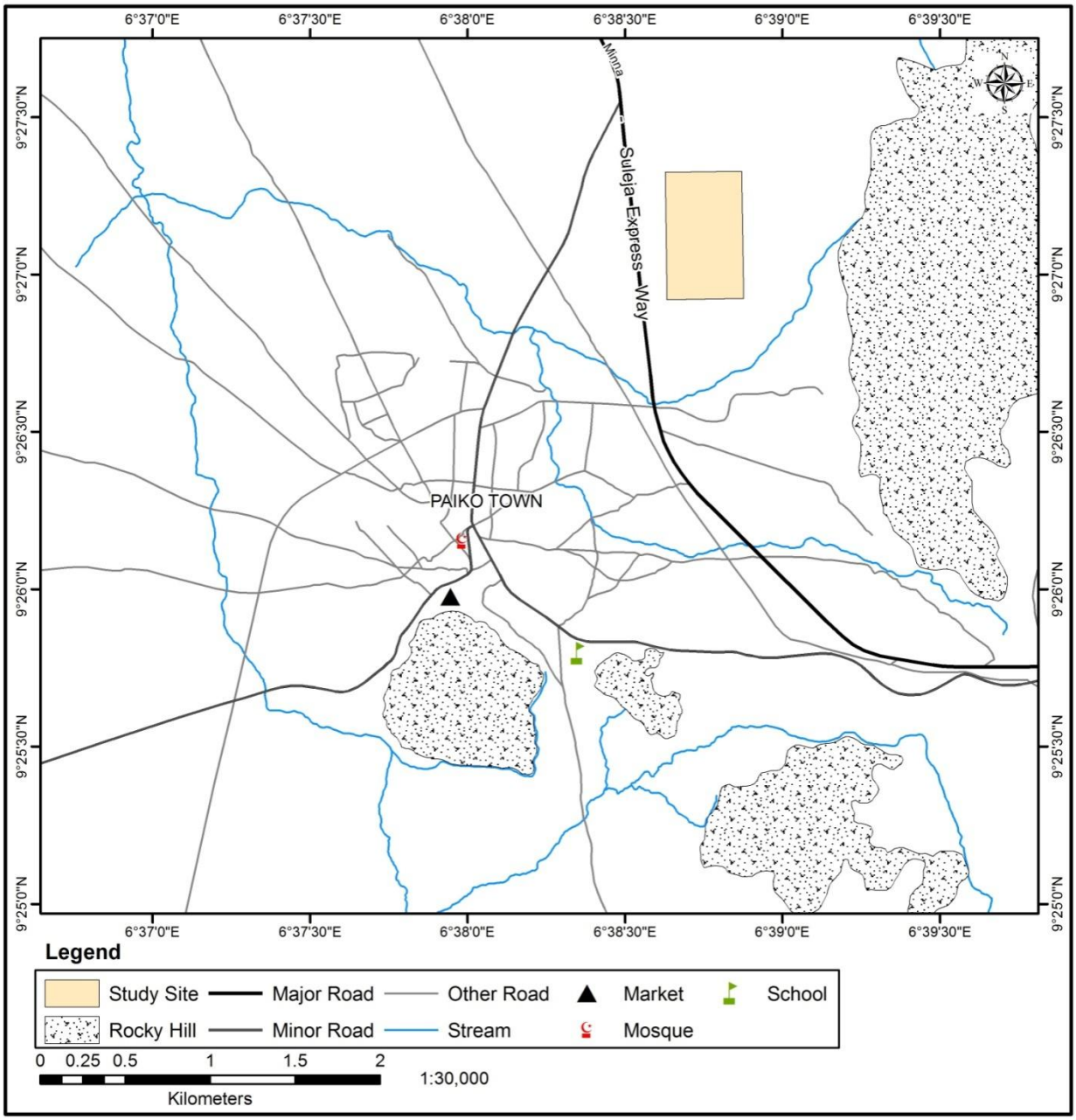

Figure 1.2: Map of Paiko showing the study site (Adapted and modified from Topo Sheet 185 North-Central Nigerian).

1.3 Climate, Relief and Vegetation

The vegetation of the area is that of the Guinea Savannah which comprises various species of shrubs and high forest plants (Ajibade and Woakes, 1976).This area is characterized by tall grasses of height 1.0 m to 1.5 m, sparsely distributed trees of up to 15.0 m high in the dry season and evenly distributed trees in the wet (rainy) season. The area lies within North-Central part of Nigeria. The annual rainfall distribution pattern shows a maximum of 1300 mm rainfall and minimum of 900–1000 mm (McCurry, 1976). The rainy season is between April and October covering a period of six months. Temperature is highest in March at about 30^0C and lowest in August at about 25^0C (Ajibade *et al*., 1983). The topography of the study area is marked by high and flat terrain, with most of the highlands visible around the vicinity of the area. Generally, the fertile soil and hydrology of the area permit the cultivation of most Nigeria's staple crops and still allows sufficient opportunities for grazing, fresh water fishing and forestry development.

1.4 Aim and Objectives of the Survey

The present survey is aimed at determining the depth to bedrock and the thickness of the weathered basement distribution in the area.

The specific research objectives include:

- Identifying strategic areas for siting high-rise buildings;
- Potential positions for the location of boreholes and
- Possible depth of sewage system that will avoid groundwater contamination.

1.5 Justification

The study area is situated on the Basement Complex of North-Central Nigeria with variable overburden thicknesses. Owing to the fixed nature and small size of the site, it is expected that with the large number of corp members, being deployed to Niger State, the erection of buildings need to be embarked upon in order to provide sufficient accommodation for corp members, N.Y.S.C. staff as well as the military training personnel. There is therefore, the need to provide information on the subsurface sequence and structural disposition necessary for the buildings. Detailed geophysical investigation will provide such information. Again, as there is no surface water near the site (Figure 1.2), it becomes imperative to locate suitable areas for tapping groundwater by siting boreholes to provide sufficient and safe water for domestic uses. This, no doubt will help avert acute shortage of water in the N.Y.S.C. orientation camp. However, it is important to know the depth to aquifer especially when constructing sewage system in order to avoid groundwater contamination. The need to ascertain the degree of the overburden protective capacity which overlies the aquifer units is also imperative, hence this called for detailed geophysical investigations on the site.

CHAPTER TWO: LITERATURE REVIEW

2.1 Some Previous Works in the Study Area

Amadi *et al*. (2013) carried out a geophysical investigation of groundwater in parts of Paiko, Sheet 185, North-Central Nigeria. They concluded that the geoelectric sections generated from the geoelectric logs indicated that three major layers exist in Paiko basement rocks at various depths. The topmost layer is the unconsolidated topsoil with resistivity value ranging from 8-710 Ωm and depth from 0.9-3.5 m. The topmost layer is underlain by a slightly weathered/fractured basement with resistivity values ranging from 70-910 Ωm and thickness of 1.6-29.0 m. The last layer is the fresh basement unit with resistivity value ranging between 900-2800 Ωm extending to a fairly infinite depth. Their study has also revealed that the fractures in the study area are discrete, localized and discontinuous.

Ishaku *et al*. (2013) in their Vertical Electrical Sounding investigations of aquifer composition and its potential to yield groundwater in some selected towns in Bida Basin of North Central Nigeria have stated that there are five geoelectric layers in the study area namely: top layer, Clay/sand, Clay, Sandstone and Sandy Clay layers. The groundwater bearing layer varies between 32–50 m in thicknesses across their study area corresponding to the fourth layer (i.e. the Sandstone layer).

Bello and Makinde (2007) have carried out a geophysical study using the Vertical Electrical Sounding (VES) techniques to investigate the subsurface layering in the southwestern part of the Niger Basin in order to determine the nature, characteristics and spatial extent of the components of the aquifer underlying the region. The results of their interpreted VES data indicated three to five layers. The geologic sections suggested that the alluvial deposits of sand, sandy clay, medium to coarse grain sandstones, as well as the weathered and fractured basement constitute

the aquifer. Furthermore the results of the interpretation of the VES data indicated that the thickness values of the aquifer vary from 6.01 m to 58.60 m. The geoelectric section generated also suggest that the resistivity values of the aquifer components range from 4 Ωm to 107 Ωm for the alluvial deposits; 34 Ωm to 109 Ωm (weathered basement); and 346 Ωm to 564 Ωm for the fractured basement rocks.

Muhammed *et al*. (2008) carried out hydrogeophysical investigation aimed at delineating the aquiferous units in the central part of Minna by determining their depths, thicknesses, resistivities and the potential borehole depth at various locations within the area employing the Vertical Electrical Sounding (VES) technique using the Schlumberger array. They found that the area was underlain by four geological formations and the aquiferous unit have resistivity value of 120 – 900 Ωm and an average thickness of 25 m – 30 m.

Okoye *et al*. (2011) evaluated the groundwater potential of Pompo village in the neighborhood of Gidan Kwano Campus of Federal University of Technology, Minna, using Vertical Electrical Resistivity Sounding. A total of 12 Vertical Electrical Soundings (VES) were carried out. The Vertical Electrical Sounding curves revealed that the area is generally characterized by five geo-electric layers. The top soil layer is a highly resistive layer with thickness ranging from 0.3 m to 1.6 m. The second geoelectric layer is a resistive dry layer with thickness ranging from 0.9m to 4.3 m. The weathered basement layer thickness varies from 0.9 m to 9.1 m. The fractured basement ranges from 2.1 m to 16.4 m in thickness, while the depth to fresh basement varies between 4.9 m and 25.3 m. Out of the 12 VES carried out, 5 VES stations were found as the most viable locations for the development of groundwater resources.

2.2 General Geology of the Study Area

The study area is within the north-central portion of the Nigerian Basement Complex rocks (Figure 2.1). This Basement Complex is characterized by three lithofacies: The Migmatite-Gneiss Complex, The Schist Belt and The Older Granite (Olarewaju *et al*., 1996; Olasehinde, 1999):

The Migmatite-Gneiss Complex is the oldest basement rock and the commonest rock type in the Nigerian Basement complex. It comprises two main types of gneisses: the biotite gneiss and the banded gneiss. Very widespread, the biotite gneisses are normally fine-grained with strong foliation caused by the parallel arrangement of alternating dark and light minerals. The banded gneisses show alternating light-coloured and dark bands and exhibit intricate folding of their bands.

Rocks of the schist belts occur predominantly in the Western half of Nigeria. Their lithologic composition ranges from schists through phyllites to pelitic, semi-pelitic, and psammatic rocks as well as marble, quartzite and amphibolite (Obaje *et al*., 2006). The Schist belts fall into two age groups: The earlier group contains assemblages of mafic igneous rocks, pelitic schists and phyllites, banded iron formation and, locally, coarse grained clastics and carbonate rocks. These belts show complex structural styles and are extensively intruded by granitic plutons belonging to the widely distributed Pan-African magmatic suite. The latter group of schist belts is characterized by coarsed to fine grained clastics and mafic igneous rocks.

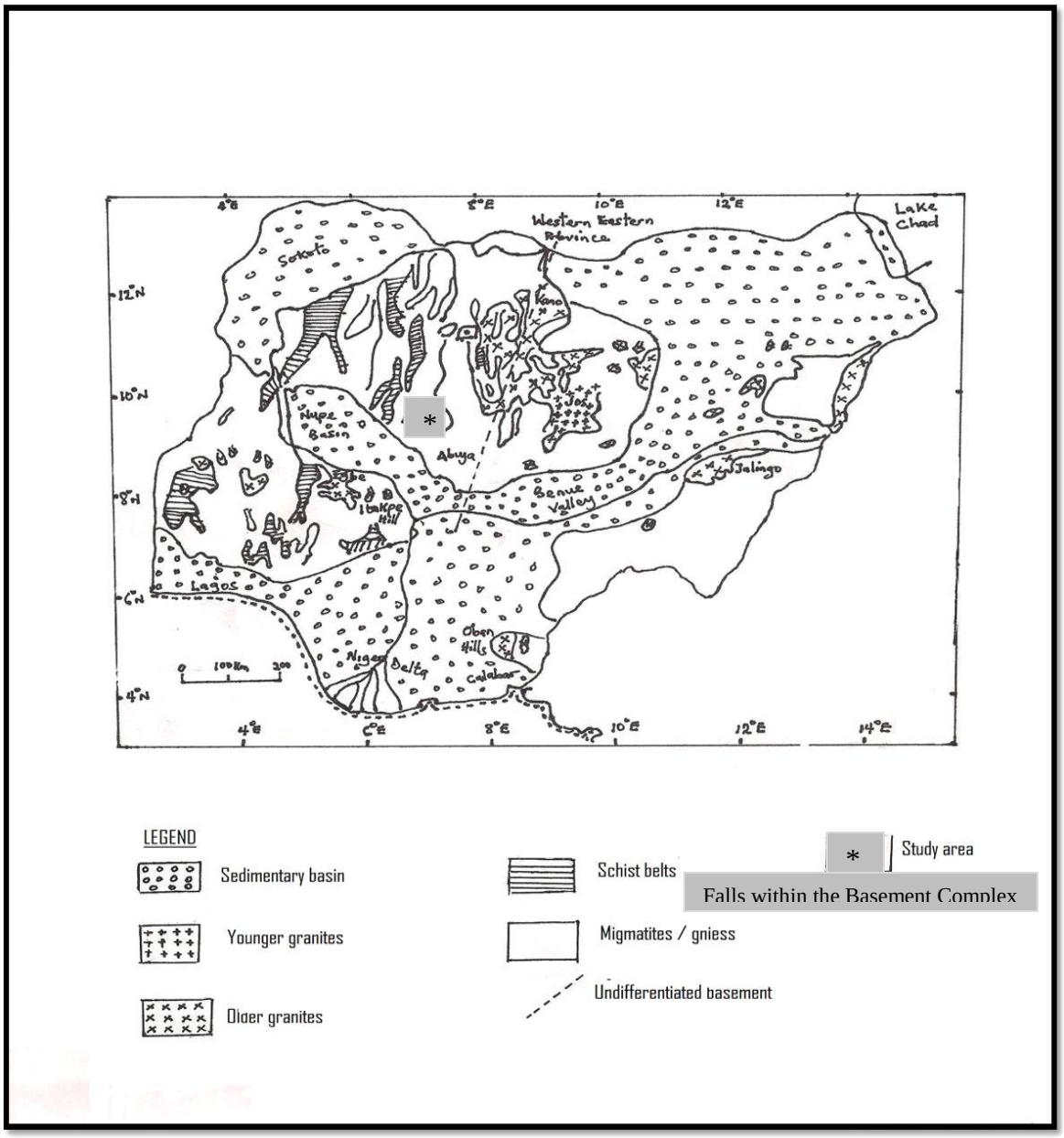

Figure 2.1: Geological Map of Nigeria showing the Study Area (Adapted and modified from the Geological Map of Nigeria, Ajibade *et al*., 1983).

The Older Granites are widespread throughout the Basement Complex and occur as large circular masses within the schists and the migmatite - gneiss complex. The older granite series comprises mainly granite, granodiorites, diorites, charnokitic rocks and gabbros which intruded during the Pan-African Orogenic Cycle and formed part of the Precambian Basement Complex. The study area, Paiko, consists predominantly of medium to coarse-grained biotite granite and granodiorites which varies from light coloured to medium dark coloured (Kogbe, 1976) as shown in (Figure 2.2). The granite types and the granodiorite together form part of the Older Granite (Rahaman, 1988). Peculiar to the area, is outcropping at different sizes, shapes and locations with noticeable fractures and joints.

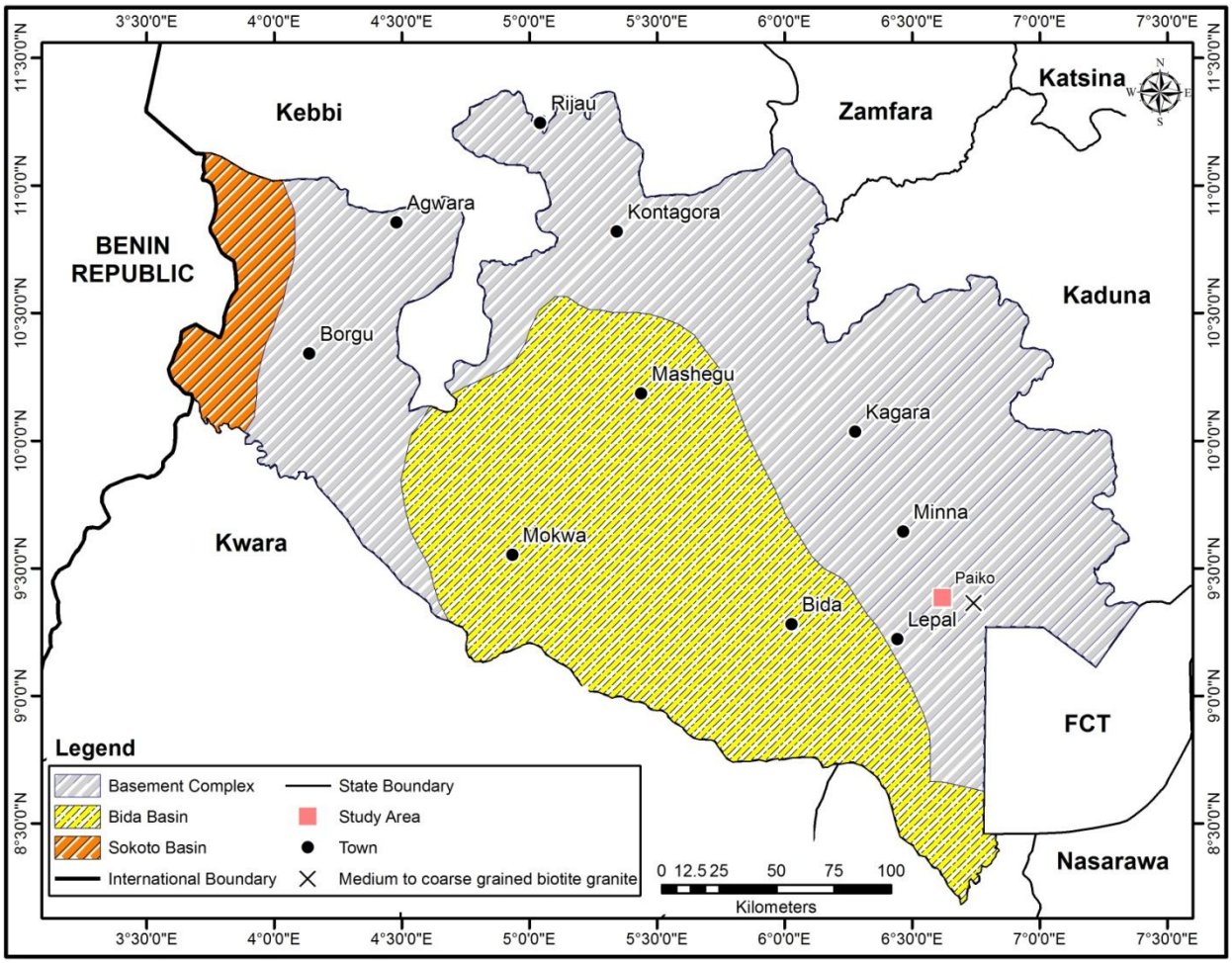

Figure 2.2: Geological Map of Niger State showing the Study Area (Adapted and modified from Niger State Geological Map).

CHAPTER THREE: MATERIALS AND METHODOLOGY

3.1 Fieldwork Planning

The fieldwork was accomplished between 5th of March and 12th of March, 2014 during the dry season. This period was chosen for the field work because during the dry season, the geologic materials (aquifer) are in their natural state.

3.1.1 Choice of Electrode Configuration

The choice of layout with its dimension largely depends upon the target; its size, depth and resistivity contrast with its surrounding. In order to achieve the aim and objectives of this work, Schlumberger electrode layout was employed based on the following reasons:

- The smaller separation of the potential electrodes reduces noise due to ground current (from industrial and telluric sources) which may limit the useful depth of penetration.
- Its ease of operation, relatively low cost and its capacity of greater depth penetration than Wenner electrode layout.

3.1.2 Resistivity Values of rocks and minerals

Of all the physical properties of rocks and minerals, electrical resistivity shows the greatest variation (Telford *et al*., 1976). While the range in density, elastic wave velocity and radioactive content is quite small, in magnetic susceptibility it may be as large as 10^5. However, the resistivity of metallic minerals may be as small as $10^{-5}\Omega$m. Those of dry, close grained rocks like gabbro are as large as $10^7\Omega$m. The maximum possible range is even greater, from native silver ($1.6 \times 10^{-8}\Omega$m) to pure sulphur ($10^{16}\Omega$m).

The following geological and hydrogeological factors affect the resistivity of rocks and minerals:

1. Mineral composition: The common rock-forming minerals such as silicates, phosphates, carbonates, nitrates, sulphates, quartz, e.t.c., are poor conductors with resistivity greater than

$10^7\Omega$m. The variation in the resistivity of minerals is quite large. Minerals like pyrrhotite and graphite are consistently good conductors while pyrite, galena and magnetite are poor conductors in bulk form, although the individual crystals have high conductivity. Hematites and sphalerite, in pure form, are practically insulators, but when combined with impurities may have resistivities as low as 0.1Ωm. Graphite is often the connecting link in mineral zones which makes them good conductors.

Igneous rocks have the highest resistivity, sedimentary the lowest, with metamorphic rocks intermediate. However, there is considerable overlapping, as in other physical properties. In addition, the resistivities of particular rock types vary directly with age and lithology, since the porosity of the rock and salinity of the contained water are affected by both. For example, the resistivity range of Precambrian volcanics is 200 - 5000Ωm, while for Quaternary rocks of the same kind; it is 10 - 200Ωm.

2. Porosity and degree of water saturation: The resistivity of subsurface rock is greatly affected by the presence of groundwater. The minerals which form the matrix of a rock are generally poorer conductors than the groundwater and hence the effective resistivity of the rock is decreased by the groundwater. Hence, a small change in the percentage of the water content affects the resistivity of the earth materials significantly. Increasing the amount of water decreases the resistivity of a water-bearing rock.

Porosity can be defined as the percentage of voids to the total volume of the rock. It is measured as a percentage and has the symbol ∅, i.e.

$$\text{Porosity } (\emptyset) = \frac{\text{volume of pores}}{\text{total volume of rock}} \text{ X } 100\ \% \qquad (3.1)$$

Porosity arises from the fact that the particles do not occupy all the possible spaces. It provides a direct measure of the total void space available for the storage of fluid. Resistivity and porosity

in sedimentary rocks can be related by the general form of Archie's law, which for rocks devoid of clay is written as,

$$F_r = \frac{a}{\emptyset^m} = \frac{\rho_r}{\rho_s} \quad (3.2)$$

where F_r is the formation resistivity factor, ρ_r is the resistivity of the rock , ρ_s is the resistivity of the solution in the pores of the rock, $\emptyset$ is the porosity, while ''a'' and ''m'' are constants peculiar to the rock type. The constant 'm' is usually referred to as the cementation exponent while the constant 'a' is referred to as the tortuosity factor.

Igneous and Metamorphic rocks usually have low porosity unless they are fractured while sedimentary rocks usually have high porosity and the higher the rock porosity, the lower the rock resistivity.

3. Water salinity: Conduction in near-surface rocks is largely electrolytic, taking place in connected pore spaces, along grain boundaries, in fractures, faults and shear zones but negligible through the silicate framework. The ions which conduct the current result from the dissociation of salts, such dissociation occurring when salts are dissolved in water. Since each ion is able to carry only a definite quantity of charge, it follows that the more ions are available in a solution, the greater will be the charge that can be carried. Hence, the solution with the larger number of ions will have the higher conductivity. In general, for a given porosity, a rock which contains saline water within its pore will have a greater conductivity when the salinity of the water is high than when it is low. Resistivity decreases with increase in salinity.

4. Temperature effect: Extreme temperature ranges greatly affect the resistivity of water bearing rocks. Particularly if the temperature is high enough to expel the water in the rock as steam or low enough to freeze the water. At moderate temperature, rock resistivity usually decreases with

increasing temperature, i.e., rocks have negative temperature coefficient of resistivity. Metals have positive temperature coefficient i.e their resistivity increases with increasing temperature.

An increase in temperature lowers the viscosity of water, with the result that ions in the water become more mobile. The increased mobility results in an observed resistivity decrease with increase in temperature according to the formula (Keller and Frischknecht, 1966):

$$\rho_r = \frac{\rho_{18^\circ C}}{1+\alpha\,(t-18)} \qquad (3.3)$$

where ρ_r is the resistivity at that temperature, ρ_{18} is the resistivity at 18^0C, α is the temperature coefficient of resistivity (about 0.025 per degree centigrade) and t is the ambient temperature.

5. Effects of Geologic Processes

In general, geological processes reduce the resistivity of a rock but there are exceptions. Weathering or hydrothermal alteration of granite significantly lowers its resistivity. Dissolution, faulting and shearing usually increase porosity and fluid permeability, and hence lower resistivity. Precipitation of calcium carbonate and silica reduces porosity and hence reduces fluid permeability and increases resistivity.

6. Structure and texture of rocks: Well sorted rocks usually have high resistivities while poorly sorted rocks usually have low resistivities. The texture of a rock also affects its resistivity. Usually the finer the rock grain size the lower the resistivity.

The geometrical arrangement of the interstices in the rock has less pronounced effect, but may make the resistivity anisotropic, that is, having different magnitudes for current flow in different directions. Anisotropy is the characteristic of stratified rock which is generally more conductive in the bedding plane. The anisotropy coefficient, which is the ratio of the maximum to minimum resistivity, may be as large as two (2) in some graphitic slates and varies from 1 to 1.2 in some rocks such as limestone, shale and rhyolite.

As an example, in considering a layered formation, having resistivities ρ_1 and ρ_2 whose respective fractional volumes are V_f and $1 - V_f$. Here the resistivity in the horizontal direction – a stack of beds effectively in parallel is

$$\rho_h = \frac{\rho_1 \rho_2}{\{\rho_1(1-Vf) + \rho_2 Vf\}} \quad ; \qquad (3.4)$$

In vertical direction, the beds are in series so that

$$\rho_v = \rho_1 V_f + \rho_2(1 - V_f). \qquad (3.5)$$

Then the ratio is

$$\frac{\rho_v}{\rho_h} = (1 - 2\,V_f + 2\,V_f^{\,2}) + \left(\frac{\rho_1}{\rho_2} + \frac{\rho_2}{\rho_1}\right) V_f\,(1 - V_f). \qquad (3.6)$$

If V_f is much less than 1 and $\frac{\rho_2}{\rho_1}$ is much greater than 1, this simplifies to

$$\frac{\rho_v}{\rho_h} \approx 1 + \left(\frac{\rho_2}{\rho_1}\right) V_f \qquad (3.7)$$

If the layer of the resistivity ρ_1, is for water- saturated beds, this ratio might be quite large.

Table 3.1 shows the resistivity values of the rock types in Basement Complex areas compiled from (Telford *et al.*, 1976).

TABLE 3.1: RESISTIVITIES OF SOME IGNEOUS, METAMORPHIC AND SEDIMENTARY ROCKS (Telford *et al*., 1976).

Rock type	**Resistivity range (ohm-metre)**
Granite	$3 \times 10^2 - 10^4$
Granite porphyry	4.5×10^3 (wet) – 10^4 (dry)
Gneiss (various)	6.8×10^4 (wet) – 3×10^4 (dry)
Sandstones	$1 – 6.4 \times 10^8$
Argillites	$10 – 8 \times 10^2$
Unconsolidated wet clay	20
Clays	1 – 100
Alluvium and Sands	10 – 800

3.1.3 Electrical Properties of Earth materials and Parameters

The electrical parameters of properties of rocks and minerals exploited in the electrical prospecting are: electrical conductivity or its inverse electrical resistivity, natural electrical potentials dielectric constant and magnetic permeability.

The most important of these parameters is the conductivity. Electrical current flow in earth's material is determined to a large extent by the medium's resistivity and to a lesser extent by the dielectric constant magnetic permeability.

3.1.3.1 Electrical Conductivity

Electric current may be propagated in rocks and minerals in three ways: electronic (ohmic) conduction, electrolytic (ionic) conduction and dielectric conduction. The first is the normal type of current flow in materials containing free electrons, such as the metals. In an electrolyte the current is carried by ions at a comparatively slow rate. Dielectric conduction takes place in poor conductors or insulators, which have very few free carriers or none at all (Telford *et al*., 1990). Under the influence of an external varying electric field, the atomic electrons are displaced slightly with respect to their nuclei; this slight relative separation of negative and positive charges is known as dielectric polarization of the material. Ionic and molecular polarization may occur in materials with ionic and molecular bonds respectively. In all these cases dielectric conduction is the result of changing electronic, ionic or molecular polarization caused by the alternating electric field.

1. Electronic Conduction: The electrical resistivity of a cylindrical solid of length *L* and cross-sectional area *A*, having resistance *R* between the end faces, is given by

$$\rho = \frac{RA}{L} \qquad (3.8)$$

If A is in metres^2, L in metres and R in ohms, the resistivity unit is the ohm-metre (Ωm). The resistance R is given in terms of the voltage V_t applied across the ends of the cylinder and the resultant current I flowing through it, by Ohm's law as:

$$R = \frac{Vt}{I} \qquad (3.9)$$

where R is in ohms and the units of V_t and I are volts and amperes respectively.

The reciprocal of resistivity is the conductivity σ, the units $(\Omega m)^{-1}$.

$$\sigma = \frac{1}{\rho} = \frac{L}{RA} = \frac{IL}{AV} = \frac{j}{E} \qquad (3.10)$$

where j = current density (amperes/m^2), E = electric field (volts/m).

2. Electrolytic Conduction**:** Since most rocks are poor conductors, their resistivities would be extremely large if not for the fact that they are usually porous and the pores are filled with fluid, mainly water. As a result the rocks are electrolytic conductors, whose effective resistivity may be defined as,

$$\rho = \frac{RA}{L} \qquad (3.11)$$

But it must be kept in mind that the conduction is electrolytic rather than ohmic. That is, the propagation of current is by ionic conduction- by molecules having an excess or deficiency of electrons. Hence the resistivity varies with the mobility, concentration and degree of dissociation of the ions; the latter depends on the dielectric constant of the solvent. As mentioned previously the current flow is slow compared to ohmic conduction and the movement represents an actual transport of material, usually resulting in chemical transformation.

The conductivity of a porous rock varies with the volume and arrangement of the pores and even more with the conductivity and amount of contained water. According to the empirical formula due to Archie (1942),

$$\rho = a\emptyset^{-m} S_w^{-n} \rho_w \quad (3.12)$$

where $\emptyset$ = fractional pore volume (porosity), S_w = fraction of the pores containing water, ρ_w = resistivity of water, n is valence and ≈ 2, *a* and m = constants, $0.5 \leq a \leq 2.5$, $1.3 \leq m \leq 2.5$.

Water conductivity varies considerably in the range of 0.05 to 3 x $10^3(\Omega m)^{-1}$, depending on the amount and conductivity of dissolved chlorides, sulphates and other minerals present.

Electronic conduction mechanisms are more important than the electrolytic conduction mechanisms through pore water in the following three cases (Telford *et al*., 1976);

i. In rocks containing a high percentage of conducting minerals such as magnetite, graphite or pyrrhotite.

ii. In rocks which are completely frozen.

iii. In rocks which lie sufficiently deep in the earth so that all the pore spaces are closed by overburden pressure.

3. Dielectric Conduction: The displacement current flows in non-conductors when the external electric field changes with time. The significant parameter in dielectric conduction is the dielectric constant, K_E, sometimes called the specific inductive capacity of the medium.

The dielectric constant is similar to the conductivity in porous formations in that it varies with the amount of water present (water has a very large dielectric constant at low frequency).

3.1.3.2 Electrical potentials

Certain natural or spontaneous potentials occurring in the subsurface are caused by electrochemical or mechanical activity. The controlling factor in all cases is the underground water. These potentials are associated with weathering of sulphide mineral bodies, variation in rock properties (mineral content) at geologic contacts, bioelectric activity of organic material, corrosion, thermal and pressure gradients in underground fluids and other phenomena of similar

nature. There are four principal mechanisms producing these potentials; the first is mechanical, the latter three chemical, in origin.

1. Electrokinetic potential**:** It is also known as streaming potential, this is a well known effect observed when a solution of electrical resistivity ρ and viscosity η is forced through a capillary or porous medium. The resultant potential difference between the ends is;

$$E_k = \frac{-\phi \Delta P K_E \rho}{(4\pi\eta)} \qquad (3.13)$$

where ϕ = adsorption (zeta) potential, ΔP = pressure difference, K_E = solution dielectric constant. The quantity ϕ is the potential of a double layer (solid-liquid) between the solid and solution. Although, generally of minor importance, the streaming effect may be the cause of occasional large anomalies associated with topography. It is also observed in self-potential well logging, where the drilling fluid penetrates porous formations.

2. Liquid junction (diffusion) potential**:** This is due to the difference in mobilities of various ions in solutions of different concentrations. The value is given by

$$E_d = \frac{-R^1\theta(Ia - Ic)}{\{Fn(Ia + Ic)\ log\ (D_1/D_2)\}} \qquad (3.14)$$

where E_d is in millivolts, R^1 = gas constant (8.31 joules/°C), F = Faraday constant (9.65 x 10^4 C/mol), θ = absolute temperature, n = valence, I_a and I_c = mobilities of anions and cations respectively, D_1 and D_2 = solution concentrations.

3. Shale (Nernst) potential: When two identical metal electrodes are immersed in homogeneous solution, there is no potential difference between them. If, however, the concentrations at the two electrodes are different, there is a potential difference given by;

$$E_s = \frac{R\theta}{Fn\ log\ (D1/D2)} \qquad (3.15)$$

where E_s *is* in millivolts.

The combined diffusion and Nernst potentials are known as the electrochemical or static, self-potential.

4. Mineralization potential: When two dissimilar metal electrodes are immersed in a homogeneous solution, a potential difference exists between the electrodes (Telford *et al*., 1990). This electrolytic contact potential, along with the static self-potential, is undoubtedly among the basic causes of the large potentials associated with certain mineral zones and known as mineralization potentials. These potentials, which are especially pronounced in zone containing sulphides, graphite and magnetite, are much larger than those containing alunite and spalerite. Values of several hundred millivolts are common and potentials greater than one volt has been observed in zones of graphite and alunite. Because of the large magnitude, mineralization potentials cannot be attributed solely to the electrochemical potentials earlier. The presence of metallic conductors in appreciable concentrations appears to be necessary condition; nevertheless, the exact mechanism is not entirely clear.

3.1.3.3 Magnetic permeability

This property of earth materials has only a slight effect on the electrical measurement except there is a large fraction of a ferromagnetic materials (concentrated magnetite, pyrrhotite and ilmenite) present. Magnetic permeability μ is related to magnetic susceptibility K_m by the following relations;

$\mu^1 = 1 + 4\pi K^1_m$ in cgs units, *(3.16)*

$\mu = 1 + K_m$ in SI units. *(3.17)*

Generally, magnetic susceptibility K_m is very small so that the above ratio is not appreciably different from unity.

3.2 Basis and Theory of D.C. Resistivity Method

The electrical properties of earth materials, consolidated or unconsolidated vary greatly. The factors upon which the electrical resistivity of earth materials depend includes, rock porosity, temperature, rock textures, and rock type. Various types of unconsolidated material differ significantly in voids and contain fluids. The general basis of the electrical method of geophysical prospecting is the detection of surface effects produced by the flow of electric current inside the earth. However, the basis of the resistivity method is that, when current is driven into the earth, any variation of the subsurface resistivity will alter the current flow which will in turn affect the distribution of electrical potential (Telford et al., 1990).

The electrical resistivity method is the measurement of an earth resistance by passing low frequency current into the ground through two metal stakes or electrodes and measuring the potential difference resulting across another two electrodes. If the distance between the four electrodes is known then, this together with the current and electrical potential measurements may be used to calculate a 'resistivity' value of the earth (Reynolds, 2003). All resistivity methods employ an artificial source of current, which is introduced into the ground through point electrodes or long line contacts (Telford *et al*., 1990).

The resistivity of rocks usually depends upon the amount of groundwater present and upon the amount of salt dissolved in it. It decreases by the presence of many ore minerals and by high temperature (Aftab and Alan, 2000). Conduction of electricity through rocks is of three types; electronic conduction which occurs when the mineral grains are electrically conductive as with minerals such as pyrite, and magnetite. Most common mineral grains such as quartz, feldspar and calcite, however, are non- conductive and in rocks composed only of these, conduction is ionic or through ions in the interstitial fluid. The third type of current conduction is dielectric

conduction which occurs in poor conductors or insulators having very few charge carriers or even none. The main uses of resistivity surveying are for mapping the presence of rocks of different porosities, particularly in connection with hydrogeology for detecting aquifers and contamination, and for mineral prospecting. But other uses include archaeological surveying, investigating saline and other types of pollution.

Schlumberger array (Figure 3.1), was used for the survey. C_1 and C_2 are current electrodes through which current is driven into the ground via points A and B, while P_1 and P_2 are two potential electrodes positioned at points M and N to record the potential distribution in the subsurface within the two current electrodes.

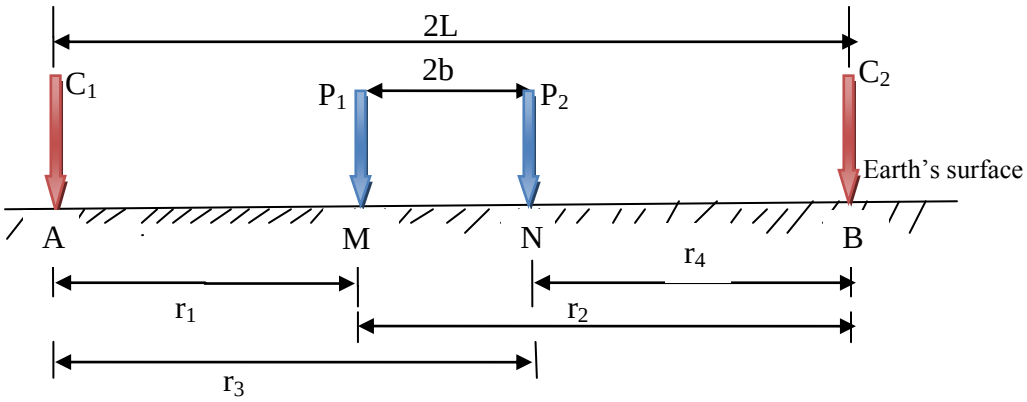

Figure 3.1: Schlumberger symmetrical Electrode Array.

where C_1 is the Current electrode at point A

C_2 is the Current electrode at point B

P_1 is the Potential electrode at point M

P_2 is the Potential electrode at point N

From Ohm's law, the current I and electric potential U in a metal conductor at constant temperature is related as follows:

$$U = IR \tag{3.18}$$

where R is the constant of proportionality termed resistance and it is measured in ohms. The resistance R, of a conductor is related to its length L and cross sectional area A by;

$$R = \frac{\rho L}{A} \tag{3.19}$$

where ρ is the resistivity and it is a property of the material considered. From equations (3.18) and (3.19),

$$U = \frac{I\rho L}{A} \tag{3.20}$$

Schlumberger array involves fixing the potential electrodes at points M and N, and symmetrically increasing the current electrode separation AB about the centre by displacing A and B outwardly in steps. This will increase the depth of penetration within the separation AB. Thus the varying resistivity measured when electrode array position is varied in an inhomogeneous medium is termed apparent resistivity.

For simple treatment, a semi-infinite solid with uniform resistivity, ρ, is considered. A potential gradient is measured between M and N when current electrodes located on the surface of the equipotential surface is semi-spherical downwards into the ground at each electrode. The surface area will then be $2\pi L^2$, where L is the radius of the sphere. Thus, from equation (3.20),

$$U = \frac{I\rho}{2\pi L} \tag{3.21}$$

By deduction then, the potential at M (U_M), due to the two current electrodes, is

$$U_M = \frac{I\rho}{2\pi}\left(\frac{1}{r_1} - \frac{1}{r_2}\right) \tag{3.22}$$

Similarly, the potential at electrode N (U_N) is given by

$$U_N = \frac{I\rho}{2\pi}\left(\frac{1}{r_3} - \frac{1}{r_4}\right) \quad (3.23)$$

where r_1, r_2, r_3 and r_4 are the inter-electrode distances as shown in (Figure 3.1).

The electric potential difference, ΔU, across electrodes M and N is given by:

$$\Delta U = U_M - U_N = \frac{I\rho}{2\pi}\left[\left(\frac{1}{r_1} - \frac{1}{r_2}\right) - \left(\frac{1}{r_3} - \frac{1}{r_4}\right)\right] \quad (3.24)$$

If the body is inhomogeneous like the study area, apparent resistivity (ρ_a) is considered,

$$\rho_a = \frac{\Delta U}{I}\left[\frac{2\pi}{\left(\frac{1}{r_1} - \frac{1}{r_2}\right) - \left(\frac{1}{r_3} - \frac{1}{r_4}\right)}\right] \quad (3.25)$$

where ρ_a is apparent resistivity in ohm-metre, and

$$K_f = \left[\frac{2\pi}{\left(\frac{1}{r_1} - \frac{1}{r_2}\right) - \left(\frac{1}{r_3} - \frac{1}{r_4}\right)}\right] \quad (3.26)$$

From equation (3.25) and (3.26), apparent resistivity ρ_a is given by,

$$\rho_a = \left(\frac{\Delta U}{I}\right)K_f \quad (3.27)$$

K_f is called the geometric factor which has to do with electrode geometry and whose value depends on the type of electrode array used. For Schlumberger symmetrical array, if MN = 2b and $\frac{AB}{2}$ = L then,

$$K_f = \pi\left(\frac{L^2}{2b} - \frac{b}{2}\right) \quad (3.28)$$

3.3 Vertical Electrical Sounding (VES)

Vertical Electrical Sounding (VES) is a geoelectrical common method to measure vertical variations of electrical resistivity (Kelly, 1993). The Vertical Electrical Sounding (VES) is also called depth sounding or sometimes electrical drilling. Its goal is to determine the variation of

resistivity with depth. Schlumberger configuration is most commonly used for VES. The mid-point of the array is kept fixed while the distance between the current electrodes is progressively increased symmetrically. This causes the current flow lines to penetrate to a great depth depending on the vertical distribution of conductivity.

3.4 Electrode configuration

An electrode configuration is an array of electrodes used for measuring either an electric current or voltage. Some electrode arrays can operate in a bidirectional fashion, in that they can also be used to provide a stimulating pattern of electric current or voltage. Many electrode spreads have been used in resistivity studies at various times. In principle, it is not necessary to use a collinear array but in practice, the electrodes are almost always in line, otherwise interpretation of result becomes difficult and the field work is complicated. The various electrode configuration used in electrical resistivity investigation includes Schlumberger, Wenner, Double-dipole, and Pole-dipole. However, for practical purposes, the most common are the Schlumberger and the Wenner.

3.4.1 Schlumberger Array

In the Schlumberger electrode configuration (Figure 3.1), though the current and potential electrodes have a common mid-point, the current electrodes are spaced much further apart than the potential electrodes. 'C_1' and 'C_2' represent the current electrodes through which the current is introduced into the ground at points A and B. P_1 at point 'M' and P_2 at point 'N' represent the potential electrodes across which the potential caused by the current flow is measured. For vertical electrical sounding, the field procedure involves the expansion of the current electrodes C_1 and C_2 at points 'A' and 'B' while keeping the potential electrodes P_1 and P_2 at points 'M' and 'N' considerably constant. That is to say, it is only the current electrodes that are essentially

moved. This is actually the case for Schlumberger array. However, for large values of current electrode spacing 2L, it may be necessary to increase MN in order to obtain a measurable potential. As distance 'AB' becomes increasingly larger, the potential set up between electrodes becomes greater than the measuring capacity of the instrument. When this happens, a new value, typically about twice larger than the preceding value is obtained for 'MN' as pointed out by Harold and Mooney (1980). The procedure for the measurement of the potential developed is then continued by duplicating the last two values with the new value 'MN'. From equation (3.27), setting $r_1 = (L-x)-b$, $r_2 = (L+x)+b$, $r_3 = (L-x)+b$, $r_4 = (L+x)-b$;

Apparent resistivity when the Schlumberger array is used symmetrically is given by;

$$\rho_a = \pi\left(\frac{L^2}{2b} - \frac{b}{2}\right)\frac{\Delta U}{I} \tag{3.29}$$

3.4.2 Wenner Array

In the Wenner array, the electrodes are uniformly spaced in line and are at equal distances apart from each other (Figure 3.2). Wenner array is suitable for Constant Separation Traversing (CST) i.e electrical profiling which is used to determine lateral variations in resistivity. However, when used for electric drilling (VES), all the four electrodes C_1, C_2, P_1, and P_2 are moved together with a constant electrode separation 'a' for each reading. For vertical electrical sounding, the Schlumberger array is preferred to Wenner array owing to the practical difficulty of dragging electrodes and cables at the same time in wooded and rugged terrain.

From equation (3.27), setting $r_1 = r_4 = a$ and $r_2 = r_3 = 2a$

Apparent resistivity is given by;

$$\rho_a = \frac{2\pi a \Delta U}{I} \tag{3.30}$$

Indeed, the advantage of Wenner array lies in its simple geometry, but the fact that the four electrodes must be moved immediately each time a measurement is taken to maintain the same electrode distance is its major disadvantage.

3.5 Preliminary operations

The choice of the survey area was engendered by the fact that Niger State government proposed a permanent orientation camp in order to provide a better and more conducive environment for the corp members deployed to the State. Hence, the need for adequate subsurface information to aid subsequent planning of the proposed site becomes necessary. The best time for a detailed geophysical survey of this kind ought to fall within the dry season ranging from November to March. The dry season is preferred to rainy season for the following reasons. During the rainy season, the survey area is waterlogged and muddy and the unpredicted heavy down pour may mar fieldwork and affect the instrument's components.

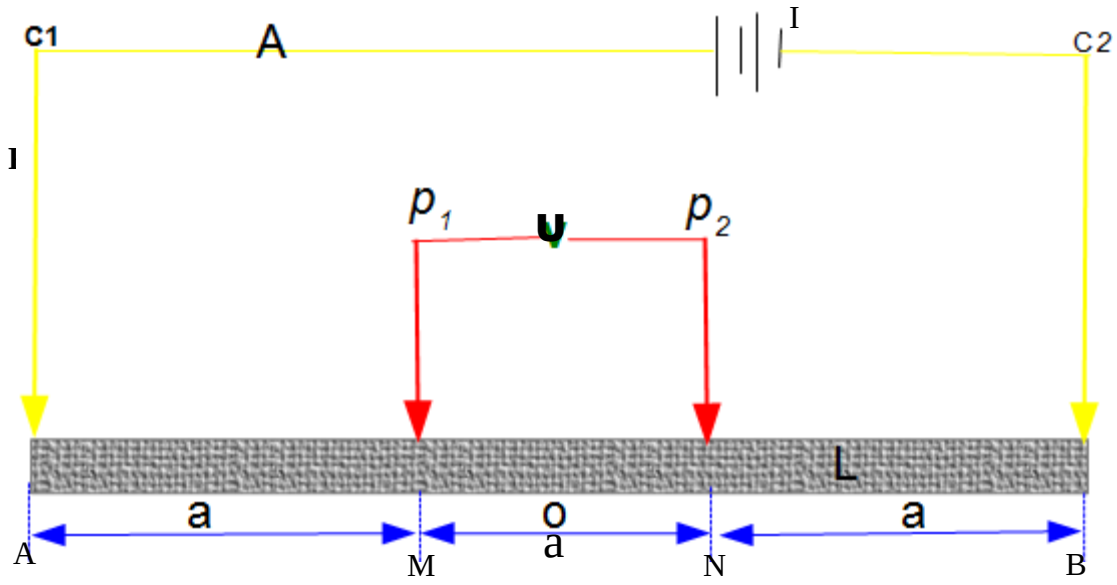

Figure 3.2: Wenner Electrode Array.

Based on the above consideration, the period of the field work was fixed in March 2014, leaving February for the preparation of the fieldwork. Preliminary testing of the equipment (ABEM Terrameter, SAS 1000) was carried out prior to the fieldwork at Government Secondary School, Paiko to calibrate the cable and ensure that the equipment was in good working condition devoid of spurious and negative readings.

Having successfully tested the equipment, the final date of the fieldwork was fixed at the second week of March 2014. The site map was drawn and was used as a guide in planning for the various layouts of the profiles and the sounding points.

3.5.1 Field procedure

In this research study, detailed geophysical investigation involving Vertical Electrical Sounding (VES) was carried out in the survey area covering an area of 480m x 880m. Measurements were taken along five (5) profiles (A-E) with ten (10) sounding points along each profile (A1-A10, B1-B10.....E1-E10) having a total of 50 VES points (A1-E10) as shown in (figure 3.3). Each profile and VES point was separated from another at a uniform interval of 80 m. The resistance measurement was done using ABEM terrameter SAS 1000 and current electrode separation (AB) was varied from a minimum of 2 m to a maximum of 200 m. The geodetic system of coordinates was obtained using Garmin GPS 12 Global Positioning System. In this case, a fixed point called the VES station was marked and noted. Two current electrodes (C_1 and C_2) of equal distance on opposite sides of the VES station were measured and driven into the ground with a sledge hammer for proper contact to be made with the ground.

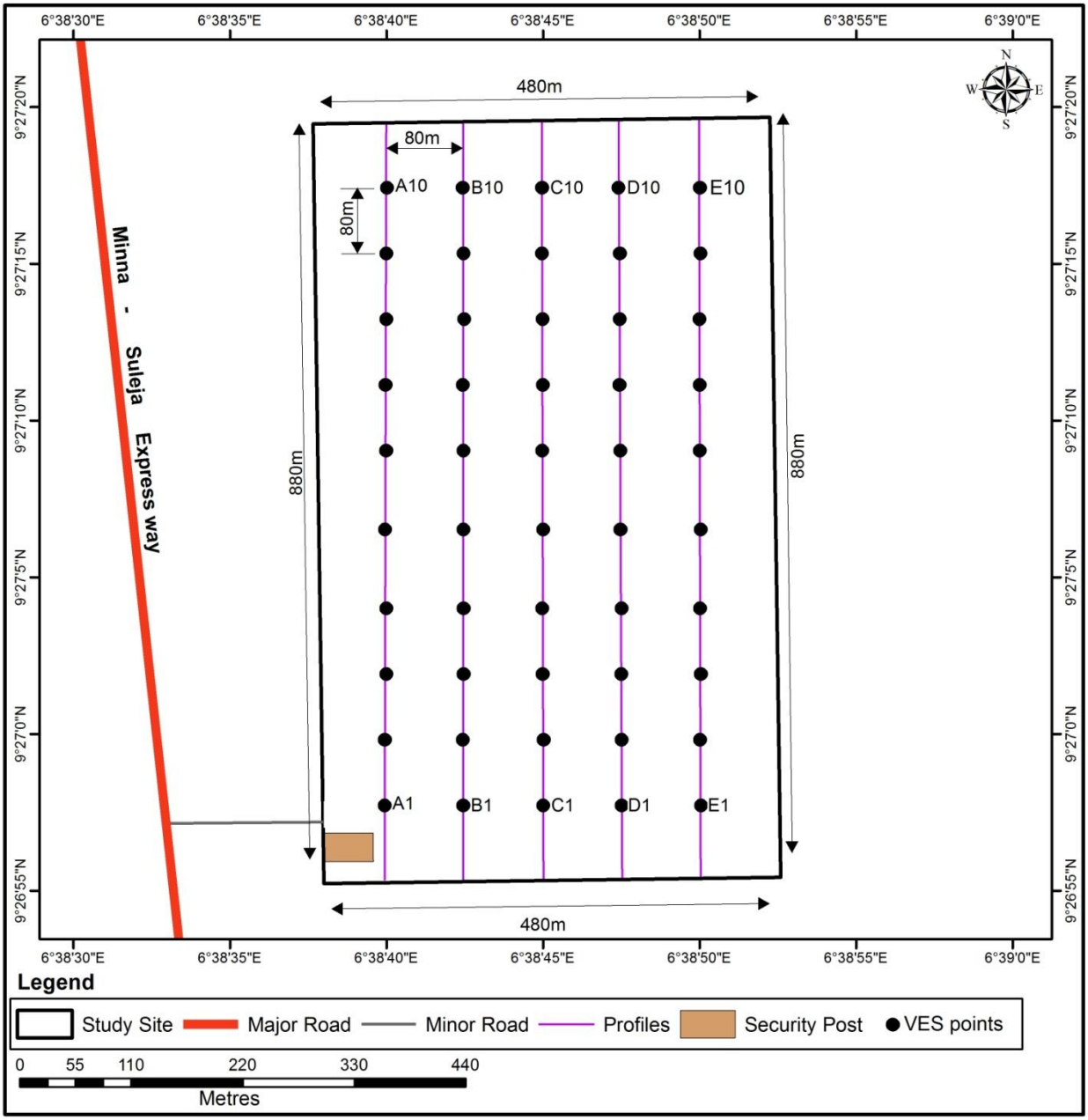

Figure 3.3: Study Site showing Profiles and VES points.

Similarly, two other electrodes called the potential electrodes (P_1 and P_2) were positioned symmetrically with respect to the VES station and were hammered into the ground with the aid of sledge hammer. The arrangements of the current and potential electrodes were in such a way as to maintain a straight line. These pairs of electrodes were connected to the terrameter through points A, B, M and N as shown in (figure 3.1).

The terrameter was switched 'ON' and current was artificially introduced into the earth through the pair of electrodes (C_1 and C_2) and the resulting potential difference due to the current flow was measured through the other pair of electrode (P_1 and P_2). Thereafter, the terrameter was switched 'OFF'. The current electrodes were equally moved away on the opposite sides of the fixed VES point according to the designed acquisition parameter and the readings were recorded at every new position. The field procedure involves the symmetrical expansion of the current electrodes (C_1 and C_2) while holding the potential electrodes distance (P_1 and P_2) fixed. However, this process yields a rapidly decreasing potential difference across P_1 and P_2, which ultimately exceeds the measuring capacity of the instrument. At this point, a new value for potential electrode distance was used, typically three times greater than the preceding value (Oseji *et al*., 2005, Okolie *et al*., 2005).

3.5.2 Difficulties encountered in the field

In the field, there were overwhelming challenges. Among them are;

i. Difficulty in driving the electrodes into the ground due to hard ground.

ii. Partial electrode-ground contact.

iii. Running down of battery in the field.

iv. Moving the equipment from one sounding station to another in a bushy terrain.

v. Entanglement of the current or potential cables.

3.5.3 Precautionary Measures used to overcome the difficulties

For difficulties (i) and (ii), they were easily overcome by moistening the ground where the electrodes were to be driven into the ground. A moderately heavy hammer was used for hammering the electrodes. For the case of battery running down (iii), a standby gasoline generator was provided for charging the battery each time the battery discharges on the field before the close of fieldwork for the day. To overcome difficulty (iv) above, enough hands were provided through hiring of labourers. For difficulty (v), care was taken during whining of the reels so as to prevent entanglement of the cables. The simultaneous observation of these precautions made the fieldwork a huge success.

3.5.4 Data Collection

The data that are normally collected at each sounding point include;

- Date of the survey
- Type of electrode configuration used
- Current electrode spacing
- Potential electrode separation
- Resistances associated with each electrode spacing
- The coordinates of the sounding points.

The choice of the sounding location was made so as to cover the whole area in order to achieve the set objectives. Previous geophysical work, carried out in some parts of Paiko, Nigeria, has shown that the overburden in the basement area is not as thick as to warrant large current electrode spacing for deeper penetration (Oyawoye, 1964). Therefore the largest current electrode separation AB used was 200m, that is, $\frac{AB}{2}$ = 100m.

The potential electrode separation, MN, is usually increased intermittently in order to maintain a measurable electrical potential difference, but the value should not exceed one-fifth of the half-current electrode separation, $\frac{AB}{2}$, as suggested by Dobrin and Savit (1988).

3.6 Instrumentation

The principal instrument used for this survey was the ABEM terrameter Signal Averaging System (SAS) 1000. No booster was used because the expected depth-to-basement in the area is within the range of penetration of instrument. The resistance reading at every point was automatically displayed on the digital read-out screen and was written down. The Terrameter and other equipment used for this survey are shown in (Figure 3.4). The GARMIN 12 channel personal navigation geographic positioning (GPS) receiver unit was used to take the coordinate of the location of the electrical sounding points and the boundary of the survey area. The site plan of the survey area showing the survey profiles and sounding points is as shown in (Figure 3.3).

3.7 IPI2win Model overview

IPI2win is designed for automated interpretation of vertical electric sounding data or induced polarization data obtained with any of a variety of the most popular electrode arrays used in electrical prospecting.

Figure 3.4: ABEM Terrameter (SAS 1000) and other equipment that were used to carry out the survey.

3.8 Data Managing

To start the process of interpreting with IPI2win, there is need for a data file of certain format containing the information on the measurement system and apparent resistivity (and apparent chargeability in the VES-IP mode) values for desegmented curves (*.dat) or for segmented curves (*.dtg).

A dtg-file may also contain potential difference and electric current values for Schlumberger and half-Schlumberger arrays.

1. Entering data: The dgt-file is generally created using the external text editor (i.e windows Notepad). IPI2win internal utility for creating data file is run by choosing the file, New VES point menu item, or by clicking the (make New VES point) button in the tool bar, or by pressing the [ctrl - Alt- N] key. The New VES point window will appear. The apparent resistivity curve (VES-IP mode – and apparent resistivity curve) is displayed in the right part of the window. The left part of the window is a table of field data, each line represents spacing. The columns of the table are spacings ($\frac{AB}{2}$column), measurement line length (MN), apparent chargeability (SP), voltage (U), current (I), coefficient (K), apparent resistivity (Ro_a). Spacing and measurement line length must be typed into the correspondent cells of the table. To enter apparent resistivity, click the input apparent resistivity button window, then type the values in the corresponding cells. When editing the table, one can use the copy and paste buttons of the window.

The table contents can be stored in the clip board by clicking the (copy table) button of the window. The stored items can be pasted then into a spreadsheet or word processor. The table contents can also be saved as the text file by clicking the (save Txt) button of the window. The array type must be selected from the array drop-down list of the window. After all the data are entered, click the (add) button of the window to append to curve to the currently opened file or

the (ok) button of the window to start creation of the new data file. In any case, save as… window will be displayed, where the file name must be pointed out or typed in the file name text box.

2. Viewing Curves and Models: The sounding curve for a certain point is displayed in the curve window titled with the sounding point name. The point name is duplicated in the name of VES location field of the status line immediately below the toolbar. Only one curve can be displayed at a time. The position of the sounding point on the profile is marked by a vertical line on the cross-sections in the cross-sections window.

The field values of the apparent resistivity are marked by circles. The curve itself is presented by a black line, which is a smoothing spline on the field values. The curve is plotted in the algorithmic scale for both spacing and apparent resistivity axes. The number of the orders on either of the axes is determined automatically, so the scale of the curve plot may vary at the different sounding points.

3. Interpreting Sounding data: in interpreting sounding data, the model parameters for the current sounding point (the resistivity and the thickness) are usually presented by a blue line of the pseudo-log plot in the curve window. The theoretical sounding curve for the current model parameter values is plotted in red in the curve window. The data for a profile are treated as a unity representing the geological structure of the survey area as a whole, rather than a set of independent objects dealt with separately. The concept is implemented mainly by using the semi-interactive mode rather than the automated interpreting model.

IPI2win is capable of solving resistivity electrical prospecting 1D forward and inverse problems for a variety of commonly used arrays for the cross-sections with resistivity contrasts within 0.001 to 10000. The forward problem is solved using linear filtering. The filters have been

developed at the near surface Electrical Prospecting Laboratory, Geophysical Department, Geological Faculty, Moscow State University, Moscow, Russia. The thoroughly tested filters and filtering algorithm implementation provide fast and accurate direct problem solution for a wide range of models, covering all reasonable geological situations.

4. Discarding Changes: Any completed editing operation can be discarded by pressing the [Alt-Backspace] keys, choosing the Edit, Undo menu item or clicking the (Undo) button on the toolbar. The editing operation is completed when the [Enter] key is pressed after typing a value in the cell of the table in the model window or the mouse button is released after dragging the pseudo-log plot segment.

5. Clearing Model: Sometimes it is necessary to delete the model for a certain point, i.e. to start interpreting from the very beginning. To do this, select the point with the desired model and choose the Edit, Cut model menu item, or press [shift-Del] keys, or click the [Cut] button on the toolbar. To clear the models for the points, currently displayed in the cross-section window, choose the Delete all results menu item.

CHAPTER FOUR: INTERPRETATION AND GENERAL DISCUSSION OF RESULTS

4.1 General Statement

The interpretation of Vertical Electrical Sounding (VES) data involves expressing the information obtained from the surface measurements in geological terms. In doing so, the combination of some subsurface structural parameters like resistivities and layer thicknesses are obtained.

For easy interpretation, it is assumed that:

1. The various geoelectric layers encountered are electrically homogeneous or uniform and isotropic. However, lateral variation in resistivity exists within a geoelectric layer. Therefore, any deviation from this ideal situation adds to the error in the final interpretation (Kearey and Brooks, 1984).

2. The computed resistivity `curves are based on the fact that the subsurface layers are horizontal and unique. This may not be true in all cases especially in a case of vertical contact. Thus, any vertical layer boundary encountered will introduce error into the interpretation.

3. Each subsurface layer is unique as regards its curve. However, the interpretation suffers from non-uniqueness arising from problems of equivalence and suppression (Kunetz, 1966). The problem of equivalence is the difficulty in distinguishing between two resistive layers of different thicknesses and resistivities where product of these parameters are the same. Similarly, two layers may not be distinguished if the ratio of their thickness to resistivity is the same. The problem of suppression is associated with those layers whose resistivities are intermediate between the resistivities of the enclosing layers. Such layers (with small thicknesses) will have no practical influence on the VES curves.

4.2 Interpretation

The field data obtained have been analysed using computer software (IPI2win) which gives an automatic interpretation of the apparent resistivity data. Figures 4.1, 4.2, 4.3, 4.4, 4.5 and 4.6 are examples of curve types and models obtained from VES stations A4, A9, B9, C5, D7 and E3. Similar plots and interpreted models were obtained for each of the 50 VES points shown in Appendix I. The results of the interpreted VES curves are shown in Appendix II.

The interpretation of these curves was based on the principle that all points of maxima and minima are indicators of different lithologies. Similarly, where the resistivity values tend to infinity is an indication of the fresh basement rock (Telford et al., 1976).

In addition, in order to help see at a glance the resistivity distributions over the whole area, comprehensive subsurface isoresistivity contours at various points at preferred depth were produced using computer software (Sufer 10.0 model). These plots are presented later on.

4.3 General Discussion of Results

For an analytical discussion of the results of the VES, the geologic equivalent of the geoelectric section for the points were drawn (Figures 4.7 - 4.11), since the interpretation of the collected geoelectrical sounding data is meaningless without some reliable geological control or some data relating to the intrinsic resistivities of the various geoelectric section (Worthington, 1977).

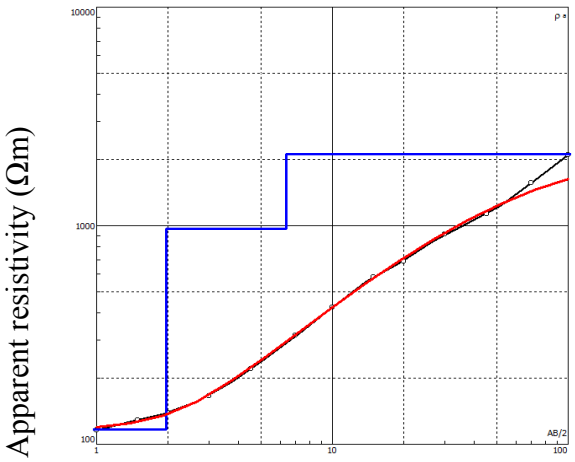

N	ρ	h	d
1	117	1.97	1.97
2	968	4.4	6.37
3	2023		

Figure 4.1: Curve at VES A4 (TYPE A)

where;

N is the layer number,
ρ is the layer resistivity in (Ωm)
h is the layer thickness in metres and
d is interface depth in metres.

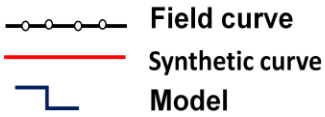

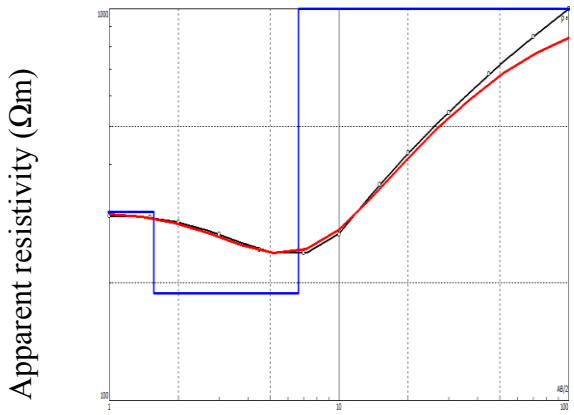

N	ρ	h	d
1	303	1.56	1.56
2	187	5.1	6.66
3	1000		

Figure 4.2: Curve at VES A9 (TYPE H)

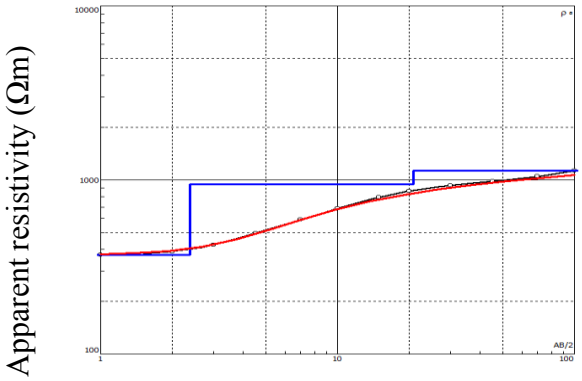

N	ρ	h	d
1	371	2.38	2.38
2	944	18.5	20.9
3	1131		

Figure 4.3: Curve at VES B9 (TYPE A)

where;

N is the layer number,
ρ is the layer resistivity in (Ωm)
h is the layer thickness in metres and
d is interface depth in metres.

Field curve
Synthetic curve
Model

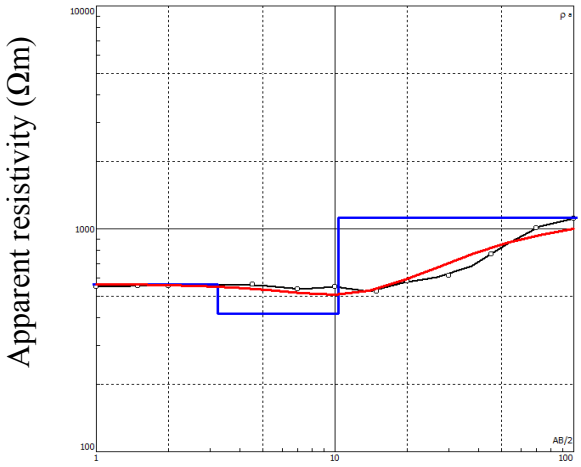

N	ρ	h	d
1	564	3.23	3.23
2	416	7.11	10.3
3	1122		

Figure 4.4: Curve at VES C5 (TYPE H)

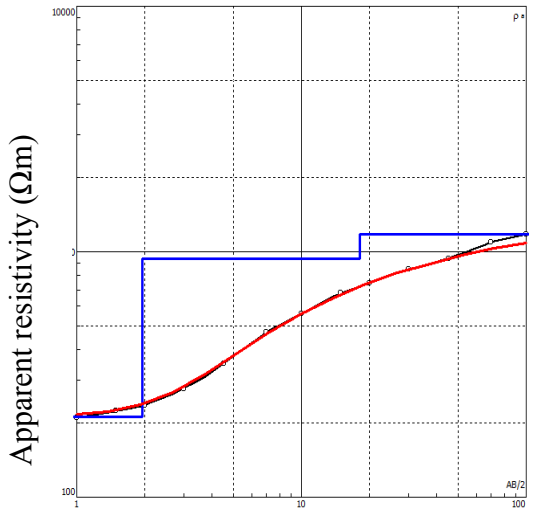

N	ρ	h	d
1	213	1.96	1.96
2	937	16.2	18.2
3	1178		

Electrode spacing (m)

Figure 4.5: Curve at VES D7 (TYPE A)

where;

N is the layer number,
ρ is the layer resistivity in (Ωm)
h is the layer thickness in metres and
d is interface depth in metres.

Field curve
Synthetic curve
Model

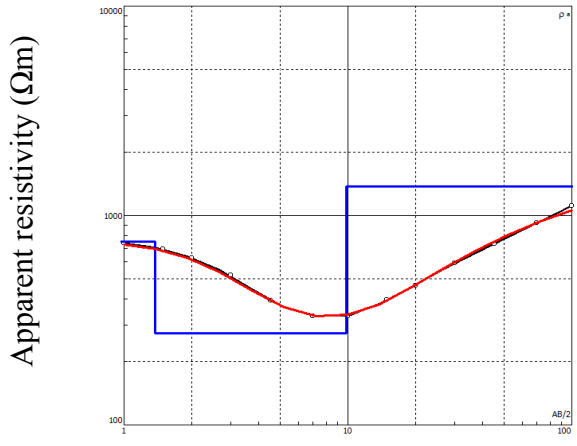

N	ρ	h	d
1	751	1.38	1.38
2	273	8.46	9.84
3	1377		

Electrode spacing (m)

Figure 4.6: Curve at VES E3 (TYPE H)

4.3.1 Geoelectric Sections along profiles

To obtain geoelectric section along a profile, the profile of interest is first drawn as shown in the map in Figure 3.3. The position of each VES station point is marked out. The resistivity values beneath each VES point along with their depth values are obtained using the interpretation data for the geoelectric cross sections automatically generated by a computer software package (IPI2win). Appropriate resistivity boundaries in form of contours are then drawn through points of equal resistivity values following the resistivity ranges obtained for various rock types. The resulting map shows the depth and thickness of a rock material at a point. Such result is referred to as geoelectric section. The equivalent geologic sections in this work were drawn based on the following controls:

1. A borehole lithology of Paiko, obtained from the Physical Planning Unit, Ibrahim Badamosi Babangida (IBB) University, Lapai, Niger State. The area is shown to be underlain by lateritic topsoil having a thickness of 2m, silty/sandy clay with 8m thickness, weathered basement with thickness of 16m extending to a depth of about 26m (Table 4.1).
2. Resistivity values obtained from previous works (Tables 4.2 and 4.3), who worked in different Basement areas of Niger State, were used to correlate the results of the present survey.

The VES interpretation results were used to prepare geoelectric sections along the five profiles (Figures 4.7 to 4.11). The geoelectric sections delineate maximum of three geoelectric/geological subsurface layers which have been interpreted to be topsoil for the uppermost layer, weathered layer for the second layer and fresh bedrock (basement) for the third layer.

TABLE 4.1: A Borehole Lithology of Paiko (obtained from the Physical Planning Unit, Ibrahim Badamosi Babangida (IBB) University, Lapai, Niger State).

Lithology	Depth(m)	Thickness(m)
Top lateritic soil	0-2	2
Silty/Sandy Clay	2-10	8
Weathered basement	10-26	16
Fresh crystalline basement rock	26- ∞	∞

TABLE 4.2: Typical Resistivity values compiled from previous works (Yadav et al., 2007).

Soil and Rock type	Resistivity (Ωm)
Dry Clay	30-70
Sandstone	40-100
Laterite	80-400
Sandy Clay	200-500
Weathered Basement	100-600
Dry sand	500-1000
Fresh basement (crystalline)	>1000

TABLE 4.3: Typical Resistivity values of common rock materials and selected ore minerals (After Olorunfemi and Fasuyi, 1993).

Soil and Rock type	Resistivity range (Ωm)
Clay	1-100
Gravel	100-600
Weathered Bedrock	100-1000
Sandstone	200-8000
Granite	200-100000
Basalt	200-100000
Galena	0.001-0.1
Chalcopyrite	0.005-100
Magnetite	0.01-1000
Hematite	0.01-1000000
Fadama Loam	20-100
Laterite	60-1000
Silt and Sand	80-400
Fresh Basement	>1000

TABLE 4.4: Resistivity values adopted for this work.

Rock type	Resistivity range (ohm-metre)
Top lateritic soil	10 – 250
Silty/Sandy Clay	100 – 500
Weathered/Fractured Basement	9 – 968
Fresh Basement	540 - ∞

4.3.2 PROFILE "A"

The geoelectric section along this profile, suggests three (3) geoelectric layer and a two (2) layer at VES A6 (Figure 4.7). The top layer whose resistivity value ranges from 14 to 303Ωm and thickness from 1.39 to 2.55m (except for VES A6 where the top soil has been probably washed off by erosion) with the thickest portion at VES A1 (2.55m) is a lateritic and a silty/sandy clay soil (Table 4.4). The second layer whose resistivity value ranges from 9 to 968Ωm and thickness from 2.47 to 24.50m with the thickest portion at VES A10 (24.50m) is an indicator of the weathered basement. The third layer which is the fresh basement rock cuts across the entire length of the profile, and is shallowest at VES A6 (2.47m) and deepest at VES A10 (26.8m). The resistivity of this layer ranges from 540 to 2023Ωm.

4.3.3 PROFILE "B"

The geoelectric section along this profile, suggests that the subsurface is made up of three (3) layers (Figure 4.8). The top soil resistivity value ranges from 128 to 559Ωm and thickness ranging from 1.15m at VES B2 to 3.39m at VES B10. The second layer, appearing to be a weathered basement has resistivity ranging from 223 to 944Ωm and thickness ranging from 4.38 to 18.60m. The resistivity of the third layer ranges from 1122 to 2718Ωm. The fresh basement is closer to the surface around VES B6 with resistivity value of 1446Ωm and its highest resistivity value appears at VES B3 with a value of 2718Ωm.

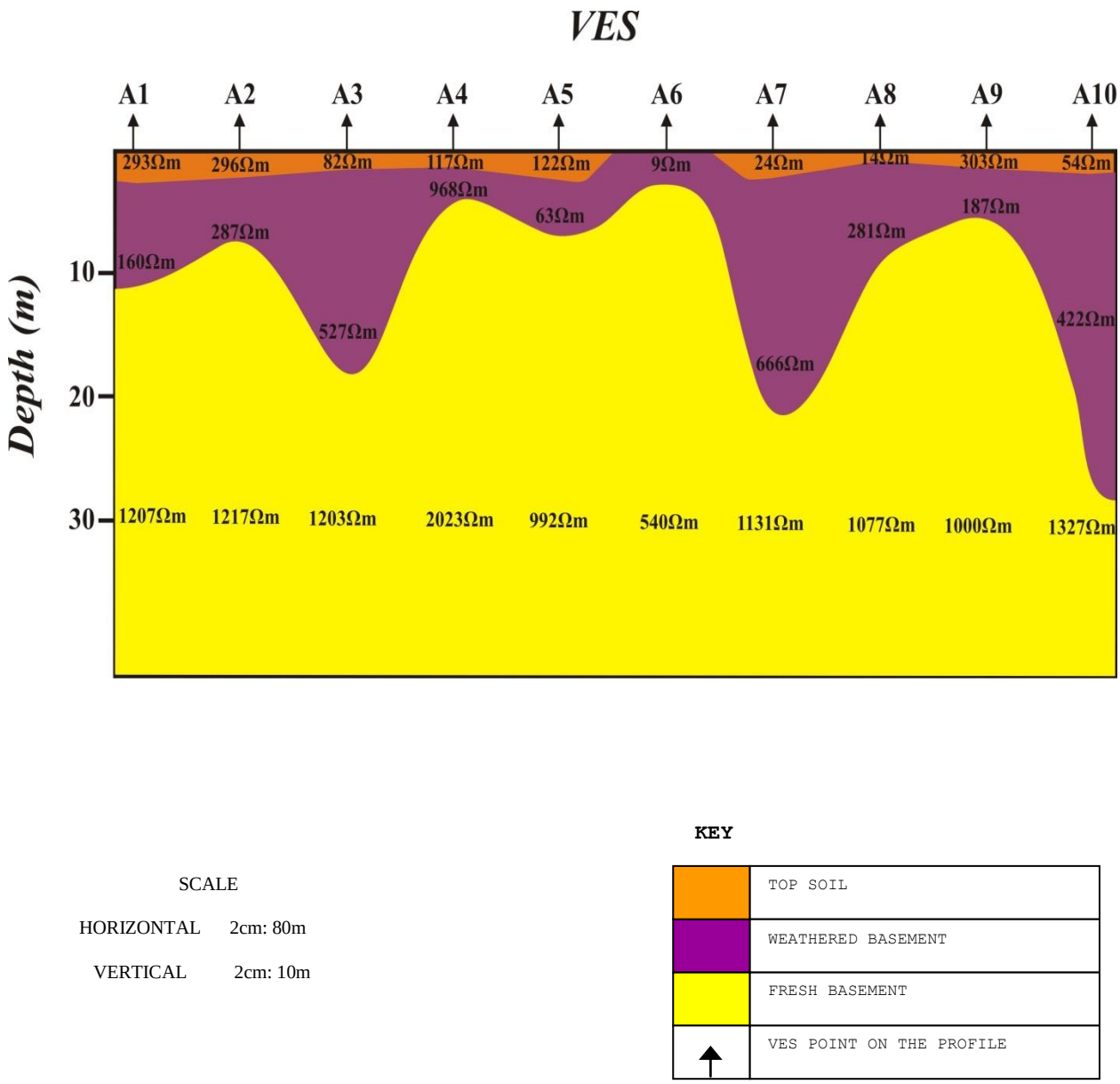

Figure 4.7: Geoelectric Section along Profile A.

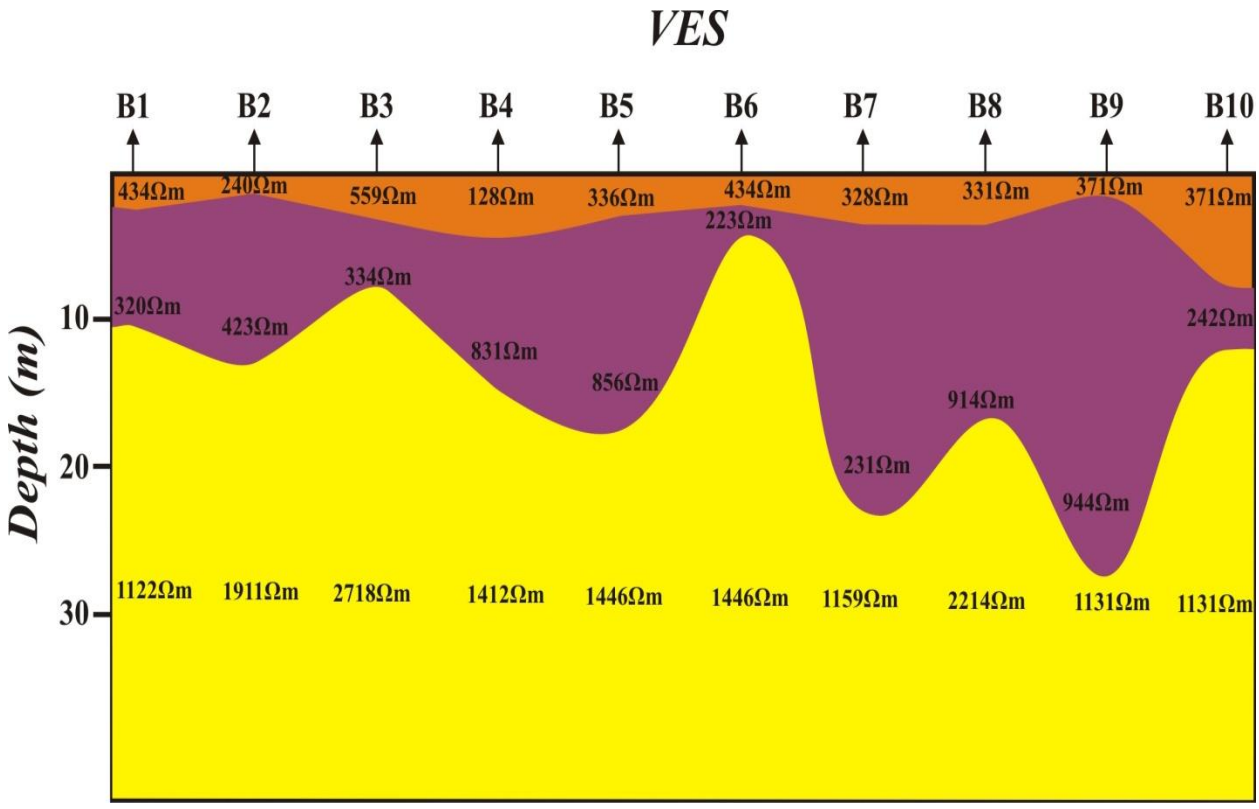

SCALE

HORIZONTAL 2cm: 80m

VERTICAL 2cm: 10m

KEY

	TOP SOIL
	WEATHERED BASEMENT
	FRESH BASEMENT
↑	VES POINT ON THE PROFILE

Figure 4.8: Geoelectric Section along Profile B.

4.3.4 PROFILE "C"

The geoelectric section for this profile shows the presence of three (3) layers (Figure 4.9). The top layer is thinnest at VES C8 which is 0.98m thick and thickest at VES C3 with a thickness of 3.34m. Its resistivity ranges from 39 to 564Ωm. The thickness of the second layer ranges from 5.08 to 22.70m and its resistivity is between 130 to 929Ωm. The range type here is generally weathered. The third layer is the fresh basement with the resistivity value ranging from 1068 to 2108Ωm. It is shallowest at 6.36m at VES C4 and deepest at 26.04m at VES C3.

4.3.5 PROFILE "D"

The geoelectric section for this profile shows three (3) layers extending all along its length (Figure 4.10). The topsoil has resistivity ranging from 10 to 403Ωm and thickness ranging from 1.26 to 4.23m. The second layer of the geoelectric section also suggests that the thickest portion is at VES D7 with a thickness of 16.20m and thinnest at VES D9 with a thickness of 3.28m. The resistivity ranges between 202 and 952Ωm. The third (3) layer with resistivity value as low as 1000Ωm and as high as 2040Ωm appears to be the fresh basement. The shallowest depth of the fresh basement was found to be about 7.51m at VES D9 and deepest at depth 18.16m at VES D7 along the chosen profile of the study area.

4.3.6 PROFILE "E"

The geoelectric section along this profile suggests three (3) layers extending all over the profile, (Figure 4.11). The topsoil has resistivity ranging from 9 to 751Ωm and thickness ranging from 1.34m at VES E7 to 3.96m at VES E2. The geoelectric section also suggests that the second layer (weathered basement) is thickest at VES E1 with a thickness of 20.80m and thinnest at VES E7 with thickness of about 0.67m. The resistivity value ranges from 102 to 772Ωm.

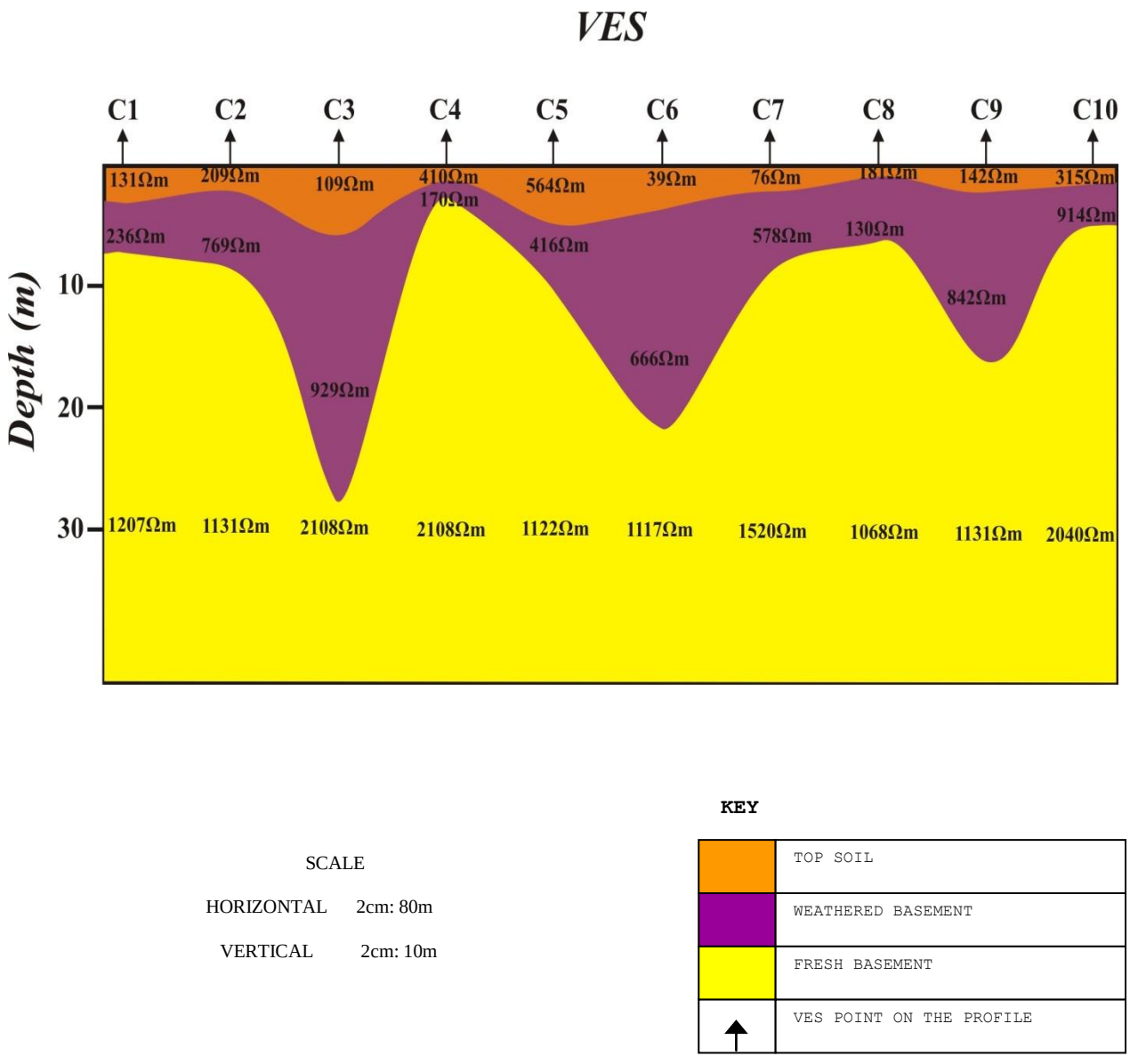

Figure 4.9: Geoelectric Section along Profile C.

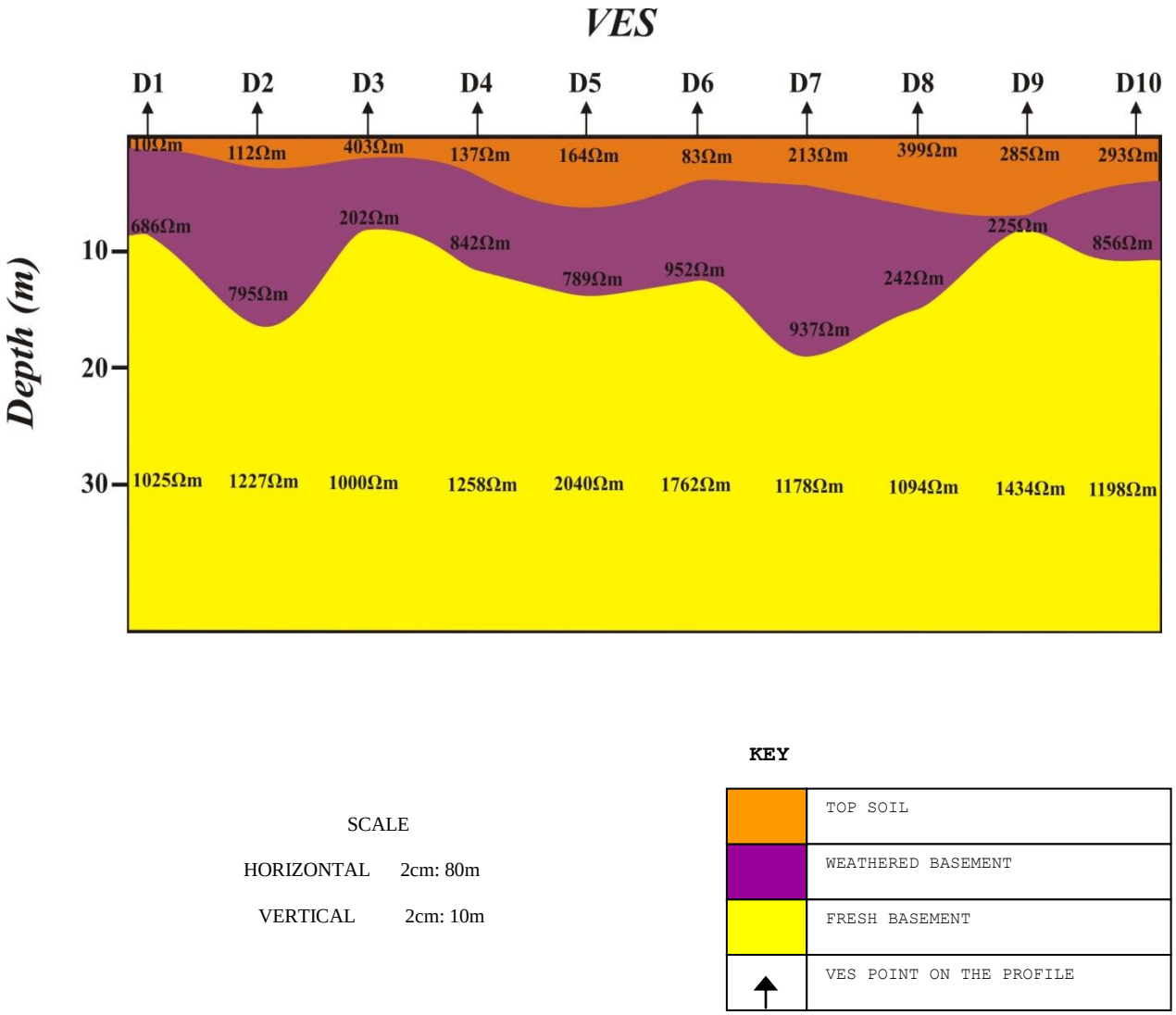

Figure 4.10: Geoelectric Section along Profile D.

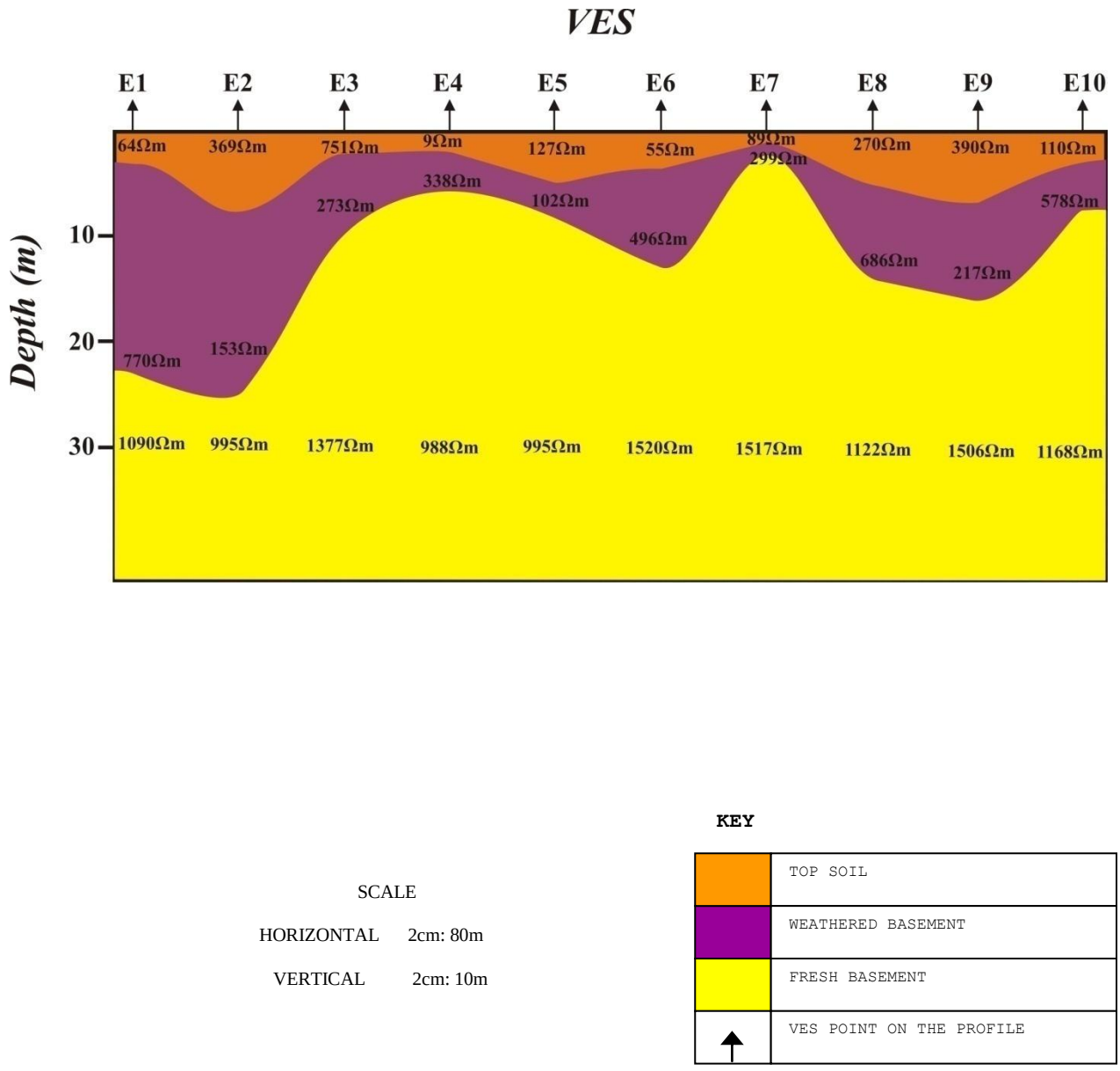

Figure 4.11: Geoelectric Section along Profile E.

The third layer which is the fresh basement has resistivity value as low 988Ωm and as high as 1520Ωm. The shallowest depth to the fresh basement (bedrock) was found to be 2.01m at VES E7 and the deepest is 24.26m at VES E2.

4.4 Isoresistivity Contour Maps

The Isoresistivity contour maps have helped to show at a glance the resistivity distributions over the whole area at preferred depths. This work shows the isoresistivity map at 5.00m, 15.00m, and 27.00m depth as shown in Figures 4.12, 4.13 and 4.14 respectively.

Figure 4.12 show that the regions around VES E3, C5 and B3 have the highest resistivity values at depth 5.00m, while most of the other areas such as VES E4, A6 and A8 have low values due to the layer of silt and clay at the top layer (topsoil). However, the highly resistive area may indicate high content of sand and silt mixed with the lateritic topsoil at this depth.

Figure 4.13 shows a high resistivity value around VES A4, D6, C10 and D10 which is an indication of outcrop of fresh basement; while other areas such as VES A5, C8 and A1 have very low resistivity values, which is an indication that the topsoil has been exceeded and another layer (weathered basement) that is water bearing has been reached.

In Figure 4.14, areas such as VES B9, D7, and C3 have very high resistivity values (low conductivity) this is because the rock in those areas are still very fresh compared to areas such as VES E2 and B7 with very low resistivity values because the rock in those areas are highly weathered.

4.5 Depth-to- Bedrock map.

The IPI2win software used for the interpretation of this work generates sets of depths with the corresponding resistivity values for each layer.

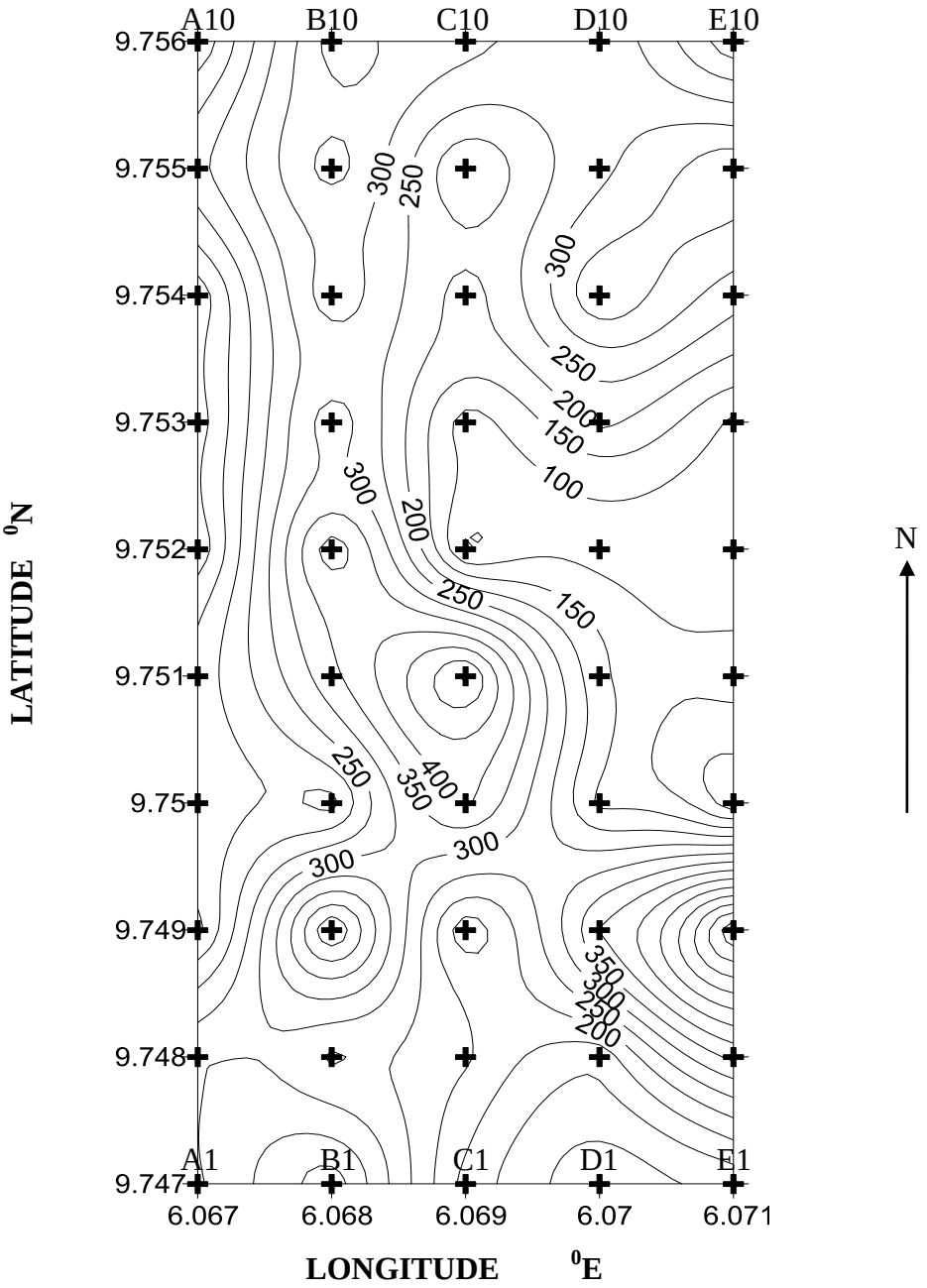

Figure 4.12: Isoresistivity map at 5.00m depth. Cont. Int. 50Ωm.

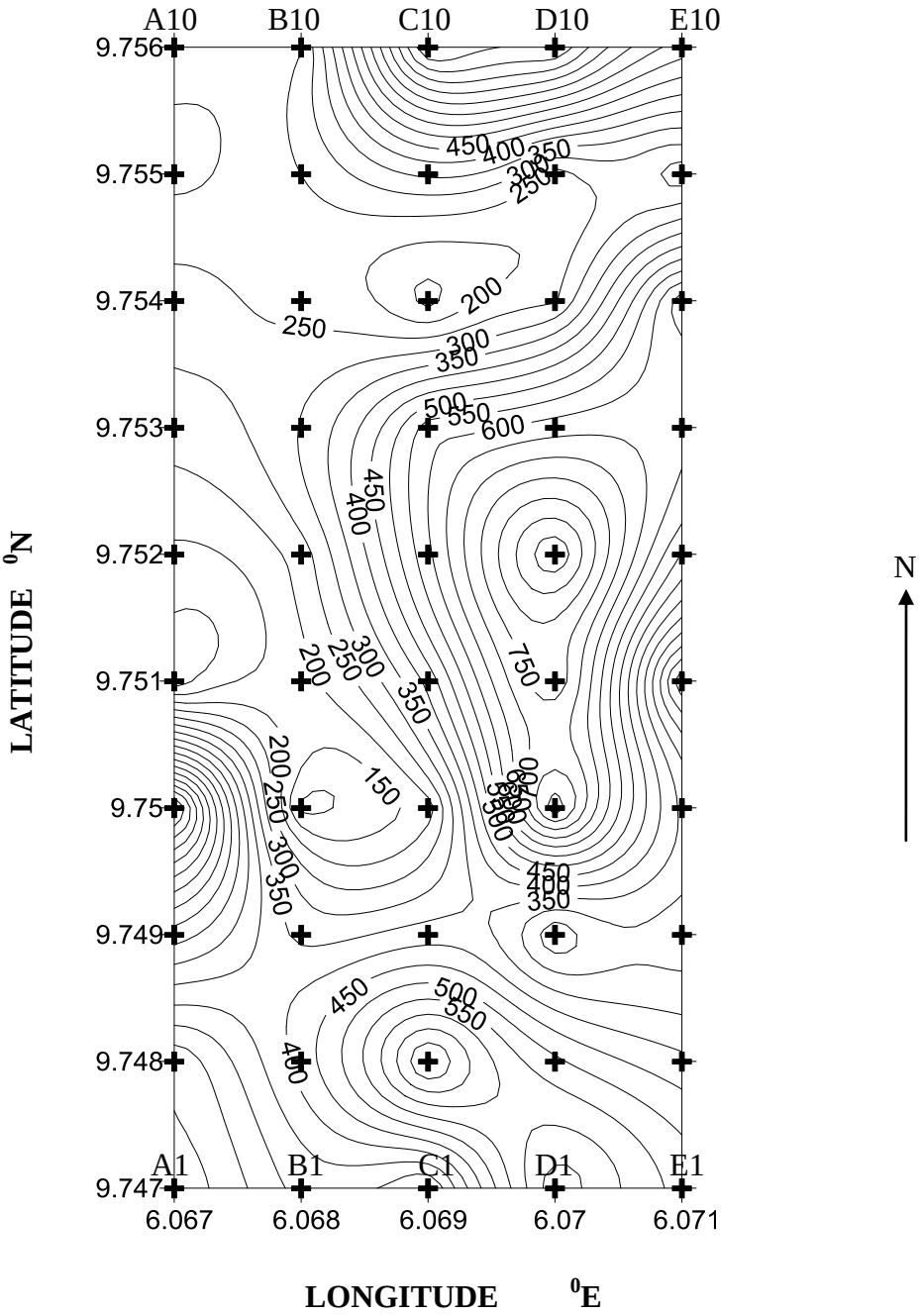

Figure 4.13: Isoresistivity Map at 15.00m depth. Cont. Int. 50Ωm.

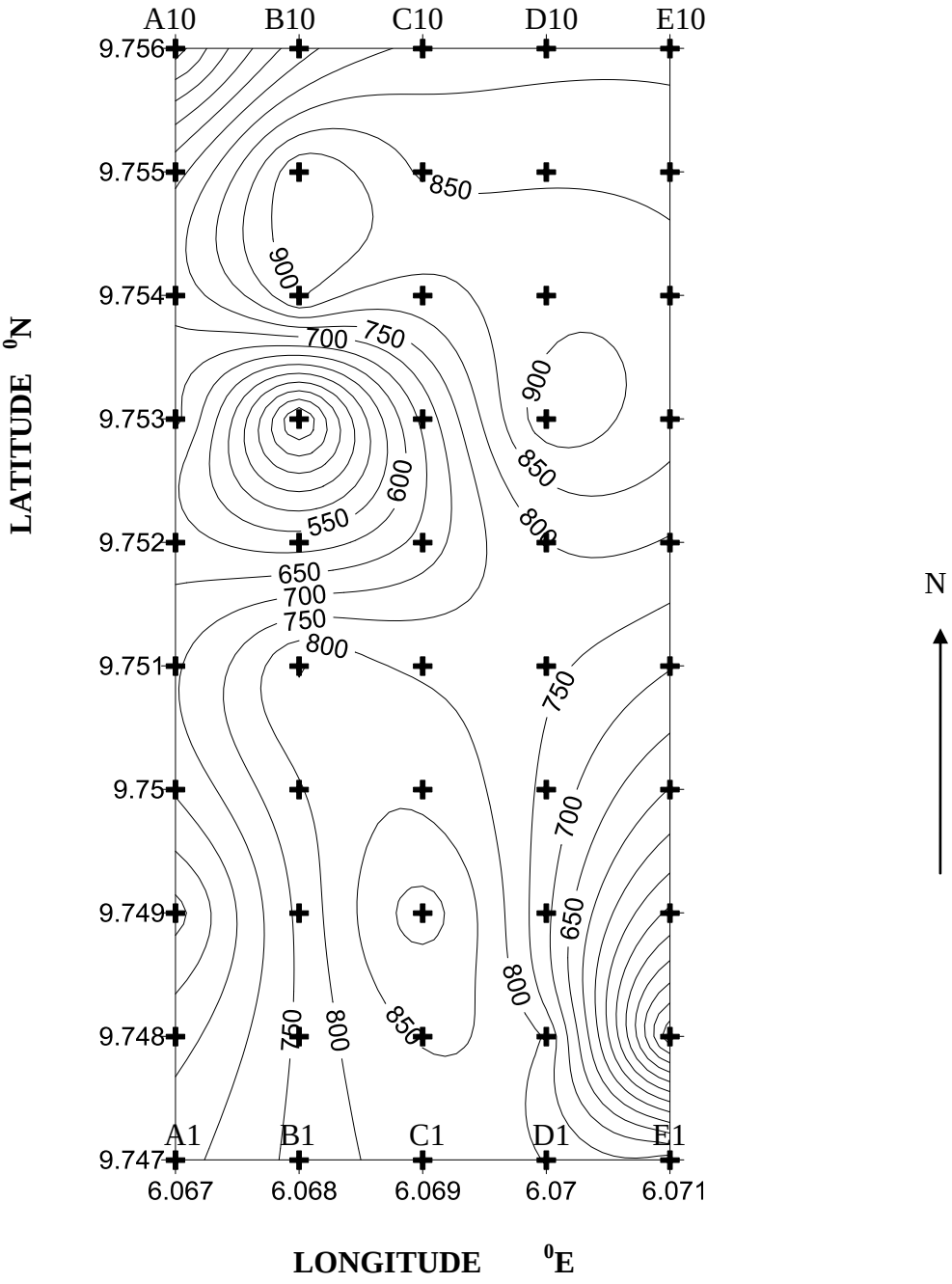

Figure 4.14: Isoresistivity Map at 27.00m depth. Cont. Int. 50Ωm.

The depth estimates (sum of thicknesses from topsoil to fresh basement) gives the depth to the fresh basement (bedrock) which is the last depth.

These data are used to plot the depth-to-bedrock image map and their corresponding fresh basement resistivity values (Figure 4.15) by picking all depth data corresponding to the resistivity assumed for bedrock at all VES points.

Figure 4.15 is an overlay of the depth to fresh basement (bedrock) and resistivity distribution within the survey area. The image map shows the depth to the fresh basement (bedrock) distribution while the contour map represents the resistivity distribution within the area of study. It can be seen that the bedrock is shallowest at VES E7 with a depth of about 2.01m and deepest at A10 with a depth of about 26.81m. A 3D surface plot for the bedrock is shown in Figure 4.16 which is a representative of the bedrock topography.

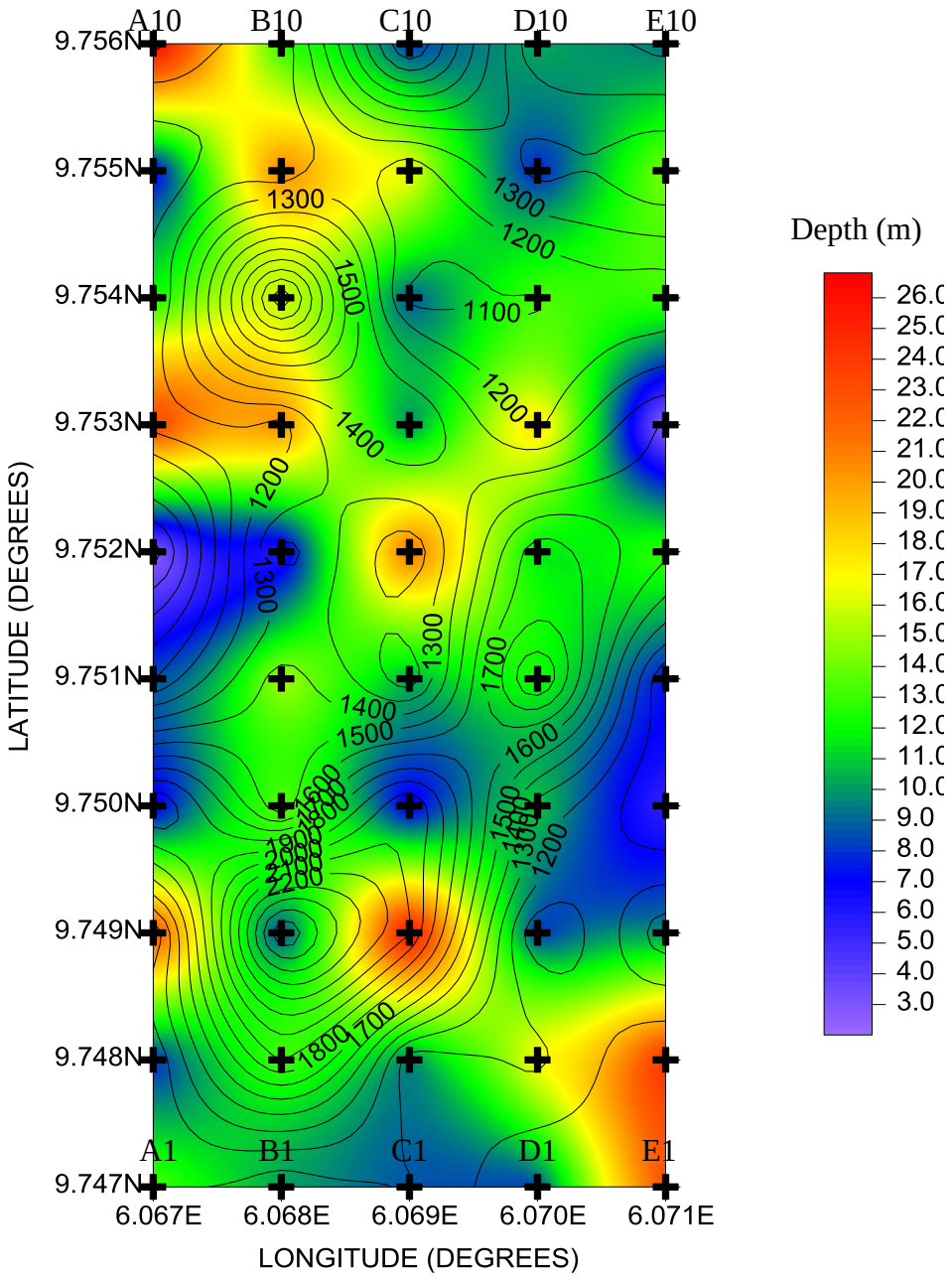

Figure 4.15: Depth-to-Bedrock Image Map and Fresh Basement Resistivity Distribution Contour Map. Cont. Int. 100Ωm.

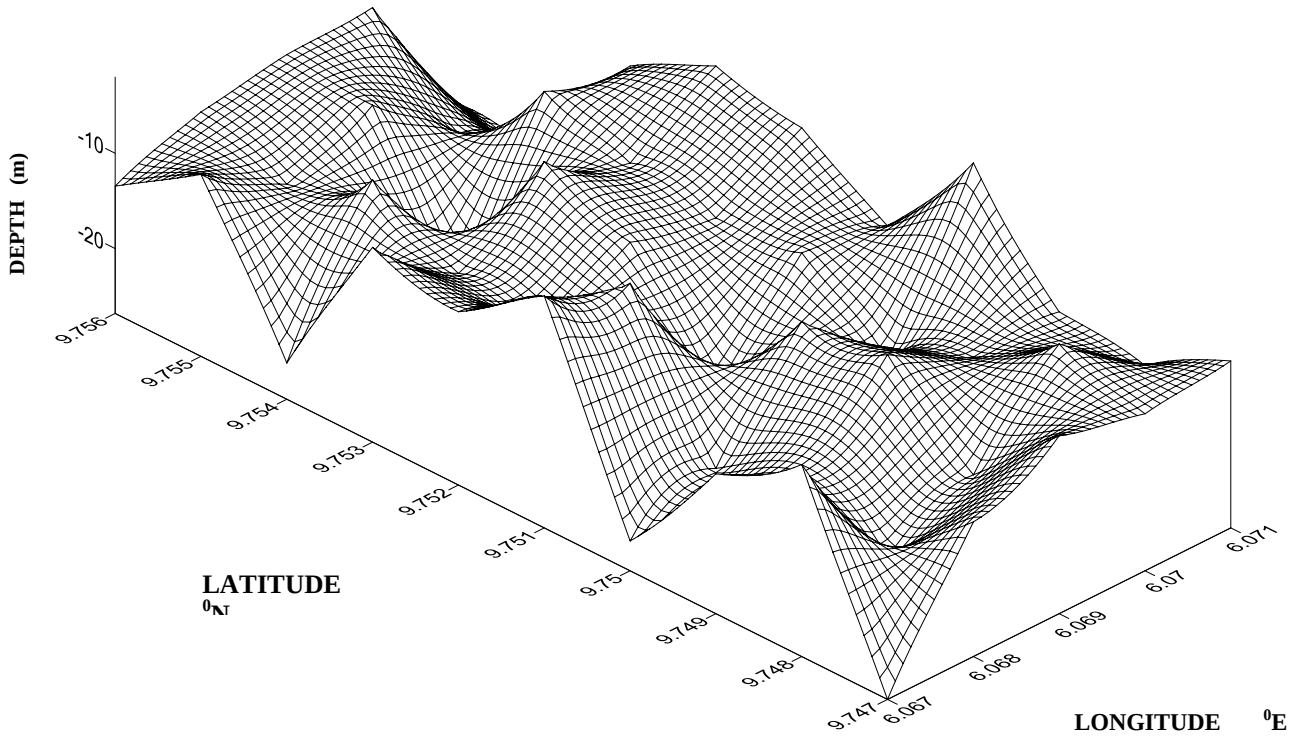

Figure 4.16: 3D Surface Plot of the Bedrock.

4.6 Depth-to-and thickness of Weathered Basement maps

In achieving depth to the weathered basement and thickness of the weathered basement, data of depths to the weathered basement (thickness of the topsoil) with the corresponding topsoil resistivity values at each VES stations were used (Figure 4.17). The same process was followed using the resistivity values for the weathered basement at each VES stations and their corresponding thicknesses distribution to plot the map of the weathered basement thickness with their corresponding resistivity (Figures 4.18). Figure 4.17 shows that weathered basement is deepest at VES D9 with a depth of about 4.23m and resistivity value of 285Ωm and shallowest at VES C8 with a depth of 0.98m and resistivity value of 181Ωm. The thickest portion of the weathered basement indicated by Figure 4.18 is about 24.50m which is at VES point A10 and with resistivity value of 422Ωm while the thinnest portion is at VES point E7 with thickness of 0.67m and with resistivity value of 299Ωm.

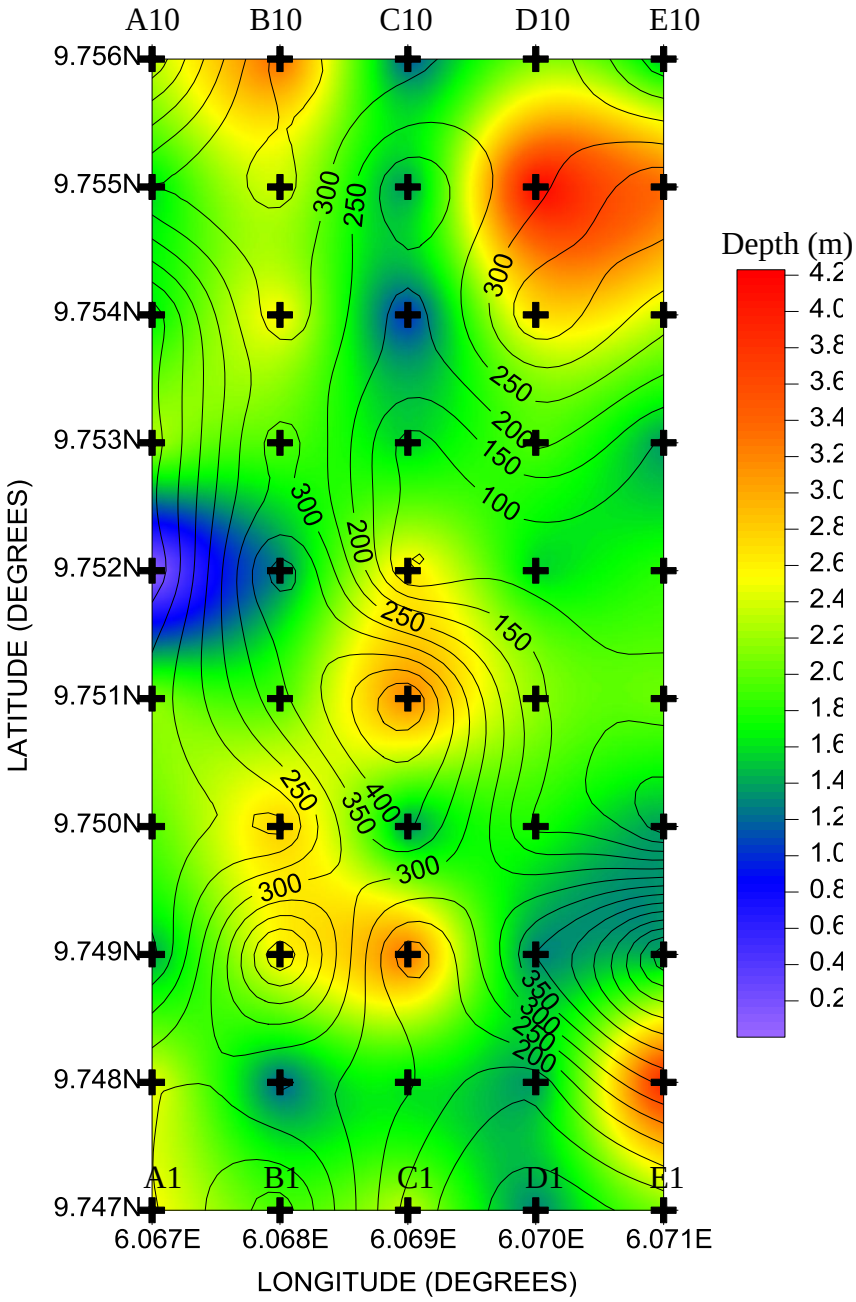

Figure 4.17: Depth-to-Weathered Basement Image Map and Top Soil Resistivity Distribution Contour Map. Cont. Int. 50Ωm.

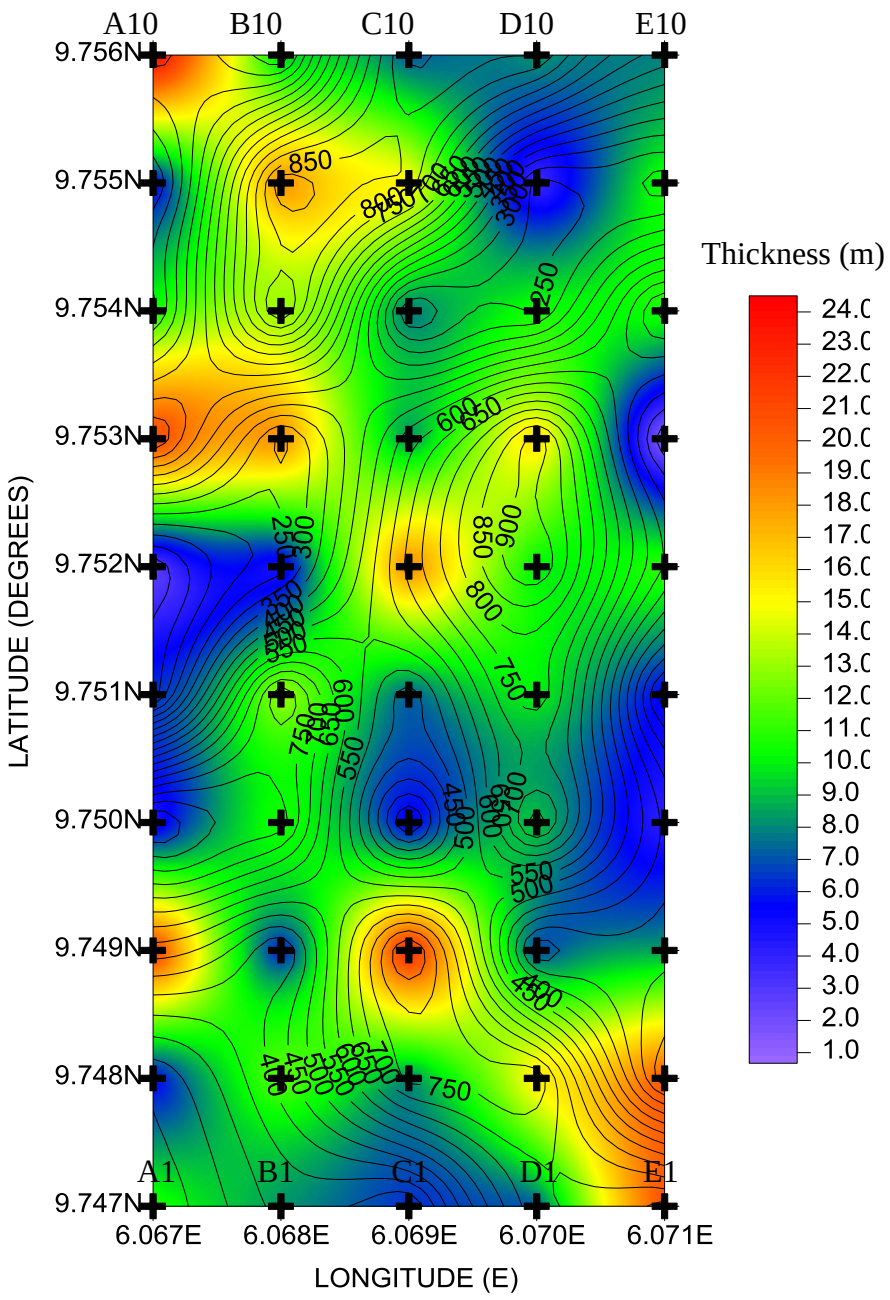

Figure 4.18: Thickness of Weathered Basement Image Map and Weathered Basement Resistivity Distribution Contour Map. Cont. Int. 50Ωm.

CHAPTER FIVE: SUMMARY, CONCLUSION AND RECOMMENDATION

5.1 SUMMARY

The aim of this work was to investigate depth to the bedrock and to determine the thickness of the weathered basement in the area.

The VES carried out at fifty (50) stations aided in deriving geoelectric sections along five (5) profiles. These revealed that there are mostly three geoelectric layers (3 - layer cases) beneath each VES station, and a two layer geoelectric case at VES A6. The predominant layers are: the topsoil consisting of lateritic and silty/sandy clay soil. The resistivity of this layer is as low as 10Ωm and as high as 751Ωm, while the thickness ranges from 0.98m at VES C8 to 4.23m at VES D9 (except for VES A6 where the top soil has been probably washed off by erosion). The weathered basement formed the second layer on each profiles (except for profile A, VES A6 where the top soil has been probably washed off by erosion and the weathered basement became the first layer) with the resistivity value as low as 9Ωm and as high as 968Ωm on some profiles. The weathered basement is considered as the aquifer and the thickness ranges from 0.67m at VES E7 to 24.50m at VES A10. The third layer is the fresh basement whose resistivity is as high as 2718Ωm. The shallowest depth to it is 2.01m at VES E7 and the deepest is 26.81m at VES A10.

5.2 CONCLUSION

In this work, the electrical d.c. resistivity method was employed to establish fifty (50) VES points which offered complimentary solution to the problem of this investigation. The study area is mostly characterized by three (3) layered geoelectric sections which include the topsoil, weathered basement and fresh basement. The topsoil has resistivity ranging from 10 to 751Ωm. The weathered basement has resistivity ranging from 9 to 968Ωm with depth to it ranging from

0.98m to 4.23m. The topsoil is lateritic and silty/sandy clay, associated with the weathering of sulphide minerals from the underlying granitic rocks. They have great amount of dissolved salts resulting in low resistivity values. The weathered basement is deepest around VES D9 with a depth to it of 4.23m. The thickest portion of the weathered basement is 24.50m at VES A10. The weathered basements are medium to fine grain porous or fractured rocks containing water. They are referred to as the aquiferrous zone. Highly fractured areas have low resistivity because of its high degree of saturated water implying that their resistivity is greatly influenced by underground water. The fresh basement has its deepest part at VES A10 of 26.81m located along profile A. The fresh basement rocks are coarse, close grained (plutonic or intrusive) rocks, constituting the rock forming minerals which are poor conductors.

The following areas can be used for siting boreholes: VES A1, A3, A7, A8, A10, B2, B4, B5, B7, B8, B9, C3, C6, C9, D2, D7, E1, E2, E8 and E9. These points have considerable thickness of weathered basement (fractured zone thickness > 10.00m) which can be a good water aquifer i.e. have identified elements for groundwater storage such as high porosity, permeability and less consolidation.

Strategic areas for siting high-rise buildings may include: VES A4, A9, B1, B6, C4, D3, E3 and E4. These are areas with shallow depths to the bedrock of about (5.00 to 10.00m) and also thin topsoil (thickness < 2.00m) because of the lateritic and silty/sandy clayey nature of the topsoil. The consolidated basement (bedrock) can serve as pillar supports for buildings. Since the study area has shallow depths to the bedrock and water aquifer, the depth of sewage system should be less than 10.00m of the aquiferrous zone (weathered basement) in order to avoid groundwater contamination.

There is no known geophysical survey that has been carried out in the site. However, this survey revealed that the average depth to the bedrock (Fresh Basement) is about 15.00m with the lowest depth to it as 2.01m and with the highest depth to it as 26.81m. The aquifer in the area has an average depth of about 10.00m and therefore the depth of sewage system should be less than 10.00m in order to avoid groundwater contamination.

5.3 RECOMMENDATIONS

The present investigation was accomplished using one of the geophysical methods which is the electrical resistivity method. However, integrated geophysical studies are highly desirable. For this reason, it is recommended that other geophysical methods such as, seismic (refraction), magnetics, gravity and VLF methods which are found to be greatly instrumental in mapping subsurface materials and determining depth to bedrock, can be used to verify the findings from this study.

The study of the overburden protective capacity in the area has revealed that there is need to site potential sources of aquifer contamination sites such as sewage tanks and waste disposal sites away from the promising aquifer units to enhance safety appraisal of groundwater consumption in the area.

Finally civil engineering structures involving underground piping utilities should be coated with corrosion prevention system to prevent corrosion as some of the areas are liable to corrosion. As an alternative, the piping utilities should be made of plastics instead of metal.

REFERENCES

Aftab, K. and Alan, E. (2000): Looking into the Earth, an introduction to geological geophysics. Cambridge University Press, 50-55.

Ajibade, A.C. and Woakes, M. (1976): Proterozoic crustal development in the Pan-African Regime of Nigeria, In: C.A. Kogbe (Editor) Geology of Nigeria; Published by Rock View (Nigeria.) Ltd., 57–63.

Ajibade, A.C., Woakes, M. and Rahaman, M.A. (1983): The origin of the Older Granites of Nigeria, some evidence from the Zungeru region. Nigerian Journal of Mineralization Geology, 19(1), 223–230.

Amadi, A. N., Ameh, M. I., Idris-Nda, A., Okoye, N. O., Ejiofor, C. I. (2013): "Geological and Geophysical Investigation of Groundwater in Parts of Paiko, Sheet 185, North-Central Nigeria" published at International Journal of Engineering Research and Development, 6, 23-25.

Archie, G.E., (1942): The electrical resistivity log as an aid in determining some reservoir characteristics. Journal of Petroleum Technology, 5, 54-62. Transactions at American Institution of Mining, Metallurgical, and Petroleum Engineers (AIME).

Bello, A. A. and Makinde, V. (2007): Delineation of the aquifer in the South- Western part of the Nupe Basin, Kwara State, Nigeria. Journal of American Science, 3(2), 36-44.

Blyth, K.T. and Freitas, G.P. (1988): Behaviour of Foundation and Structures', in proceedings of the 9th International Conference of Soil Mechanics, Tokyo, Session 2, 8-10.

Dobrin, M.B. and Savit, C.H. (1988): Introduction to Geophysical Prospecting, McGraw-Hill Book Company, New York, United States, 867-868.

Gomes, N. (2006): Access to Water, Pastoral Resource Management and Pastoralists' Livelihoods; Lessons Learned From Water Development in Selected Areas of Eastern Africa (Kenya, Ethiopia and Somalia); In NATIONS, Food And Agriculture Organization Of The United Nations (F. A. A. O. O. T. U. N). Livelihood Support Programme Working Paper 26, Access to Natural Resources Sub-Programme.

Harold, M. And Mooney, T., (1980): Hand Book of Engineering Physic; Electrical Resistivity Bison Instruments Inc., Minnesota, U.S.A., 2, 27-34.

Ishaku, Y. B., Mohamad, Y. I. and Rindam, M. (2013): Vertical Electrical Sounding Investigation of Aquifer Composition and Its Potential to Yield Groundwater in Some Selected Towns in Bida Basin of North Central Nigeria. Journal of Geography and Geology; Published by Canadian Center of Science and Education, 6(1), 30-35.

Kearey, P. and Brooks, M. (1984): An introduction to geophysical exploration, Blackwell Scientific Publications, Geological Journal, 21-25.

Keller, G.K. and Frishknecht, F.C. (1966): Electrical methods in Geophysical Prospecting. Pergamon Press, Oxford, New York, Toronto, Sydney, Braunschweig, 45-48.

Kelly, W.E. (1993): Applied Geophysics in hydrogeological and engineering practice. Elsevier, Amsterdam Press, United Kingdom, 345-348.

Kogbe, C. A., (1976): Geology of Nigeria (2nd Revised Edition). Rockview Publishing Company, Jos, Nigeria, 531–538.

Kunetz, G., (1966): Principle of Direct Current Resistivity. Geoexploration Monographs, series No.1, Gebruder Borntraeger, Berlin, 710-712.

McCurry, P. (1976): The Geology of the Precambrian to Lower Palaeozoic rocks of Northern

Nigeria-a review in: C.A. Kogbe (Editor), Geology of Nigeria. Elizebethan Publishing Company, Lagos, 15–39.

Muhammed, I. N., Aboh, H. O., and Emenike, E. A. (2008): A regional geoelectric investigation for groundwater exploration in Minna area, northwest Nigeria. *Science World Journal*, *2*(4), 22-24.

Obaje, N.G., Lar, U.A., Nzegbuna, A.I., Moumouni, A., Chaanda, M.S. and Goki, N.G. (2006): Geology and Mineral Resources of Nasarawa State, an investor Guide. Elizabethan Publishers, Lagos, 21-34.

Offodile, M.E. (1992): An Approach to Groundwater Study and Development in Nigeria. Mecon Services Ltd., Jos, Nigeria, 224-236.

Okolie, E. C., Osemeikhian, J. E., Oseji, J. O. and Atakpo, E. (2005): "Geophysical Investigation of the source of River Ethiope" in Ukwuani Local Government area of Delta State. Nigeria Institute of Physics, 17, 6-8.

Okoye, N.O., Okunlola, N.A., and Nnuevho, C.I. (2011): Evaluation of the Groundwater Potential in Pompo Village, Gidan Kwano, Minna Using Vertical Electrical Resistivity Sounding. British Journal of Applied Science & Technology, 1(3), 53-66.

Olarewaju, V.O., Olorunfemi, M.O. and Alade, O., (1996): Chemical Charateristicts of Groundwater from some Parts of the Basement Complex of Central Nigeria. Journal of Mineralization Geology, 33 (2), 135-139.

Olasehinde, P. I., (1999): An Integrated Geological and Geophysical Exploration Technique for Groundwater in the Basement Complex of West Central Part of Nigeria. Journal of National Association of Hydrogeologist (Water Resources), 10 (1), 46-49.

Olorunfemi, M. and Fasuyi, S. (1993): Aquifer types and the geoelectric/hydrogeologic characteristics of part of the central basement terrain of Nigeria (Niger State). Journal of African Earth Sciences (and the Middle East), 16, 309-317.

Omoyoloye, N.A., Oladipo, M.I. and Adeoye, O.O. (2008): 'Engineering Geophysical Study of Adagbakuja Newton Development, Southwestern Nigeria. Medwell Online Journal of Earth Science, 2(2), 55-63.

Oseji, J. O., Atakpo, E. A. and Okolie, E. C. (2005): Geoelectric investigation of the aquifer characteristics and groundwater potential in Kwale, Delta State. Nigeria Journal of Applied Sciences and Environmental Management, 9, 157-160.

Oyawoye, M.O. (1964): Geology of Nigerian Basement Complex; Journal of Mining and Geology, 1, 110 -121.

Rahaman, M.A. (1988): Recent Advance in the study of the Basement Complex of Nigeria, Symposium on the geology of the Basement Complex of Nigeria, Obafemi Awolowo University, Ile-Ife, Nigeria (doi:1016/0899-5362(91)90102-5), 7(2), 223-228.

Reynolds, J.M. (2003): An Introduction to Applied and Environmental Geophysics, John Wiley and Son, Reynolds Geosciences Ltd, UK, 450-452.

Telford,W.M., Geldart, L.P., Sheriff, R.E. and Keys, D.A., (1976): *Applied Geophysics*. Cambridge University Press, London, 620 - 623.

Telford, W.M., Geldart, L.P. and Sherif, R.E. (1990): Introduction to Geophysical Methods, Techniques and Targets. Cambridge University Press, Cambridge; 530-538.

Worthington, P.F., (1977): Geophysical Investigation of Groundwater Resources in the Kalahari Basin, Geophysics, 42, 838 – 849.

Yadav, G. S., Singh, S.K. and Tsepav, M.N. (2007): Integrated resistivity surveys for delineation of fractures for groundwater exploration in basement complex. Journal of Applied Geophysics, 62(3), 301-312.

APPENDIX I

VES RESULTS FOR THE ACQUIRED FIELD DATA.

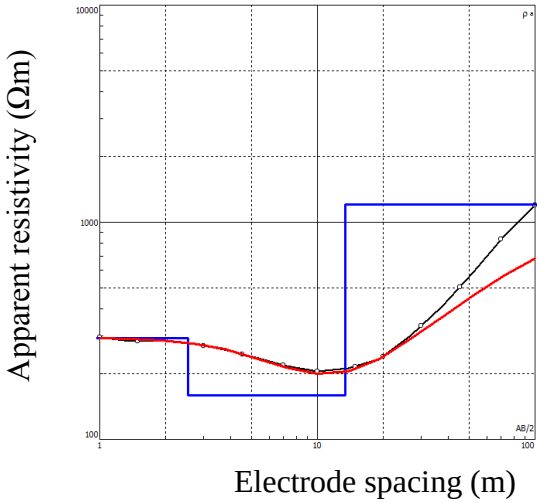

N	ρ	h	d
1	293	2.55	2.55
2	160	10.9	13.4
3	1207		

CURVE AT VES A1 (TYPE H)

where;

N is the layer number,
ρ is the layer resistivity in (Ωm)
h is the layer thickness in metres and
d is interface depth in metres.

Field curve
Synthetic curve
Model

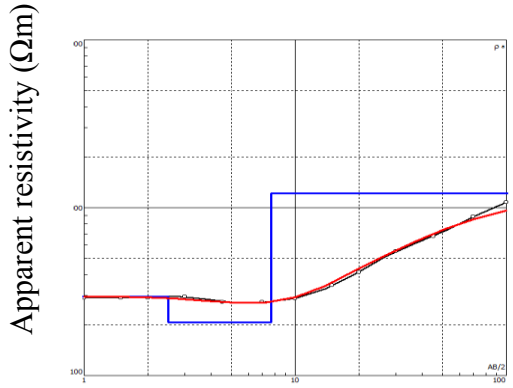

N	ρ	h	d
1	296	2.5	2.5
2	207	5.22	7.72
3	1217		

CURVE AT VES A2 (TYPE H)

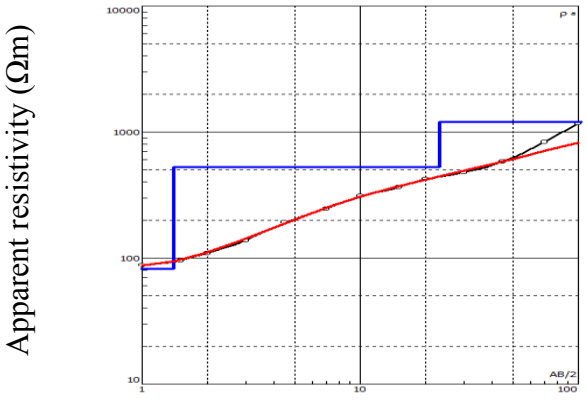

N	ρ	h	d
1	82	1.39	1.39
2	527	21.7	23.1
3	1203		

Electrode spacing (m)

CURVES AT VES A3 (TYPE A)

where;

N is the layer number,
ρ is the layer resistivity in (Ωm)
h is the layer thickness in metres and
d is interface depth in metres.

Field curve
Synthetic curve
Model

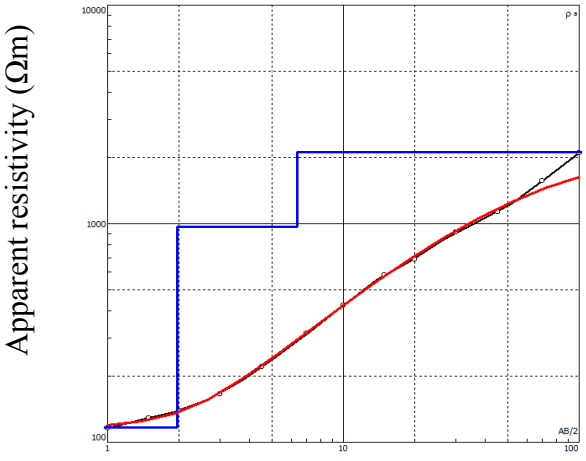

N	ρ	h	d
1	117	1.97	1.97
2	968	4.4	6.37
3	2023		

Electrode spacing (m)

CURVE AT VES A4 (TYPE A)

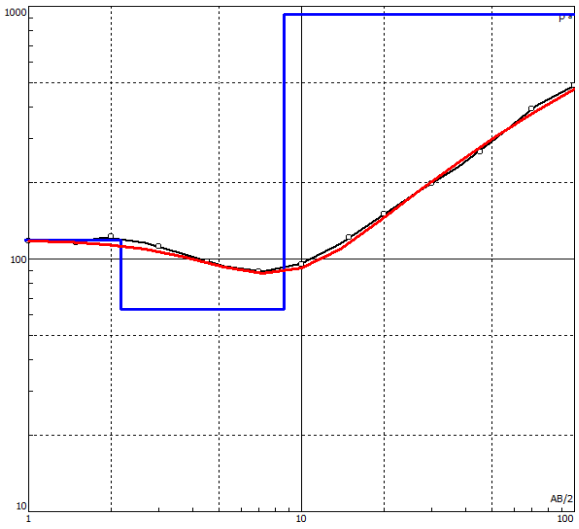

N	ρ	h	d
1	122	2.17	2.17
2	63	6.46	8.63
3	992		

CURVE AT VES A5 (TYPE H)

where;

N is the layer number,
ρ is the layer resistivity in (Ωm)
h is the layer thickness in metres and
d is interface depth in metres.

Field curve
Synthetic curve
Model

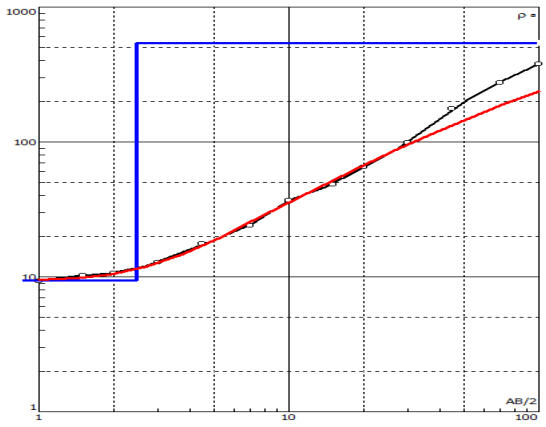

N	ρ	h	d
1	9	2.47	2.47
2	540		

CURVE AT VES A6 (Two layers)

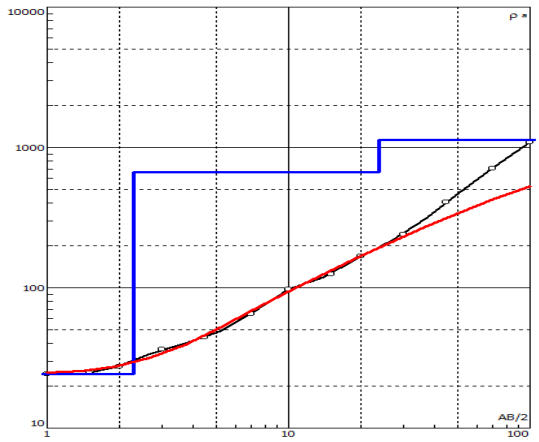

N	ρ	h	d
1	24	2.28	2.28
2	666	21.4	23.7
3	1131		

CURVES AT VES A7 (TYPE A)

where;

N is the layer number,
ρ is the layer resistivity in (Ωm)
h is the layer thickness in metres and
d is interface depth in metres.

Field curve
Synthetic curve
Model

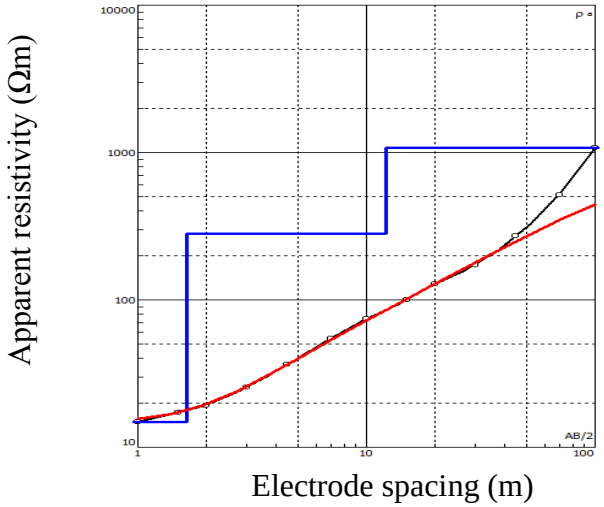

N	ρ	h	d
1	14	1.64	1.64
2	281	10.5	12.1
3	1077		

CURVE AT VES A8 (TYPE A)

Apparent resistivity (Ωm)

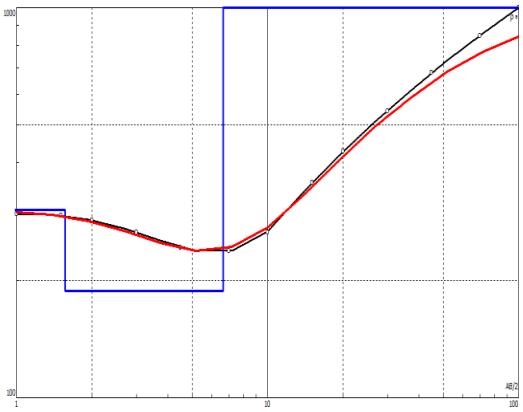

Electrode spacing (m)

N	ρ	h	d
1	303	1.56	1.56
2	187	5.1	6.66
3	1000		

CURVE AT VES A9 (TYPE H)

where;

N is the layer number,
ρ is the layer resistivity in (Ωm)
h is the layer thickness in metres and
d is interface depth in metres.

Field curve
Synthetic curve
Model

Apparent resistivity (Ωm)

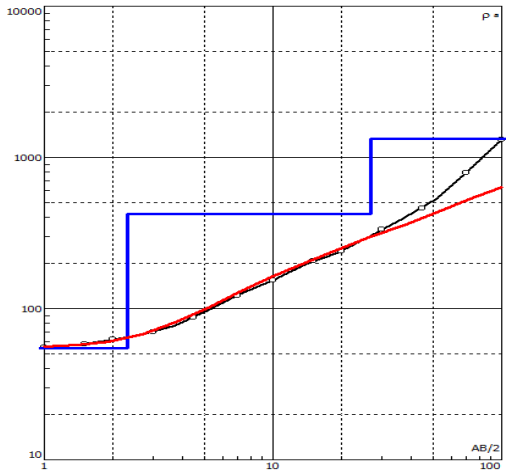

Electrode spacing (m)

N	ρ	h	d
1	54	2.31	2.31
2	422	24.5	26.8
3	1327		

CURVE AT VES A10 (TYPE A)

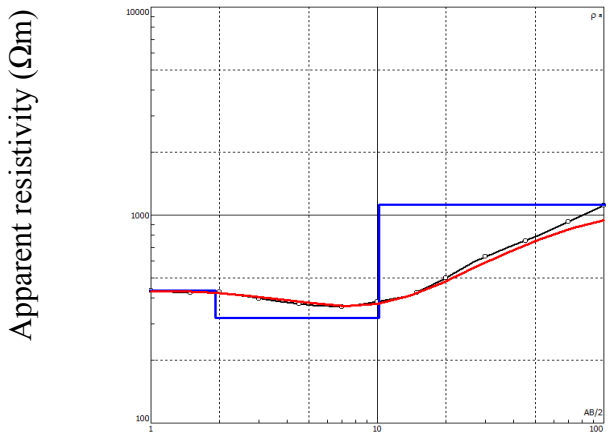

N	ρ	h	d
1	434	1.93	1.93
2	320	8.24	10.2
3	1122		

CURVE AT VES B1 (TYPE H)

where;

N is the layer number,
ρ is the layer resistivity in (Ωm)
h is the layer thickness in metres and
d is interface depth in metres.

Field curve
Synthetic curve
Model

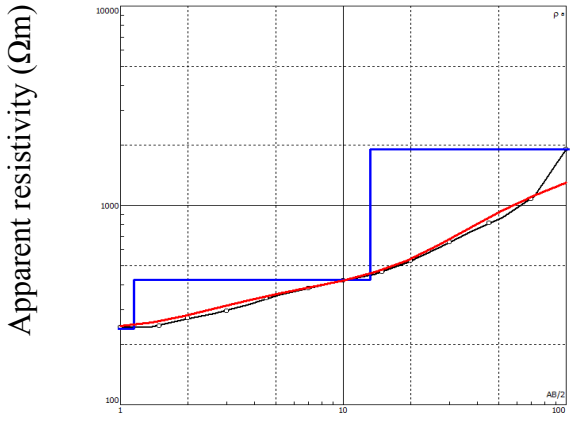

N	ρ	h	d
1	240	1.15	1.15
2	423	12.1	13.2
3	1911		

CURVE AT VES B2 (TYPE A)

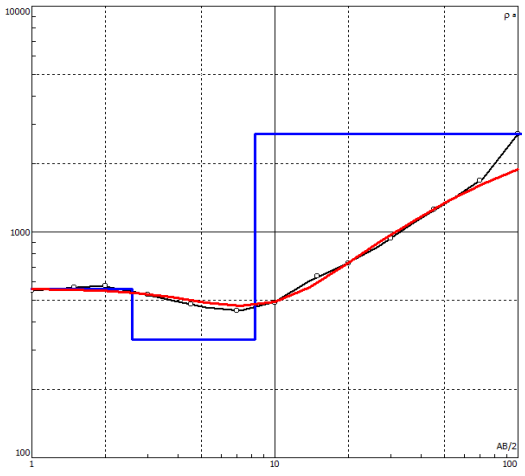

N	ρ	h	d
1	559	2.59	2.59
2	334	5.69	8.28
3	2718		

CURVE AT VES B3 (TYPE H)

where;

N is the layer number,
ρ is the layer resistivity in (Ωm)
h is the layer thickness in metres and
d is interface depth in metres.

Field curve
Synthetic curve
Model

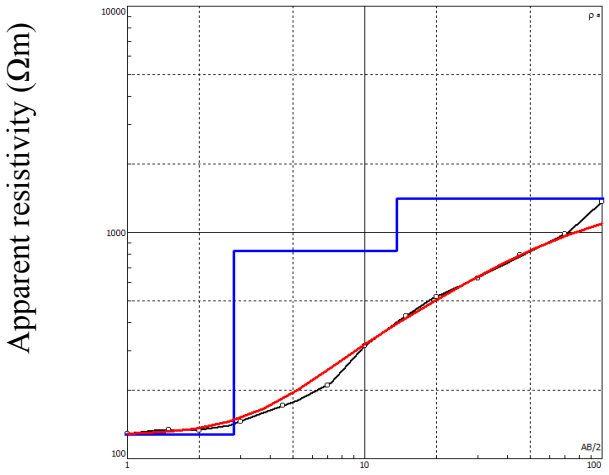

N	ρ	h	d
1	128	2.81	2.81
2	831	10.8	13.6
3	1412		

CURVE AT VES B4 (TYPE A)

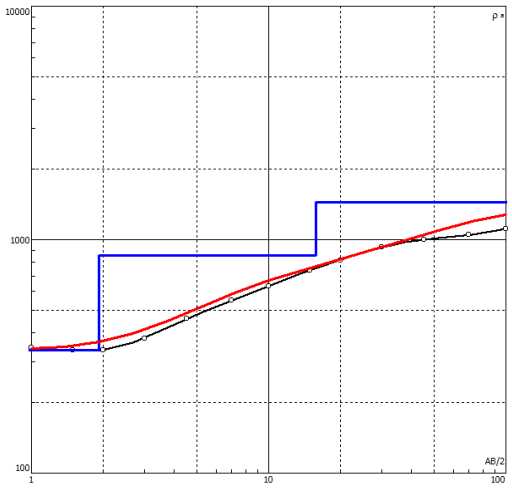

N	ρ	h	d
1	336	1.93	1.93
2	856	13.9	15.8
3	1446		

CURVE AT VES B5 (TYPE A)

where;

N is the layer number,
ρ is the layer resistivity in (Ωm)
h is the layer thickness in metres and
d is interface depth in metres.

Field curve
Synthetic curve
Model

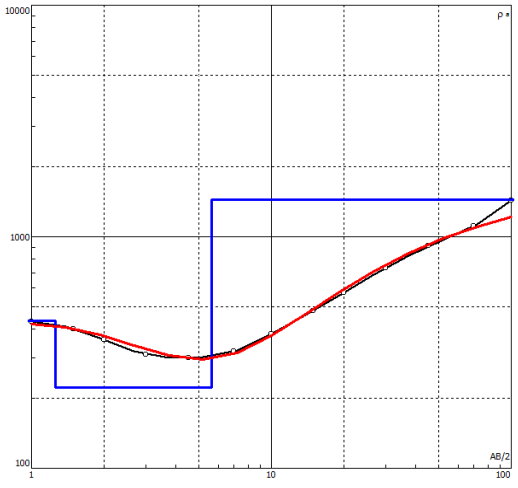

N	ρ	h	d
1	434	1.26	1.26
2	223	4.38	5.64
3	1446		

CURVE AT VES B6 (TYPE H)

Apparent resistivity (Ωm)

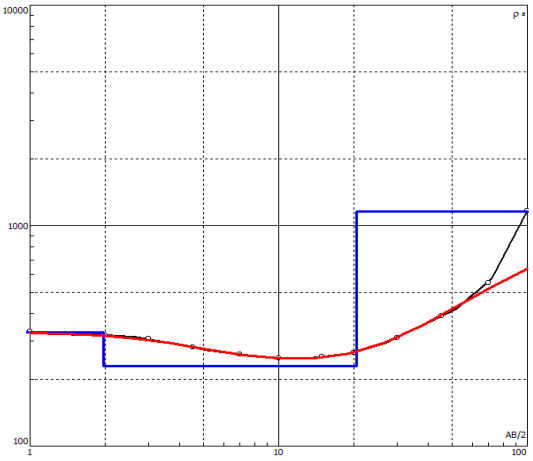

Electrode spacing (m)

N	ρ	h	d
1	328	1.97	1.97
2	231	18.6	20.6
3	1159		

CURVE AT VEES B7 (TYPE H)

where;

N is the layer number,
ρ is the layer resistivity in (Ωm)
h is the layer thickness in metres and
d is interface depth in metres.

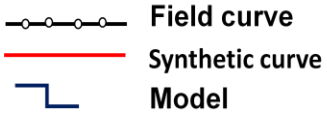

Apparent resistivity (Ωm)

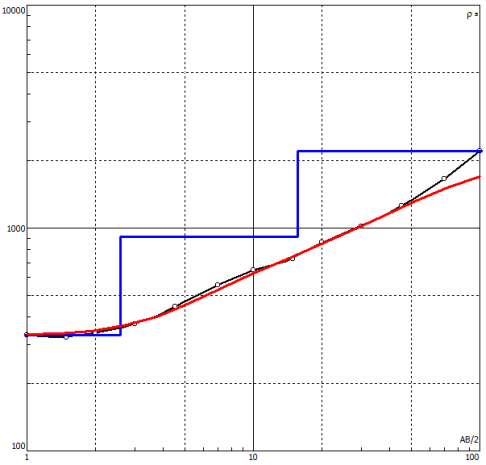

Electrode spacing (m)

N	ρ	h	d
1	331	2.59	2.59
2	914	13.1	15.7
3	2214		

CURVE AT VES B8 (TYPE A)

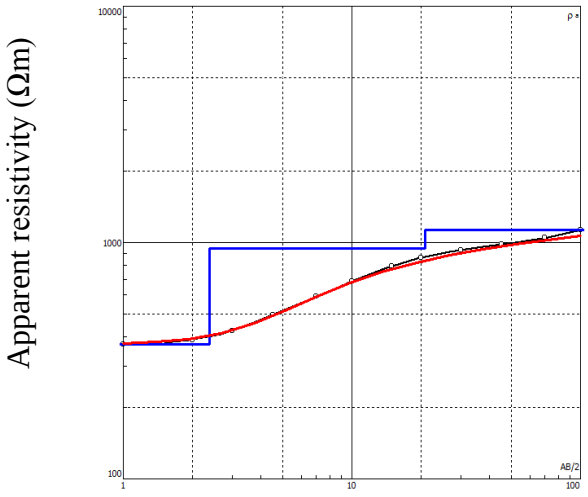

N	ρ	h	d
1	371	2.38	2.38
2	944	18.5	20.9
3	1131		

CURVE AT VES B9 (TYPE A)

where;

N is the layer number,
ρ is the layer resistivity in (Ωm)
h is the layer thickness in metres and
d is interface depth in metres.

Field curve
Synthetic curve
Model

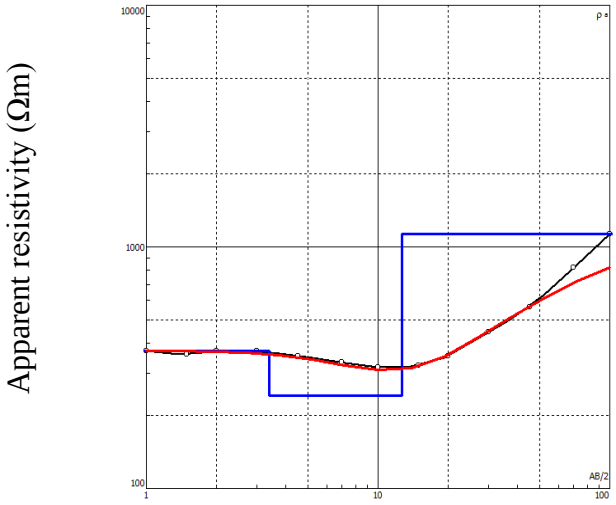

N	ρ	h	d
1	371	3.39	3.39
2	242	9.29	12.7
3	1131		

CURVE AT VES B10 (TYPE H)

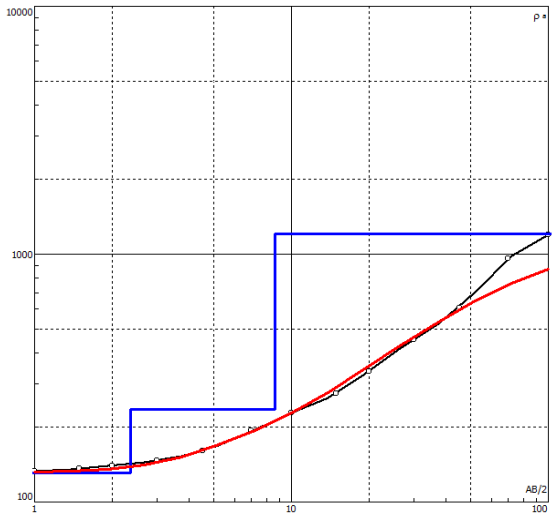

N	ρ	h	d
1	131	2.36	2.36
2	236	6.3	8.65
3	1207		

CURVE AT VES C1 (TYPE A)

where;

N is the layer number,

ρ is the layer resistivity in (Ωm)

h is the layer thickness in metres and

d is interface depth in metres.

Field curve

Synthetic curve

Model

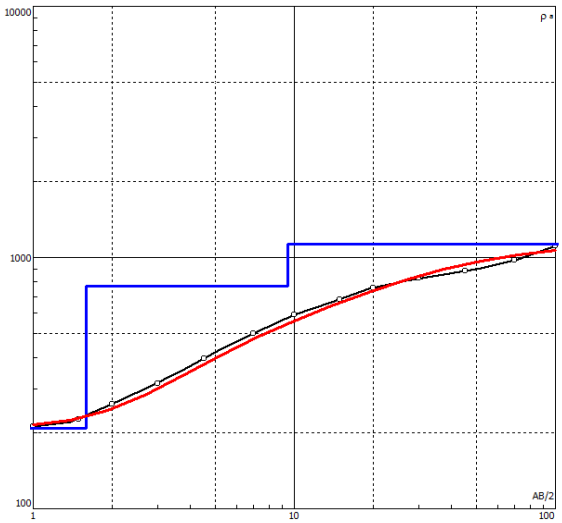

N	ρ	h	d
1	209	1.6	1.6
2	769	7.85	9.44
3	1131		

CURVE AT VES C2 (TYPE A)

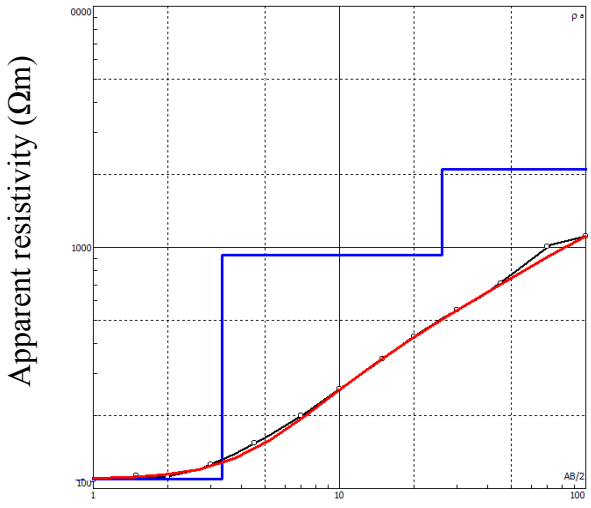

N	ρ	h	d
1	109	3.34	3.34
2	929	22.7	26.1
3	2108		

CURVE AT VES C3 (TYPE A)

where;

N is the layer number,
ρ is the layer resistivity in (Ωm)
h is the layer thickness in metres and
d is interface depth in metres.

Field curve
Synthetic curve
Model

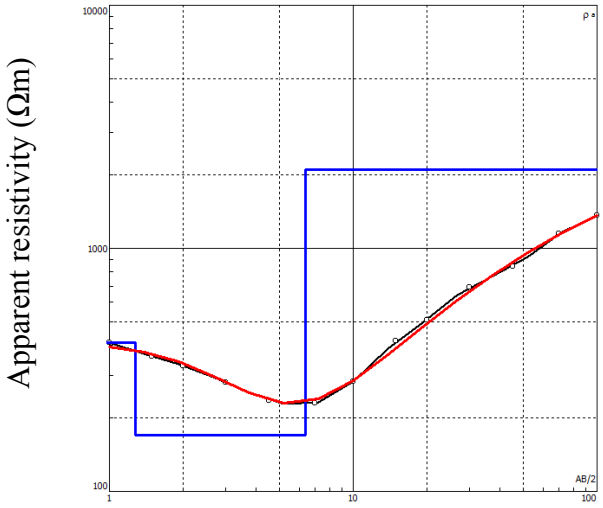

N	ρ	h	d
1	410	1.28	1.28
2	170	5.08	6.35
3	2108		

CURVE AT VES C4 (TYPE H)

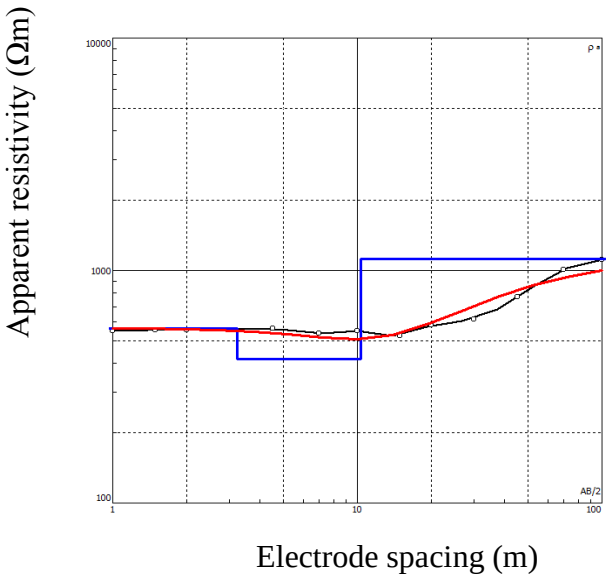

N	ρ	h	d
1	564	3.23	3.23
2	416	7.11	10.3
3	1122		

CURVE AT VES C5 (TYPE A)

where;

N is the layer number,
ρ is the layer resistivity in (Ωm)
h is the layer thickness in metres and
d is interface depth in metres.

Field curve
Synthetic curve
Model

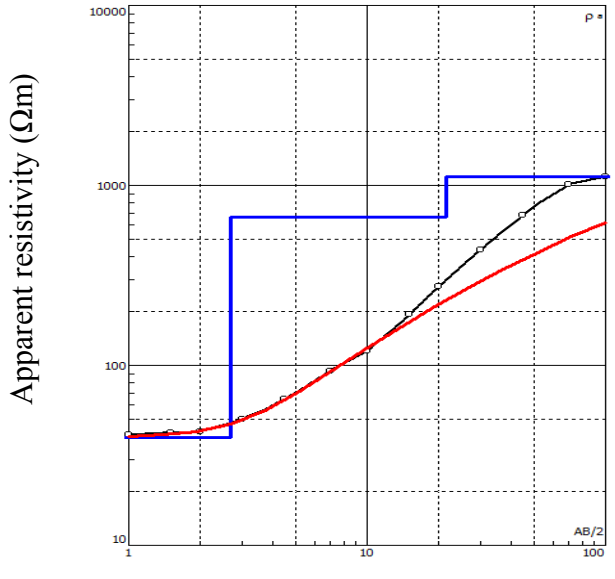

N	ρ	h	d
1	39	2.68	2.68
2	666	18.8	21.5
3	1117		

CURVE AT VES C6 (TYPE A)

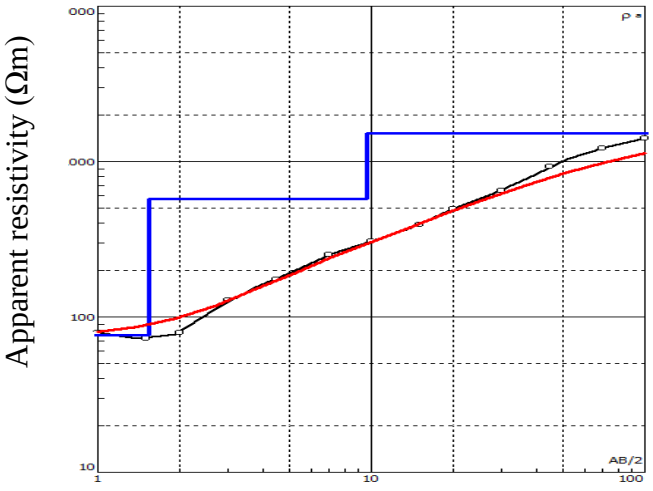

Electrode spacing (m)

N	ρ	h	d
1	76	1.54	1.54
2	578	8.1	9.64
3	1520		

CURVE AT VES C7 (TYPE A)

where;

N is the layer number,
ρ is the layer resistivity in (Ωm)
h is the layer thickness in metres and
d is interface depth in metres.

Field curve
Synthetic curve
Model

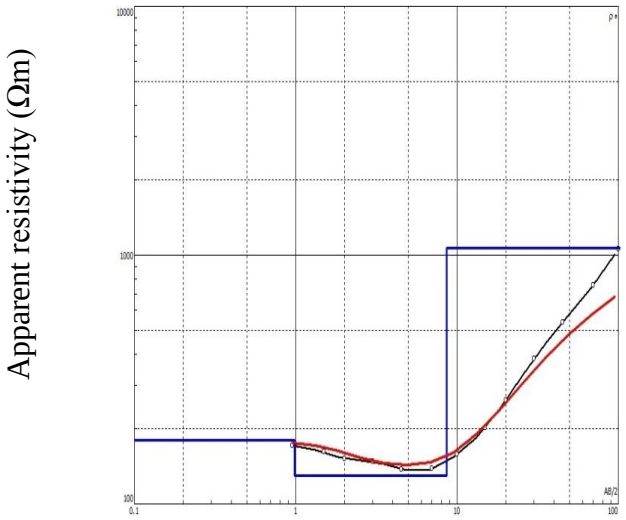

Electrode spacing (m)

N	ρ	h	d
1	181	0.98	0.98
2	130	7.65	8.63
3	1068		

CURVE AT VES C8 (TYPE H)

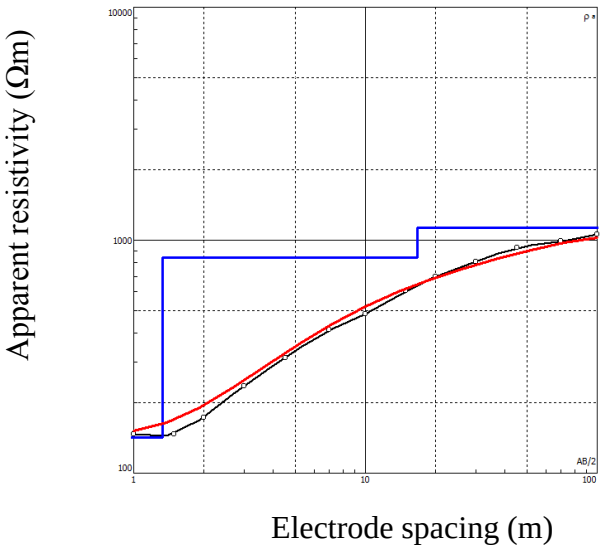

N	ρ	h	d
1	142	1.34	1.34
2	842	15.4	16.8
3	1131		

CURVE AT VES C9 (TYPE A)

where;

N is the layer number,
ρ is the layer resistivity in (Ωm)
h is the layer thickness in metres and
d is interface depth in metres.

Field curve
Synthetic curve
Model

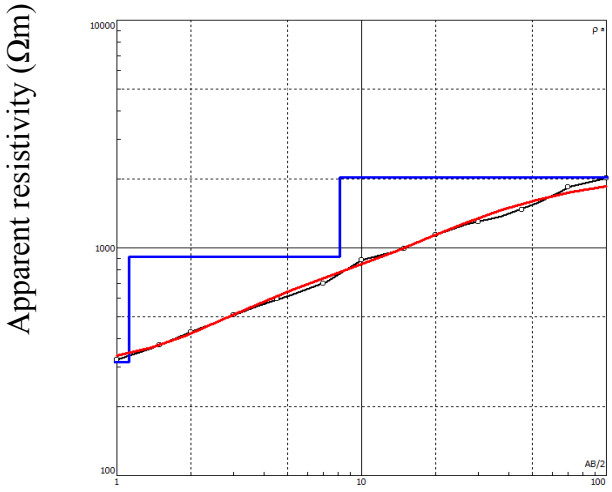

N	ρ	h	d
1	315	1.12	1.12
2	914	7.03	8.15
3	2040		

CURVE AT VES C10 (TYPE A)

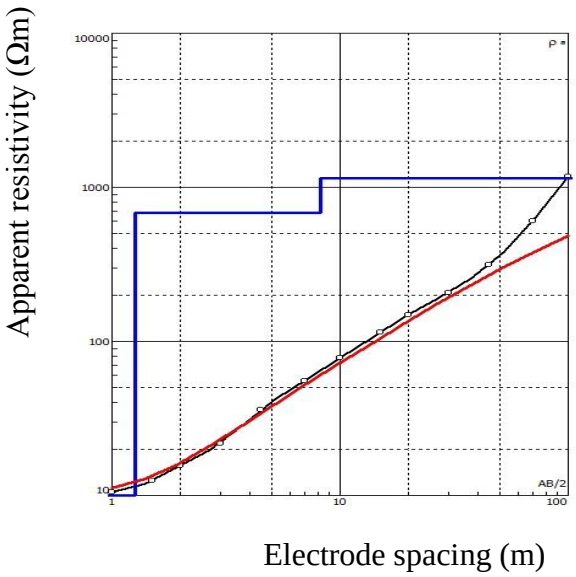

N	ρ	h	d
1	10	1.26	1.26
2	686	6.95	8.21
3	1025		

CURVE AT VES D1 (TYPE A)

where;

N is the layer number,
ρ is the layer resistivity in (Ωm)
h is the layer thickness in metres and
d is interface depth in metres.

Field curve
Synthetic curve
Model

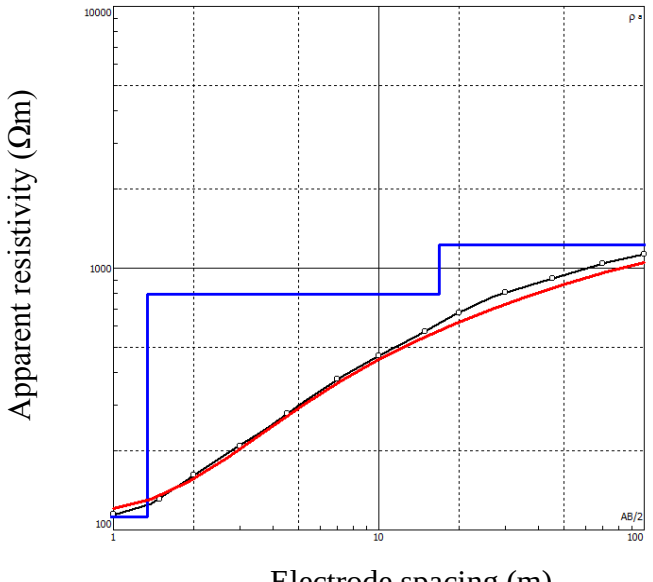

N	ρ	h	d
1	112	1.34	1.34
2	795	15.6	16.9
3	1227		

CURVE AT VES D2 (TYPE A)

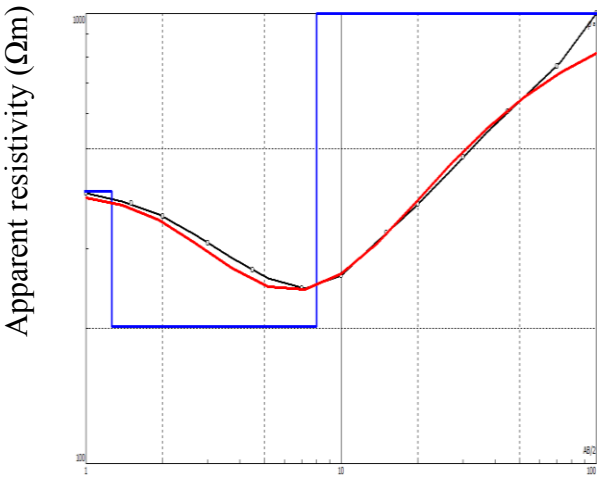

N	ρ	h	d
1	403	1.26	1.26
2	202	6.75	8.01
3	1000		

CURVE AT VES D3 (TYPE H)

where;

N is the layer number,
ρ is the layer resistivity in (Ωm)
h is the layer thickness in metres and
d is interface depth in metres.

Field curve
Synthetic curve
Model

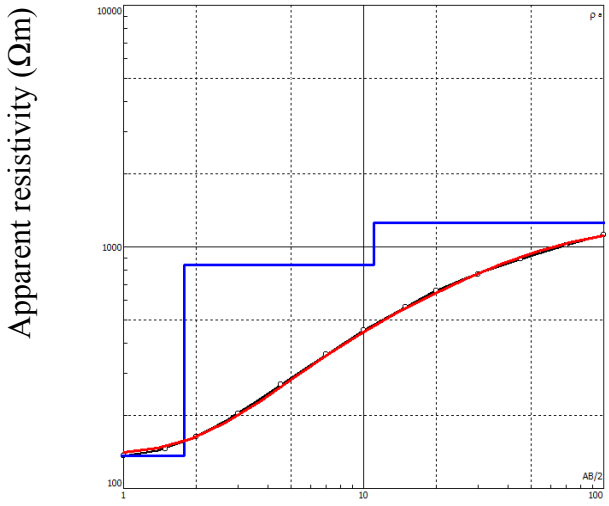

N	ρ	h	d
1	137	1.79	1.79
2	842	9.24	11
3	1258		

CURVE AT VES D4 (TYPE A)

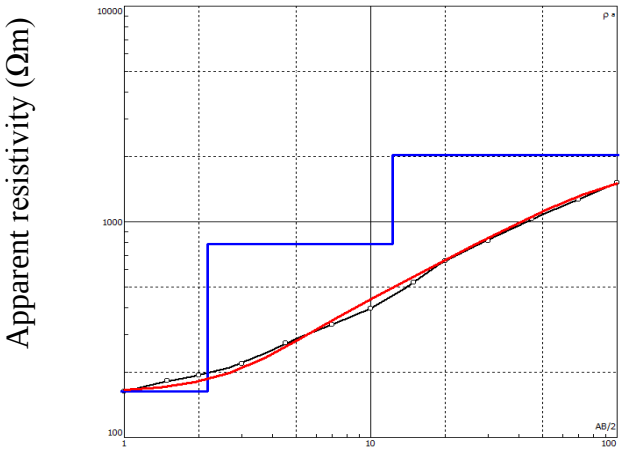

N	ρ	h	d
1	164	2.18	2.18
2	789	10.1	12.3
3	2040		

CURVE AT VES D5 (TYPE A)

where;

N is the layer number,
ρ is the layer resistivity in (Ωm)
h is the layer thickness in metres and
d is interface depth in metres.

Field curve
Synthetic curve
Model

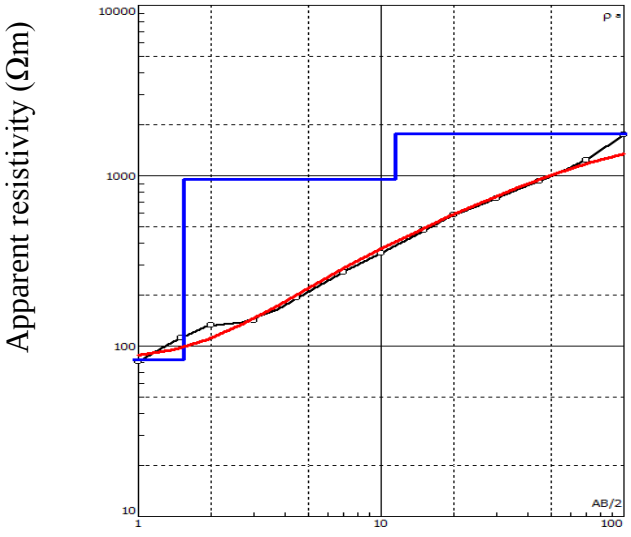

N	ρ	h	d
1	83	1.54	1.54
2	952	9.91	11.4
3	1762		

CURVE AT VES D6 (TYPE A)

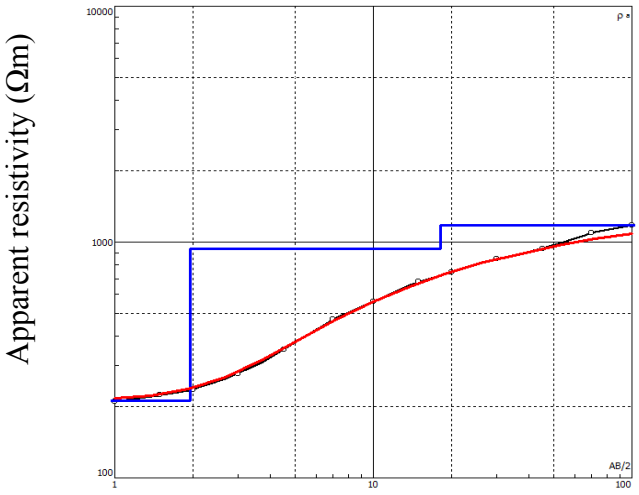

N	ρ	h	d
1	213	1.96	1.96
2	937	16.2	18.2
3	1178		

CURVE AT VES D7 (TYPE A)

where;

N is the layer number,
ρ is the layer resistivity in (Ωm)
h is the layer thickness in metres and
d is interface depth in metres.

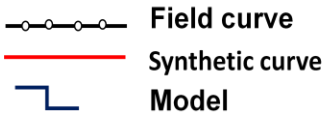

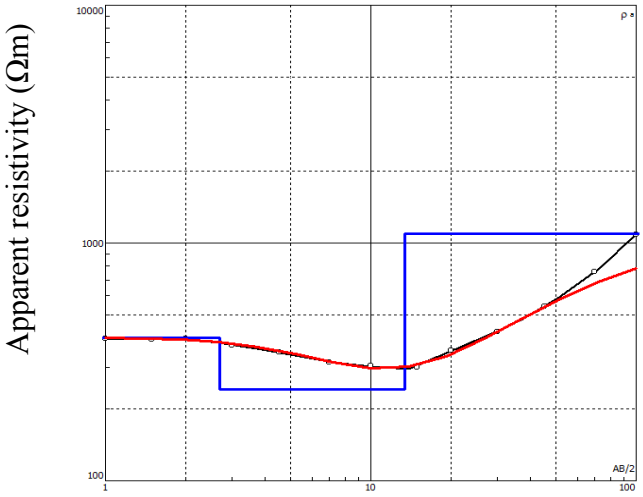

N	ρ	h	d
1	399	2.7	2.7
2	242	10.7	13.4
3	1094		

CURVE AT VES D8 (TYPE H)

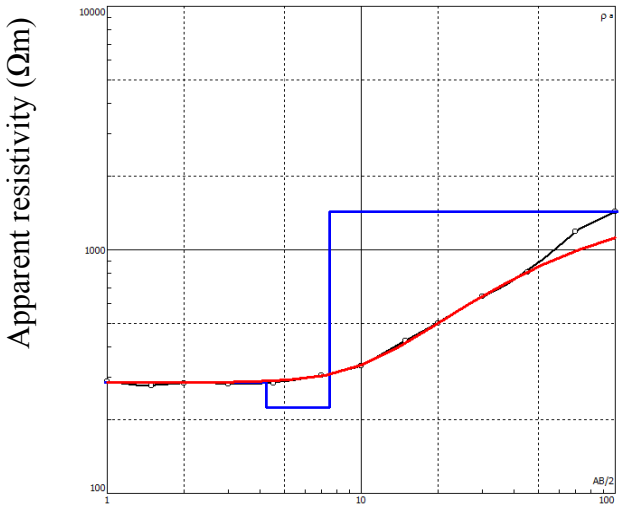

N	ρ	h	d
1	285	4.23	4.23
2	225	3.28	7.51
3	1434		

CURVE AT VES D9 (TYPE H)

where;

N is the layer number,
ρ is the layer resistivity in (Ωm)
h is the layer thickness in metres and
d is interface depth in metres.

Field curve
Synthetic curve
Model

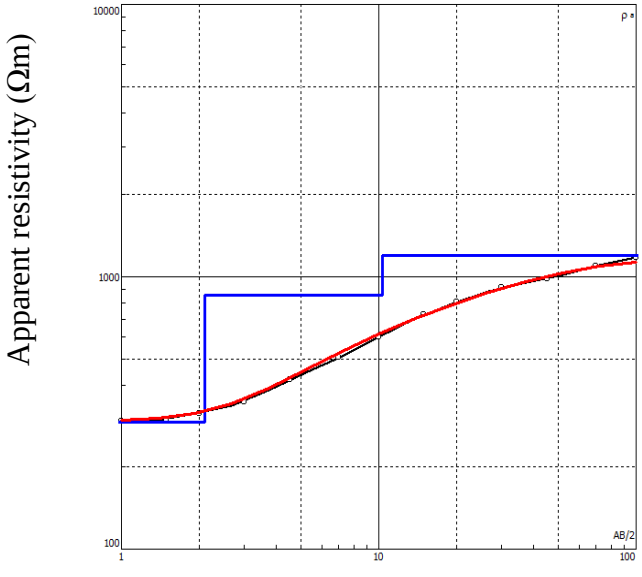

N	ρ	h	d
1	293	2.11	2.11
2	856	8.23	10.3
3	1198		

CURVE AT VES D10 (TYPE A)

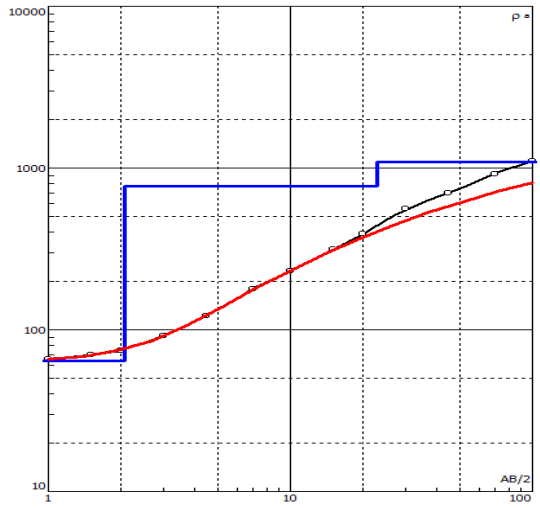

CURVE AT VES E1 (TYPE A)

N	ρ	h	d
1	64	2.07	2.07
2	772	20.8	22.9
3	1090		

where;

N is the layer number,
ρ is the layer resistivity in (Ωm)
h is the layer thickness in metres and
d is interface depth in metres.

Field curve
Synthetic curve
Model

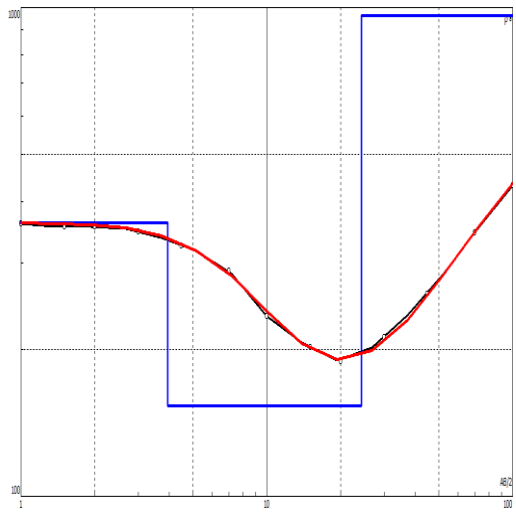

CURVE AT VES E2 (TYPE H)

N	ρ	h	d
1	363	3.96	3.96
2	153	20.3	24.2
3	995		

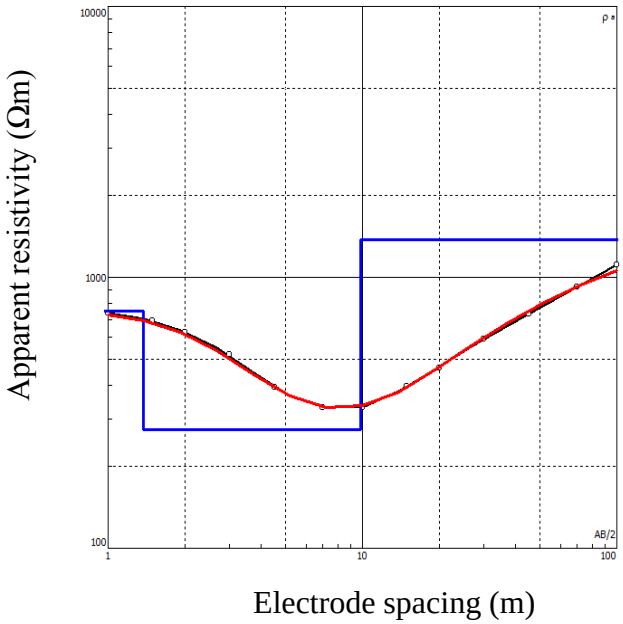

N	ρ	h	d
1	751	1.38	1.38
2	273	8.46	9.84
3	1377		

CURVE AT VES E3 (TYPE H)

where;

N is the layer number,
ρ is the layer resistivity in (Ωm)
h is the layer thickness in metres and
d is interface depth in metres.

Field curve
Synthetic curve
Model

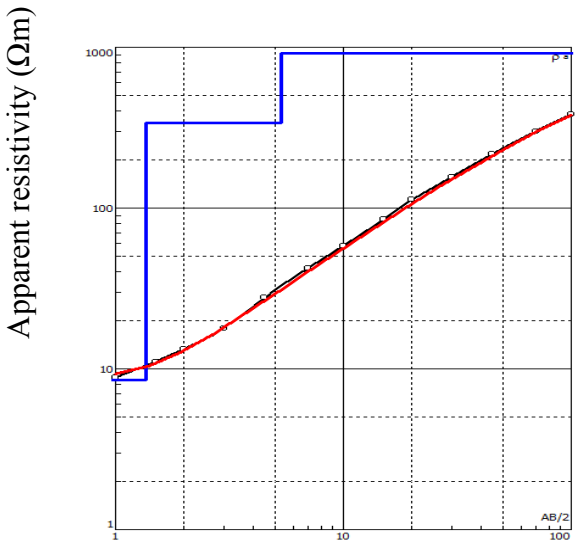

N	ρ	h	d
1	9	1.36	1.36
2	338	3.98	5.34
3	988		

CURVE AT VES E4 (TYPE A)

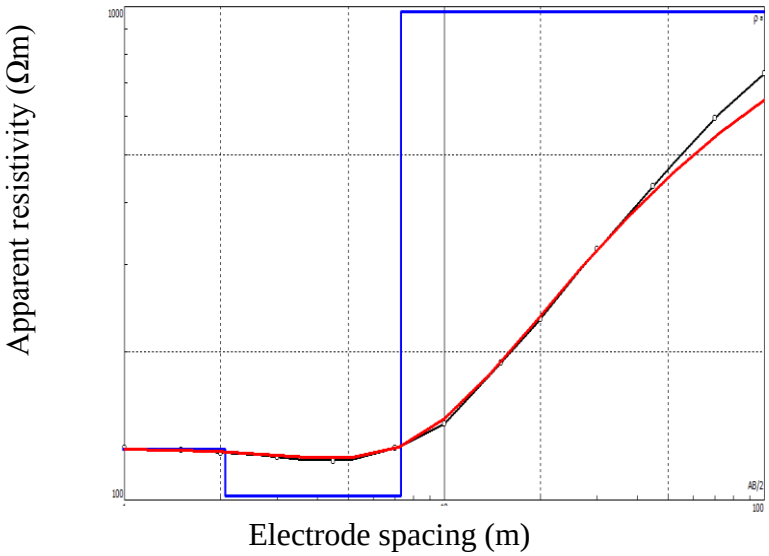

N	ρ	h	d
1	127	2.06	2.06
2	102	5.27	7.32
3	995		

CURVE AT VES E5 (TYPE H)

where;

N is the layer number,
ρ is the layer resistivity in (Ωm)
h is the layer thickness in metres and
d is interface depth in metres.

Field curve
Synthetic curve
Model

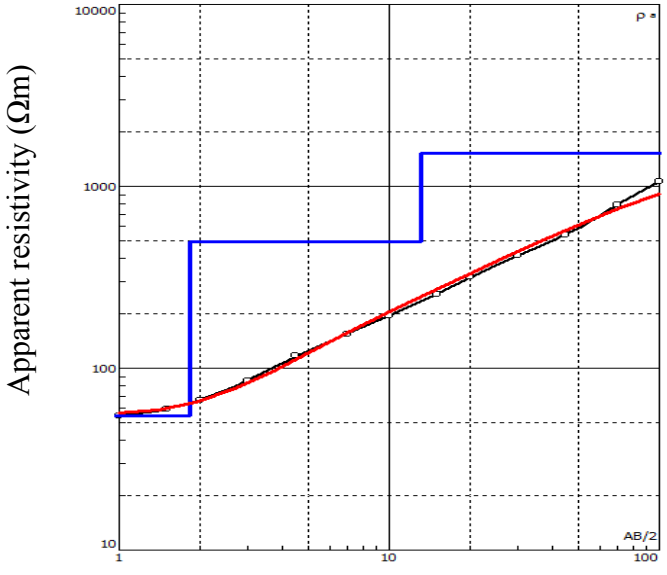

N	ρ	h	d
1	55	1.83	1.83
2	496	11.3	13.1
3	1520		

CURVE AT VES E6 (TYPE A)

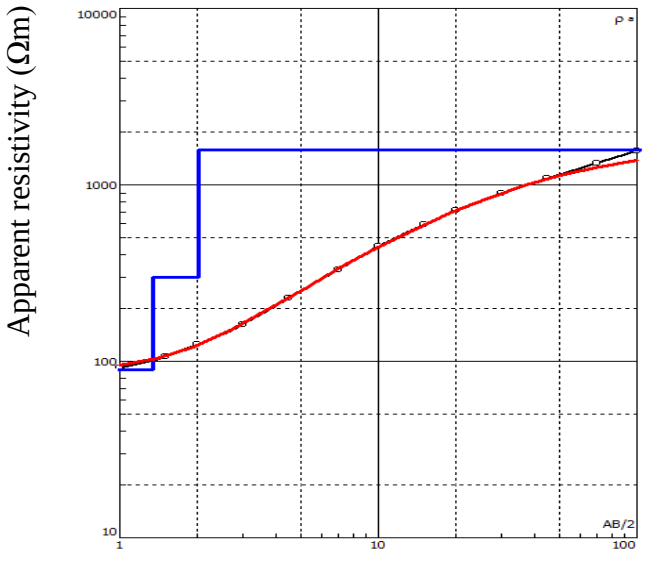

N	ρ	h	d
1	89	1.34	1.34
2	299	0.67	2.01
3	1577		

CURVE AT VES E7 (TYPE A)

where;

N is the layer number,
ρ is the layer resistivity in (Ωm)
h is the layer thickness in metres and
d is interface depth in metres.

Field curve
Synthetic curve
Model

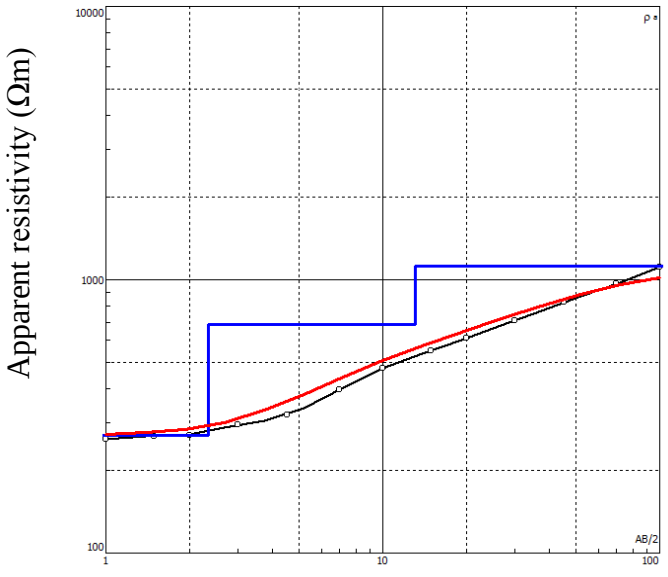

N	ρ	h	d
1	270	2.34	2.34
2	686	10.8	13.1
3	1122		

CURVE AT VES E8 (TYPE A)

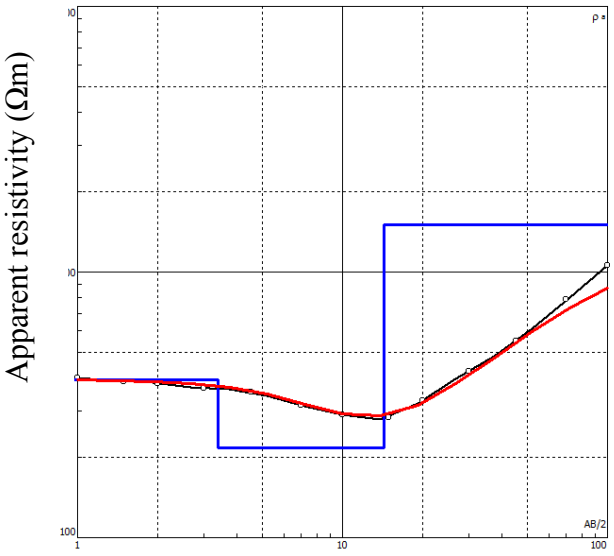

N	ρ	h	d
1	392	3.38	3.38
2	217	10.9	14.3
3	1506		

CURVE AT VES E9 (TYPE H)

where;

N is the layer number,
ρ is the layer resistivity in (Ωm)
h is the layer thickness in metres and
d is interface depth in metres.

Field curve
Synthetic curve
Model

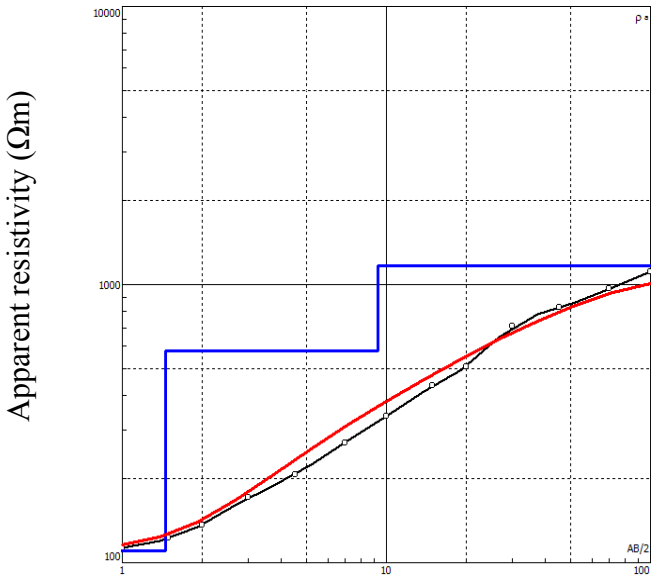

N	ρ	h	d
1	110	1.46	1.46
2	578	7.83	9.29
3	1168		

CURVE AT VES E10 (TYPE A)

APPENDIX II: The Results of the Interpreted VES Curves.

Stations	Station coordinate	Layer thickness (m)	Depth (m)	Layer resistivity (Ωm)	Remarks	Curve types	Number of Layers
A1	$9^0$26'59.5''N $6^0$38'40.0"E	2.55 10.90 -	2.55 13.45 ∞	293 160 1207	TP WB FB	H	3
A2	$9^0$27'01.0''N $6^0$38'40.4"E	2.50 5.22 -	2.50 7.72 ∞	296 207 1217	TP WB FB	H	3
A3	$9^0$27'03.5''N $6^0$38'40.8"E	1.39 21.70 -	1.39 23.09 ∞	82 527 1203	TP WB FB	A	3
A4	$9^0$27'05.0''N $6^0$38'40.2"E	1.97 4.40 -	1.97 6.37 ∞	117 968 2023	TP WB FB	A	3
A5	$9^0$27'07.5''N $6^0$38'40.0"E	2.17 6.46 -	2.17 8.63 ∞	122 63 992	TP WB FB	H	3
A6	$9^0$27'09.0''N $6^0$38'40.6"E	2.47 -	2.47 ∞	9 540	WB FB		2
A7	$9^0$27'11.5''N $6^0$38'40.0"E	2.28 21.40 -	2.28 23.68 ∞	24 666 1131	TP WB FB	A	3
A8	$9^0$27'13.5''N $6^0$38'40.5"E	1.64 10.50 -	1.64 12.14 ∞	14 281 1077	TP WB FB	A	3
A9	$9^0$27'15.0''N $6^0$38'40.7"E	1.56 5.10 -	1.56 6.66 ∞	303 187 1000	TP WB FB	H	3
A10	$9^0$27'17.5''N $6^0$38'40.5"E	2.31 24.50 -	2.31 26.81 ∞	54 422 1327	TP WB FB	A	3
B1	$9^0$26'59.6''N $6^0$38'42.5"E	1.93 8.24 -	1.93 10.17 ∞	434 320 1122	TP WB FB	H	3
B2	$9^0$27'01.0''N $6^0$38'42.4"E	1.15 12.10 -	1.15 13.25 ∞	240 423 1911	TP WB FB	A	3
B3	$9^0$27'03.5''N $6^0$38'42.8"E	2.59 5.69 -	2.59 8.28 ∞	559 334 2718	TP WB FB	H	3

Stations	Station coordinate	Layer thickness (m)	Depth (m)	Layer resistivity (Ωm)	Remarks	Curve types	Number of Layers
B4	$9^0$27’05.0’’N $6^0$38’42.2”E	2.81 10.80 -	2.81 13.61 ∞	128 831 1412	TP WB FB	A	3
B5	$9^0$27’07.5’’N $6^0$38’42.0”E	1.93 13.30 -	1.93 15.23 ∞	336 856 1446	TP WB FB	A	3
B6	$9^0$27’9.3’’N $6^0$38’42.6”E	1.26 4.38 -	1.26 5.64 ∞	434 223 1446	TP WB FB	H	3
B7	$9^0$27’11.8’’N $6^0$38’42.9”E	1.97 18.60 -	1.97 20.57 ∞	328 231 1159	TP WB FB	H	3
B8	$9^0$27’13.5’’N $6^0$38’42.5”E	2.59 13.10 -	2.59 15.69 ∞	331 914 2214	TP WB FB	A	3
B9	$9^0$27’15.3’’N $6^0$38’42.7”E	2.38 18.50 -	2.38 20.88 ∞	371 944 1131	TP WB FB	A	3
B10	$9^0$27’17.5’’N $6^0$38’42.5”E	3.39 9.29 -	3.39 12.68 ∞	371 242 1131	TP WB FB	H	3
C1	$9^0$26’59.6’’N $6^0$38’45.5”E	2.36 6.30 -	2.36 8.66 ∞	131 236 1207	TP WB FB	A	3
C2	$9^0$27’01.0’’N $6^0$38’45.4”E	1.60 7.85 -	1.60 9.45 ∞	209 769 1131	TP WB FB	A	3
C3	$9^0$27’03.5’’N $6^0$38’45.8”E	3.34 22.70 -	3.34 26.04 ∞	109 929 2108	TP WB FB	A	3
C4	$9^0$27’05.6’’N $6^0$38’46.00”E	1.28 5.08 -	1.28 6.36 ∞	410 170 2108	TP WB FB	H	3
C5	$9^0$27’07.9’’N $6^0$38’45.9”E	3.23 7.11 -	3.23 10.34 ∞	564 416 1122	TP WB FB	A	3
C6	$9^0$27’09.3’’N $6^0$38’45.8”E	2.68 18.80 -	2.68 21.48 ∞	39 666 1117	TP WB FB	A	3
C7	$9^0$27’11.8’’N $6^0$38’45.9”E	1.54 8.10 -	1.54 9.64 ∞	76 578 1520	TP WB FB	A	3

Stations	Station coordinate	Layer thickness (m)	Depth (m)	Layer resistivity (Ωm)	Remarks	Curve types	Number of Layers
C8	$9^0$27’13.9’’N $6^0$38’45.2”E	0.98 7.65 -	0.98 8.63 ∞	181 130 1068	TP WB FB	H	3
C9	$9^0$27’15.8’’N $6^0$38’45.1”E	1.34 15.40 -	1.34 16.74 ∞	142 842 1131	TP WB FB	A	3
C10	$9^0$27’17.5’’N $6^0$38’45.0”E	1.12 7.03 -	1.12 8.15 ∞	315 914 2040	TP WB FB	A	3
D1	$9^0$26’59.6’’N $6^0$38’47.5”E	1.26 6.95 -	1.26 8.21 ∞	10 686 1025	TP WB FB	A	3
D2	$9^0$27’01.0’’N $6^0$38’47.6”E	1.34 15.60 -	1.34 16.94 ∞	112 795 1227	TP WB FB	A	3
D3	$9^0$27’03.6’’N $6^0$38’47.8”E	1.26 6.75 -	1.26 8.01 ∞	403 202 1000	TP WB FB	H	3
D4	$9^0$27’05.0’’N $6^0$38’47.4”E	1.79 9.24 -	1.79 11.03 ∞	137 842 1258	TP WB FB	A	3
D5	$9^0$27’07.9’’N $6^0$38’47.8”E	2.18 10.10 -	2.18 12.28 ∞	164 789 2040	TP WB FB	A	3
D6	$9^0$27’09.0’’N $6^0$38’47.6”E	1.54 9.91 -	1.54 11.45 ∞	83 952 1762	TP WB FB	A	3
D7	$9^0$27’11.5’’N $6^0$38’47.7”E	1.96 16.20 -	1.96 18.16 ∞	213 937 1178	TP WB FB	A	3
D8	$9^0$27’13.0’’N $6^0$38’47.5”E	2.70 10.70 -	2.70 13.40 ∞	399 242 1094	TP WB FB	H	3
D9	$9^0$27’15.7’’N $6^0$38’47.4”E	4.23 3.28 -	4.23 7.51 ∞	285 225 1434	TP WB FB	H	3
D10	$9^0$27’17.5’’N $6^0$38’47.6”E	2.11 8.23 -	2.11 10.34 ∞	293 856 1198	TP WB FB	A	3
E1	$9^0$26’59.6’’N $6^0$38’50.2”E	2.07 20.80 -	2.07 22.87 ∞	64 772 1090	TP WB FB	A	3

Stations	Station coordinate	Layer thickness (m)	Depth (m)	Layer resistivity (Ωm)	Remarks	Curve types	Number of Layers
E2	$9^0$27’01.0’’N $6^0$38’50.0”E	3.96 20.30 -	3.96 24.26 ∞	363 153 995	TP WB FB	H	3
E3	$9^0$27’03.6’’N $6^0$38’50.3”E	1.38 8.46 -	1.38 9.84 ∞	751 273 1377	TP WB FB	H	3
E4	$9^0$27’05.0’’N $6^0$38’50.0”E	1.36 3.98 -	1.36 5.34 ∞	9 338 988	TP WB FB	A	3
E5	$9^0$27’07.7’’N $6^0$38’49.9”E	2.06 5.27 -	2.06 7.33 ∞	127 102 995	TP WB FB	H	3
E6	$9^0$27’09.0’’N $6^0$38’50.4”E	1.83 11.30 -	1.83 13.13 ∞	55 496 1520	TP WB FB	A	3
E7	$9^0$27’11.5’’N $6^0$38’50.3”E	1.34 0.67 -	1.34 2.01 ∞	89 299 1517	TP WB FB	A	3
E8	$9^0$27’13.3’’N $6^0$38’50.0”E	2.34 10.80 -	2.34 13.14 ∞	270 686 1122	TP WB FB	A	3
E9	$9^0$27’15.5’’N $6^0$38’50.1”E	3.38 10.90 -	3.38 14.28 ∞	392 217 1506	TP WB FB	H	3
E10	$9^0$27’17.5’’N $6^0$38’50.3”E	1.46 7.83 -	1.46 9.29 ∞	110 578 1168	TP WB FB	A	3

Where;

TP is the Top Layer

WB is the Weathered Basement

FB is the Fresh Basement.